PACIFIC EARTHQUAKE ENGINEERING RESEARCH CENTER

Nonlinear Horizontal Site Response for the NGA-West2 Project

Ronnie Kamai
Pacific Earthquake Engineering Research Center
University of California, Berkeley

Norman A. Abrahamson
Pacific Gas & Electric Company
San Francisco, California

Walter J. Silva
Pacific Engineering and Analysis
El Cerrito, California

PEER 2013/12
MAY 2013

Nonlinear Horizontal Site Response for the NGA-West2 Project

Ronnie Kamai
Pacific Earthquake Engineering Research Center
University of California, Berkeley

Norman A. Abrahamson
Pacific Gas & Electric Company
San Francisco, California

Walter J. Silva
Pacific Engineering and Analysis
El Cerrito, California

PEER Report 2013/12
Pacific Earthquake Engineering Research Center
Headquarters, University of California, Berkeley

May 2013

ABSTRACT

The nonlinear soil amplification models developed by Walling et al. (2008) are revisited for two main reasons: (a) the simulation database on which the models were developed has been updated and extended, with additional magnitudes and soil profiles, and (b) two alternatives for the input shaking parameter are explored – the Peak Ground Acceleration (PGA) and the spectral acceleration for each period, (Sa(T)). The benefits and limitations of each alternative are discussed.

The model is based on site amplification factors, relative to a V_{S30}=1170 m/sec site, computed for 53 base soil profiles using the RASCALS computer program. The base profiles include ten V_{S30} values (160 m/sec, 190 m/sec, 270 m/sec, 400 m/sec, 560 m/sec, 760 m/sec, 900 m/sec, 1170 m/sec, 2830 m/sec, and 3150 m/sec), up to eight soil depths (25 ft, 50 ft, 120 ft, 250 ft, 500 ft, 1000 ft, 2000 ft, 3000 ft), and four nonlinear soil models (EPRI and Peninsular range models for cohesionless soils and Imperial Valley and Bay Mud models for cohesive soils). For each soil profile, the site response is computed for 11 levels of input rock motion: PGA_{1170}= 0.01g, 0.05g, 0.1g, 0.2g, 0.3g, 0.4g, 0.5g, 0.75g, 1.0, 1.25g, 1.5g, produced by three point-source magnitudes: M = 5.0, 6.0, 7.0.

For each base soil profile, the shear-wave velocities, layer thickness and the nonlinear soil properties (strain dependence of the G/G_{max} and hysteretic damping) are randomized. Correlation of the velocities and layer thickness variations are considered. For each base profile, source magnitude and input ground motion level, the median amplification and the standard deviation of the amplification are computed from 30 realizations of the soil profiles and material properties. These results are intended for use by the NGA developers to constrain the nonlinear scaling of the site response for the ground motion models.

ACKNOWLEDGMENTS

This study was sponsored by the Pacific Earthquake Engineering Research Center (PEER) and funded by the California Earthquake Authority, California Department of Transportation, and the Pacific Gas & Electric Company. Any opinions, findings, and conclusions or recommendations expressed in this material are those of the authors and do not necessarily reflect those of the above mentioned agencies.

CONTENTS

LIST OF FIGURES

LIST OF TABLES

1 Introduction

The objective of the NGA project is to develop ground motion models for shallow crustal earthquakes in California that cover all relevant sources in California (excluding subduction earthquakes). In the past, the authors of the empirical ground motion models often set limits on their applicability based on the data set used to derive the models. However, these limits are typically ignored in the application of the models in PSHA because a PSHA needs to have the ground motion estimates for all relevant scenarios and for the site-specific site conditions.

Rather than having the hazard analyst blindly extrapolate the ground motion models, the NGA project required the developers of the models to extrapolate their models. To help the model developers in this extrapolation, analytical models were used to develop constraints on the ground motion scaling.

This report is divided into two main parts; Chapters 2 and 3 describe the results of a large suite of 1-D site response calculations that can be used by the NGA developers to constrain the nonlinear site amplification and to constrain the soil depth scaling for shallow soil sites. The objective of these chapters is to document the site amplification factors that were made available to the NGA developers. Chapter 4 presents and describes an update to the work conducted by Walling et al. (2008). The motivation for updating the horizontal nonlinear site amplification model is driven by two main reasons: (1) the simulation dataset was extended to include a wider range of possible conditions, and (2) the functional form is modified to include two variations – one with PGA and one with Sa(T) as the input shaking parameter.

2 Analytical Site Response Model and Input Parameters

2.1 ANALYTICAL MODEL

The site response calculations are conducted using the computer program RASCALS (Silva and Lee, 1987). The RASCALS program combines the stochastic point-source analytical model commonly used in seismology to define the source and path scaling of earthquakes with the equivalent-linear approach response commonly used in geotechnical engineering to estimate the non-linear behavior of soils. This method is summarized below.

2.1.1 Point-Source Model

The point-source model used in RASCALS is based on the omega-squared model with a constant stress-drop (e.g., Boore, 1983). Random vibration theory (RVT) is used to relate root-mean-square (RMS) values computed from the power spectrum to peak values of acceleration and oscillator response in the time domain (Silva and Lee, 1987).

The acceleration spectral density for outcrop rock, a(f), is given by:

$$a(f) = C \frac{f^2}{1+(f/f_c)^2} \frac{M_o}{R} P(f) A(f) \exp\left(\frac{-\pi f R}{\beta_0 Q(f)}\right) \tag{2.1}$$

where f is frequency in Hz and

C	=	constant
M_o	=	seismic moment
R	=	equivalent point-source distance
β_0	=	shear-wave velocity at the source
ρ_0	=	density at the source
Q(f)	=	frequency dependent quality factor (anelastic attenuation)
A(f)	=	crustal amplification
P(f)	=	high-frequency truncation filter
f_c	=	corner frequency (Hz)

C is a constant which contains source region properties (density and shear-wave velocity) and accounts for the free-surface effect, the source radiation pattern, and the partition of the energy into two horizontal components:

$$C = \frac{1.1\pi}{\sqrt{2}\rho_0 \beta_0^3} \tag{2.2}$$

Source scaling is provided by specifying two parameters: the seismic moment (M_o) and the stress-drop ($\Delta\sigma$). The seismic moment is related to magnitude through the definition of moment magnitude, M:

$$\log M_0 = 1.5M + 16.05 \tag{2.3}$$

The stress-drop relates the corner frequency to the moment:

$$f_c = \beta_0 \left(\frac{\Delta\sigma}{8.44 M_0} \right) \tag{2.4}$$

The amplification accounts for the increase in wave amplitude due to the impedance contrast from the source to the rock outcrop. The amplification depends on the shear-wave velocity and density structure from the surface to the source depth.

The P(f) filter accounts for the observation that the high-frequency content decays faster than predicted by the omega-squared model. The Anderson and Hough (1984) model for the high frequency filter is adopted:

$$P(f) = \exp(-\pi k f) \tag{2.5}$$

The kappa can be related to the Q in the shallow crust:

$$k = \frac{H}{\bar{\beta}_R \bar{Q}_S} \tag{2.6}$$

where the over-bar indicates an average over a depth H.

2.1.2 Site Effects Model

To model soil and soft-rock response, an RVT-based equivalent-linear approach is used. The outcrop rock power spectral density from the point-source model described in Section 2.1.1 is propagated through a one-dimensional soil column. RVT is used to predict the peak time domain values of shear-strain based on the shear-strain power spectrum. In this sense, the procedure is analogous to the program SHAKE (Schnabel et al., 1972) except that in SHAKE, the peak shear-strains are measured in the time domain. The RVT approach does not use a time history, thereby eliminating the need to conduct multiple analyses using a suite of input time histories consistent with the outcrop rock power spectrum.

In addition to the shear-wave velocity profile, the site effects model requires models for the strain dependence of the normalized shear modulus (G/G_{max}) and the hysteretic damping. The sets of G/G_{max} and hysteretic damping models used in this study are described in Section 2.2.

2.1.3 Input Rock Motion

Three point-source earthquakes, with magnitudes 5.0, 6.0 and 7.0 and a constant stress drop of 50 bars, were used to define the reference rock outcrop motion. The distance for the point-source model was adjusted so that the PGA for the rock outcrop (V_{S30}=1170 m/sec profile described in Section 2.3) matched the desired PGA. For each combination of Magnitude and PGA_{Rock}, the point-source distance was kept fixed, and the velocity profile was replaced with the profile for the desired case. The kappa value for the input rock motion, however, was not kept fixed, as described below.

The kappa for recorded surface ground motion on generic soil and generic rock sites in California are similar with a kappa of about 0.04 sec. If the input rock motion kappa was held fixed at 0.04 sec, then for soil sites, the additional damping in the soil profile will lead to a larger kappa for the surface soil ground motions. Since the observed data does not show a larger kappa on California soil sites than on California rock sites, the kappa for the input rock motion (e.g., the kappa used in the point-source model) was reduced so that the total kappa for a 1000 ft profile would remain at 0.04 sec, consistent with observations. An illustration of this is shown in Figure 2.1.

For hard-rock sites, the kappa for surface recordings is lower than for soil sites, so this approach of maintaining the total kappa of 0.04 sec breaks down for hard-rock sites. Two sets of hard-rock site response calculations were computed: one with a kappa of 0.04 sec and one with a reduced kappa of 0.006 sec. The lower kappa value is consistent with the kappa for hard-rock sites in the eastern U.S.

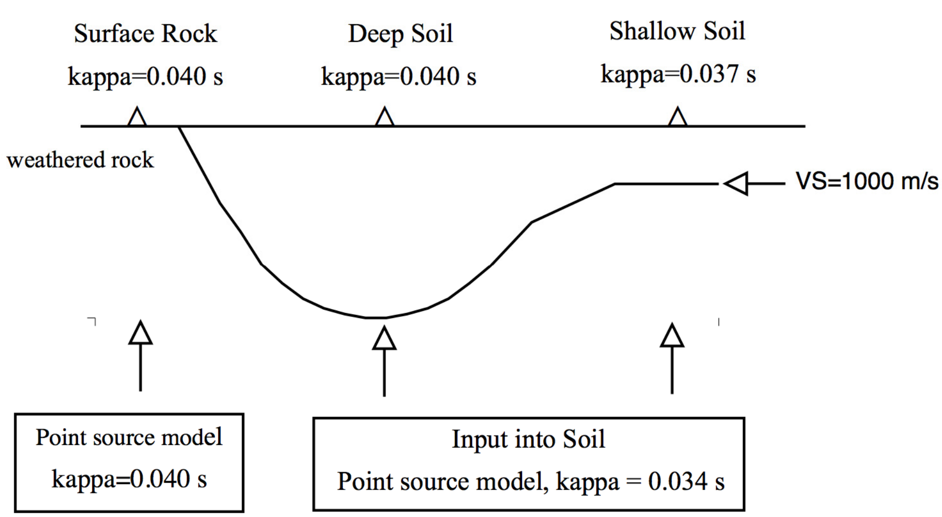

Figure 2.1 Example of kappa for the point source model used for input rock motion.

2.2 G/GMAX AND HYSTERETIC DAMPING MODELS

Four sets of G/G_{max} and hysteretic damping models are used: two for cohesionless soils (EPRI and Peninsular Range) and two for cohesive soils (Imperial Valley and Bay Mud). These four models are described below.

2.2.1 Cohesionless Soil Models

The EPRI model was developed following the 1989 Loma Prieta earthquake using strong-motion data from three earthquakes: the 1979 Coyote Lake earthquake, the 1984 Morgan Hill earthquake, and the 1989 Loma Prieta earthquake. This model was validated by Silva et al. (1997) using strong motion recordings from 48 San Francisco Bay area cohesionless soil sites. The G/G_{max} and the hysteretic damping curves for the EPRI (1993) model are shown in Figure 2.2. The EPRI G/G_{max} and damping curves were developed for generic applications to cohesionless soils in the general range of gravelly sands to low plasticity silts or sandy clays.

Following the 1994 Northridge earthquake, the EPRI soil model was tested against the strong motion data from about 80 sites in the Los Angeles region that recorded the Northridge earthquake. This test showed that the EPRI model had greater nonlinearity than was observed in the Northridge data. As a result, a revised set of G/G_{max} and hysteretic damping curves was developed for cohesionless soils in the Peninsular Range based on the Northridge data. The G/G_{max} and the hysteretic damping curves for the Peninsular Range (PR) model are shown in Figure 2.3.

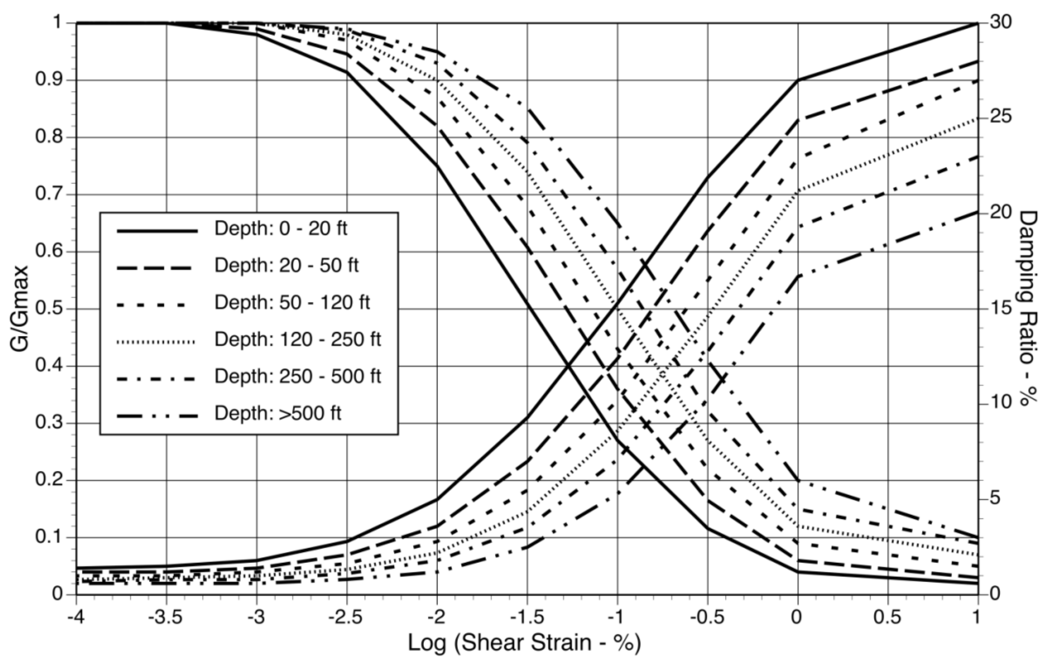

Figure 2.2 Modulus and damping curves for the EPRI soil model.

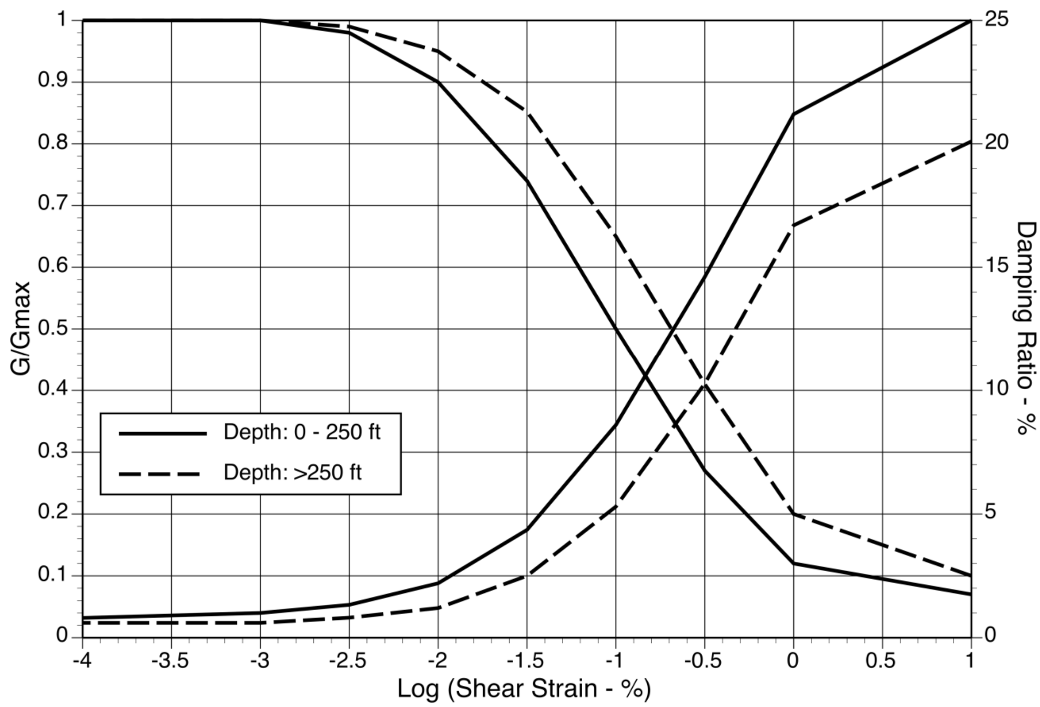

Figure 2.3 Modulus and damping curves for the PR soil model.

2.2.2 Cohesive Soil Models

For the Young Bay Muds and Old Bay Clay, the Vucetic and Dobry (1991) cohesive soil curves for a PI of 30% are used. The 30% value represents an average value for these cohesive soils. The G/Gmax and the hysteretic damping curves for the Young Bay Muds and Old Bay Clay (BM) are shown in Figure 2.4.

To cover the potential range in nonlinearity for cohesive soils, a second model based on the Imperial Valley data is used. Based on laboratory dynamic testing (Turner and Stokoe, 1982) and recordings from the 1979 Imperial Valley earthquake (Silva et al., 1997), these soils appear to behave much more linearly than the soft soils along the margins of the San Francisco Bay area and Mendocino, California (Silva et al., 1997). Although the Imperial Valley soils contain clays, typical PI values are less than 30% and the Vucetic and Dobry G/G_{max} and hysteretic damping curves appear to have too much nonlinearity to be consistent with the large peak acceleration values (about 0.5g) recorded during the 1979 Imperial Valley earthquake. As a result, a suite of G/G_{max} and hysteretic damping curves was developed for these soils based on the results of the Turner and Stoke (1982) laboratory dynamic testing and modeling of the ground motions (Silva et al., 1997). The G/G_{max} and the hysteretic damping curves for the Imperial Valley (IV) are shown in Figure 2.5. The IV curves remain nearly linear at high strain. Since neither laboratory testing nor the recorded ground motions resulted in strains exceeding about 0.1%, the curves are unconstrained at larger strain values. For high strain levels, the curves were linearly extrapolated.

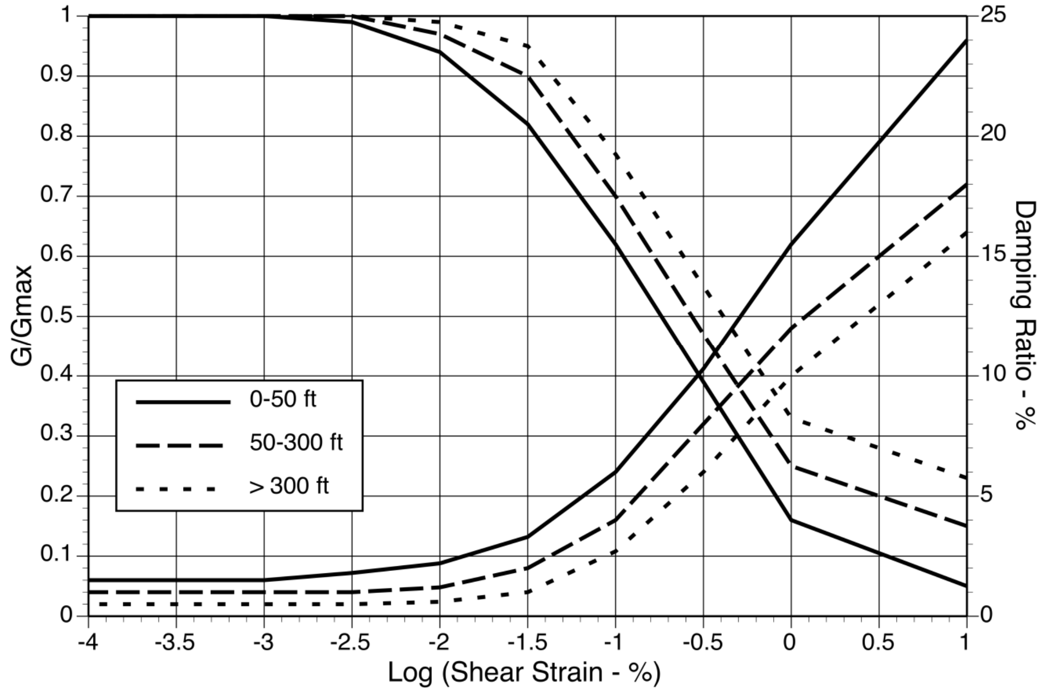

Figure 2.4 Modulus and damping curves for the IV soil model.

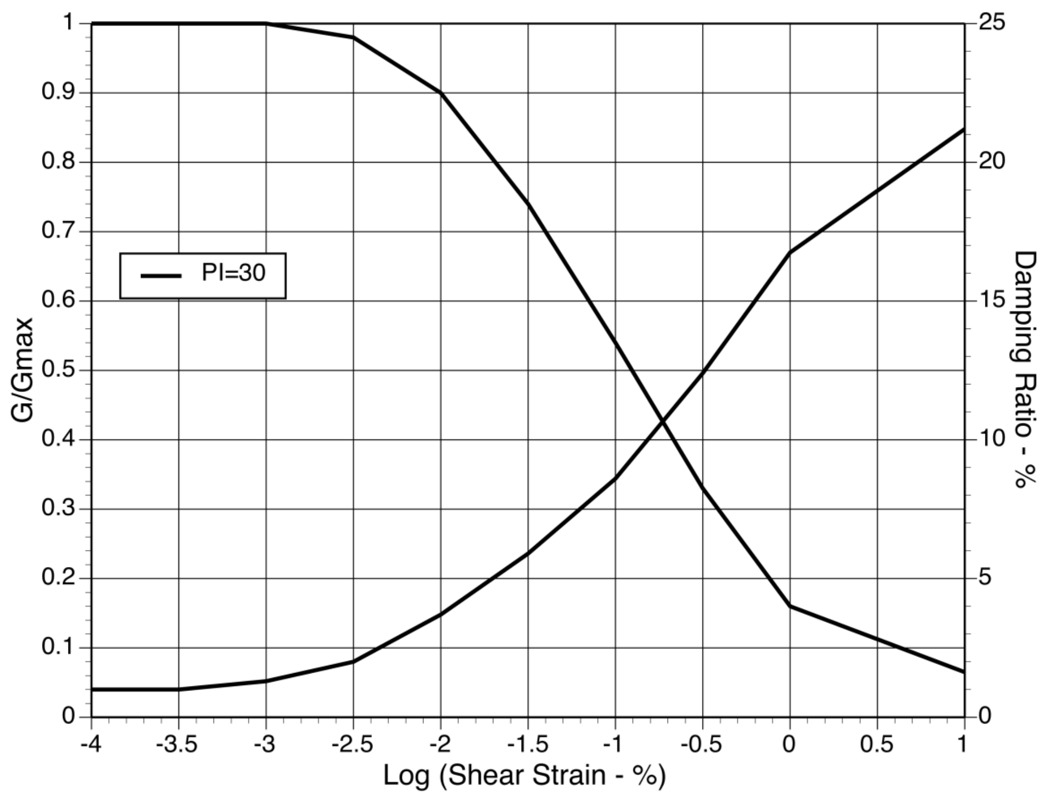

Figure 2.5 Modulus and damping curves for the BM soil model.

2.3 SHEAR-WAVE VELOCITY PROFILES

The simulations were conducted for a range of soil profiles parameterized by the V_{S30} and the depth to V_S=1000 m/sec. The soil profiles are summarized in Table 2.1 and are plotted in Figure 2.6. The four models of the nonlinear material properties described in Section 2.2 were used for the soil profiles as indicated in Table 2.1. In all, 53 combinations of V_{S30}, soil depth, and nonlinear properties were evaluated. The 53 cases are listed in Table 2.2.

For each case listed in Table 2.2, the site response was conducted for three magnitudes: M5.0, M6.0, M7.0 and 11 different PGA values of the outcrop rock motion: 0.001g, 0.05g, 0.1g, 0.2g, 0.3g, 0.4g, 0.5g, 0.75g, 1.0g, 1.25g, 1.5g. For each run, the amplification with respect to V_{S30}=1170 m/sec was computed.

As noted in Section 2.1.3, the kappa for the input rock motion was adjusted to maintain a constant total kappa of 0.04 sec for deep soil profiles. The kappa values used for the input rock motion in each case are listed in Table 2.2. For hard-rock sites, two values of the total kappa were used: 0.04 sec and 0.006 sec. The lower total kappa reflects the observed reduction in total kappa for hard-rock sites.

Table 2.1 Summary of site response cases.

V_{S30} (m/sec)	Soil Depth (ft)	Nonlinear Material Properties	Input Rock Kappa (sec)
160	25, 50, 120, 250, 500, 1000, 2000, 3000, 30-1000	BM	0.030
190	25, 50, 120, 250, 500, 1000, 2000, 3000, 30-1000	IV	0.032
190	30-1000	PR	0.032
270	25, 50, 120, 250, 500, 1000, 2000, 3000, 30-1000	PR	0.035
270	30-1000	EPRI	0.034
400	25, 50,120, 250, 500, 1000, 30-1000	PR	0.037
400	30-1000	EPRI	0.036
560	25, 50,120, 250, 500, 30-1000	PR	0.037
560	30-1000	EPRI	0.036
760	25, 50, 260	PR	0.038
760	260	EPRI	0.038
900	25, 260	PR	0.038
1170	0	Linear	0.040
3150	0	Linear	0.040
2830	0	Linear	0.006

Table 2.2 List of site response cases.

Case	Depth to V_S=1.0 km/sec (ft)	V_{S30} (m/sec)	Soil Model	Input Rock Kappa(sec)
1	25	160	BM	0.030
2	50	160	BM	0.030
3	120	160	BM	0.030
4	250	160	BM	0.030
5	500	160	BM	0.030
6	1000	160	BM	0.030
7	2000	160	BM	0.030
8	3000	160	BM	0.030
9	30-1000	160	BM	0.030
10	25	190	IV	0.032
11	50	190	IV	0.032
12	120	190	IV	0.032
13	250	190	IV	0.032
14	500	190	IV	0.032
15	1000	190	IV	0.032
16	2000	190	IV	0.032
17	3000	190	IV	0.032
18	30-1000	190	IV	0.032
19	30-1000	190	PR	0.032
20	25	270	PR	0.035
21	50	270	PR	0.035
22	120	270	PR	0.035
23	250	270	PR	0.035
24	500	270	PR	0.035
25	1000	270	PR	0.035
26	2000	270	PR	0.035
27	3000	270	PR	0.035
28	30-1000	270	PR	0.035
29	30-1000	270	EPRI	0.034
30	25	400	PR	0.037
31	50	400	PR	0.037
32	120	400	PR	0.037
33	250	400	PR	0.037
34	500	400	PR	0.037
35	1000	400	PR	0.037
36	30-1000	400	PR	0.037
37	30-1000	400	EPRI	0.036
38	25	560	PR	0.037
39	50	560	PR	0.037
40	120	560	PR	0.037
41	250	560	PR	0.037
42	500	560	PR	0.037
43	30-1000	560	PR	0.037
44	30-1000	560	EPRI	0.036
45	25	760	PR	0.038
46	50	760	PR	0.038
47	260	760	PR	0.038
48	260	760	EPRI	0.038
49	25	900	PR	0.038
50	260	900	PR	0.038
51	20	1170	Linear	0.04
52	0	2830	Linear	0.006
53	0	3150	Linear	0.04

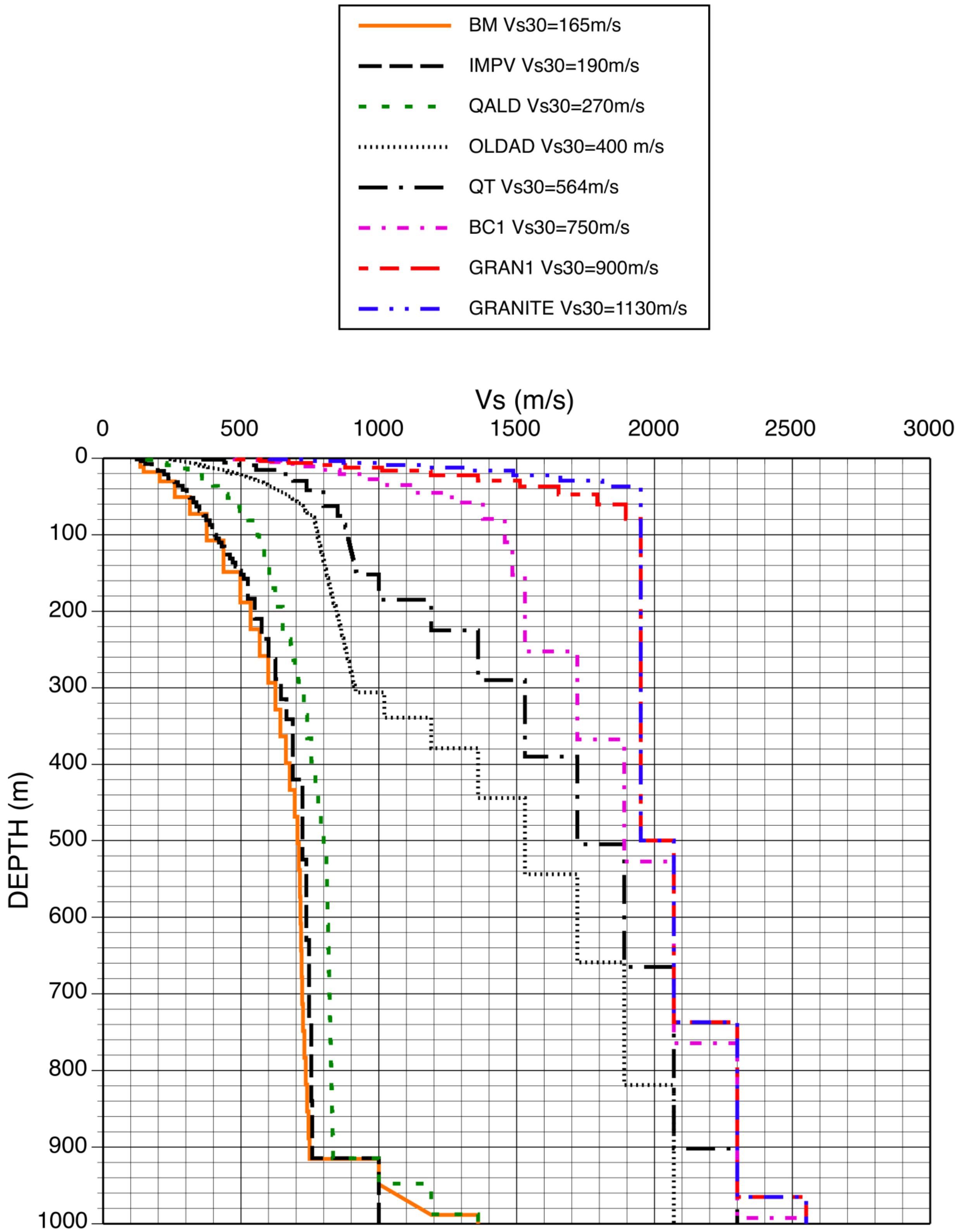

Figure 2.6 **Shear-wave velocity profiles for the eight V_{S30} cases.**

2.4 SOIL PROFILE RANDOMIZATION

Both the shear-wave velocities and the layer thicknesses are varied using correlation models based on an analysis of 557 measured shear-wave velocity profiles (Silva et al, 1997). The algorithm starts with a given base-case profile and generates a suite of random profiles about the base-case profile accounting for the correlations. The details of the procedure are given in Silva et al. (1997). The correlation models are summarized below.

2.4.1 Velocity Profile Randomization

The development of the randomization of the shear-wave velocity profile is described in Appendix C of Silva et al. (1996). The model is summarized here. For each base profile, the depth to the V_S=1.0 km/sec layer is randomized within plus and minus 50% of the depth for the base profile. Within the soil profile, the layer thicknesses are assumed to follow a Poisson process with a depth-dependent rate. The depth-dependent rate is modeled by

$$\lambda(h) = 1.98\left[h + 10.86\right]^{-0.89} \tag{2.7}$$

where λ is the rate of layer boundaries (m^{-1}) and h denotes the layer depth in m.

The layer velocities are developed by defining the normalized quantity, Z_i, given by

$$Z_i = \frac{\ln(V_i) - \ln\left(V_{median}(h_i)\right)}{\sigma_{\ln V}} \tag{2.8}$$

The lognormal distribution of the velocities and the correlation among layers is modeled by a first-order auto-regressive model:

$$Z_1 = \varepsilon_1$$
$$Z_i = \rho(h,t)\, Z_i - 1 + \sqrt{1 - \rho(h,t)^2}\; \varepsilon_i \quad for\, i > 1 \tag{2.9}$$

where ρ is the serial auto-correlation coefficient of Z, and ε_i are independent normal variates with zero mean and unit variance.

$$\rho(h,t) = \left(1 - \rho_d(h)\right)\rho_t(t) + \rho_d(h) \tag{2.10}$$

where ρ_d is the depth-dependent correlation and ρ_t is the thickness-dependent correlation and are given by

$$\rho_d(h) = \begin{cases} \rho_{200}\left(\dfrac{h + h_0}{200 + h_0}\right)^b & for\, h \le 200 \\ \rho_{200} & for\, h > 200 \end{cases} \tag{2.11}$$

and

$$\rho_t(t) = \rho_0 \exp\left(\frac{-t}{\Delta}\right) \tag{2.12}$$

The model coefficients, $\sigma_{\ln V}$, ρ_{200}, h_0, b, ρ_0, and Δ are listed in Table 2.3.

Table 2.3 Coefficients for velocity profile randomization model.

Parameter	VS30 (m/sec) Range			
	> 750 m/sec	**360 to 750**	**180 to 360**	**<180**
$\sigma_{\ln V}$	0.36	0.27	0.31	0.37
ρ_0	0.95	0.97	0.99	0.00
Δ	3.4	3.8	3.9	5.0
ρ_{200}	0.42	1.00	0.98	0.50
h_0	0.0	0.0	0.0	0.0
b	0.063	0.293	0.344	0.744

2.4.2 Nonlinear Soil Property Randomization

The modulus reduction and damping curves were independently randomized about the base case values. A truncated log normal distribution was assumed with a standard deviation of 0.35 natural log units at a cyclic shear strain of $3\text{x}10^{-2}$%. The distribution was truncated at plus and minus 2 standard deviations to avoid cases that are not considered physically possible. The random curves are generated by sampling the log normal distribution, computing the scale factor on the modulus or damping at $3\text{x}10^{-2}$% shear strain, and then applying this factor at all strains. The random variations are reduced at the ends of the strain range to preserve the general shape of the base case curves (Silva, 1992).

3 Summary of Resulting Amplification Factors

3.1 INTRODUCTION

This section presents summary plots of the amplification factors for a subset of the 53 cases. Results of the scaling with V_{S30} and PGA_{1170} using the cases with randomized soil depths (cases 17, 18, 27, 28, 35, 36, 42, 43) are shown in Section 3.2. Results of the scaling with soil depth for the linear range (e.g., cases with the rock input motion of 0.001g) are shown in Section 3.3. The complete set of results for all cases is attached as an electronic appendix.

3.2 MAGNITUDE SCALING

The period dependence of the amplification for a soil profile with V_{s30} = 270 m/sec at the linear range (PGA_{Rock}=0.01g) is shown in Figure 3.1. The amplification for the PR and EPRI models is shown in the top and bottom panels, respectively. In each panel, the amplification from three point-source magnitudes is presented. There is very little difference in the amplification for this low shaking level at periods smaller than 2sec. The increase in amplification for the M5.0 input at periods greater than 2sec is believed to be a numerical artifact of the simulation procedure and therefore results in that range (M=5, T>2sec) are not used for regression of the parametric model.

At higher shaking levels, such as PGA_{Rock}=1.0g (see Figure 3.2), the difference in amplification for the M5.0 simulations is more significant, with a clear resonant peak at T=1 sec. It should be noted here again, that for a M5.0 point source to reach PGA_{Rock} of 1.0g, the source-to-site distance must be much shorter than for the larger point-source magnitudes, leading to such differences.

Figures 3.3 and 3.4 show a similar comparison for a profile with V_{s30}=400 m/sec with PGA_{Rock} = 0.01g and PGA_{Rock}=1.0g, respectively. The trends are similar to those shown for the softer profile but less significant. For example, for the EPRI model with PGA_{Rock}=1.0g, the increase in the peak amplification between M5.0 and M6.0 is about 30% for the V_{s30}=270 m/sec profile but only about 6% for the V_{s30}=400 m/sec profile.

The Magnitude scaling of the amplification for a PR profile with V_{s30}=270 m/sec is shown again in the top panel of Figure 3.5, this time as a function of Rock PGA. The increased Magnitude dependence as input shaking increases is clearly seen. The Magnitude scaling on the PGV amplification, however, shown for the same profile in the bottom panel of Figure 3.5, presents different trends. For PGV amplification, the nonlinearity with respect to Rock PGA has opposite trends between the M5.0 simulations and M6.0-M7.0 simulations. This is related with different frequency contents for different point-source magnitude simulations, resulting with PGV for those simulations being associated with a different frequency range. Since nonlinearity is mostly expected to occur from larger magnitude simulations, the regression for the nonlinear model at PGV will be based on M6.0 and M7.0 simulation results only.

For purposes of brevity, all plots in the following sections will present simulation results for a M6.0 point-source only; trends for the M5.0 and M7.0 are similar other than the differences that were mentioned above.

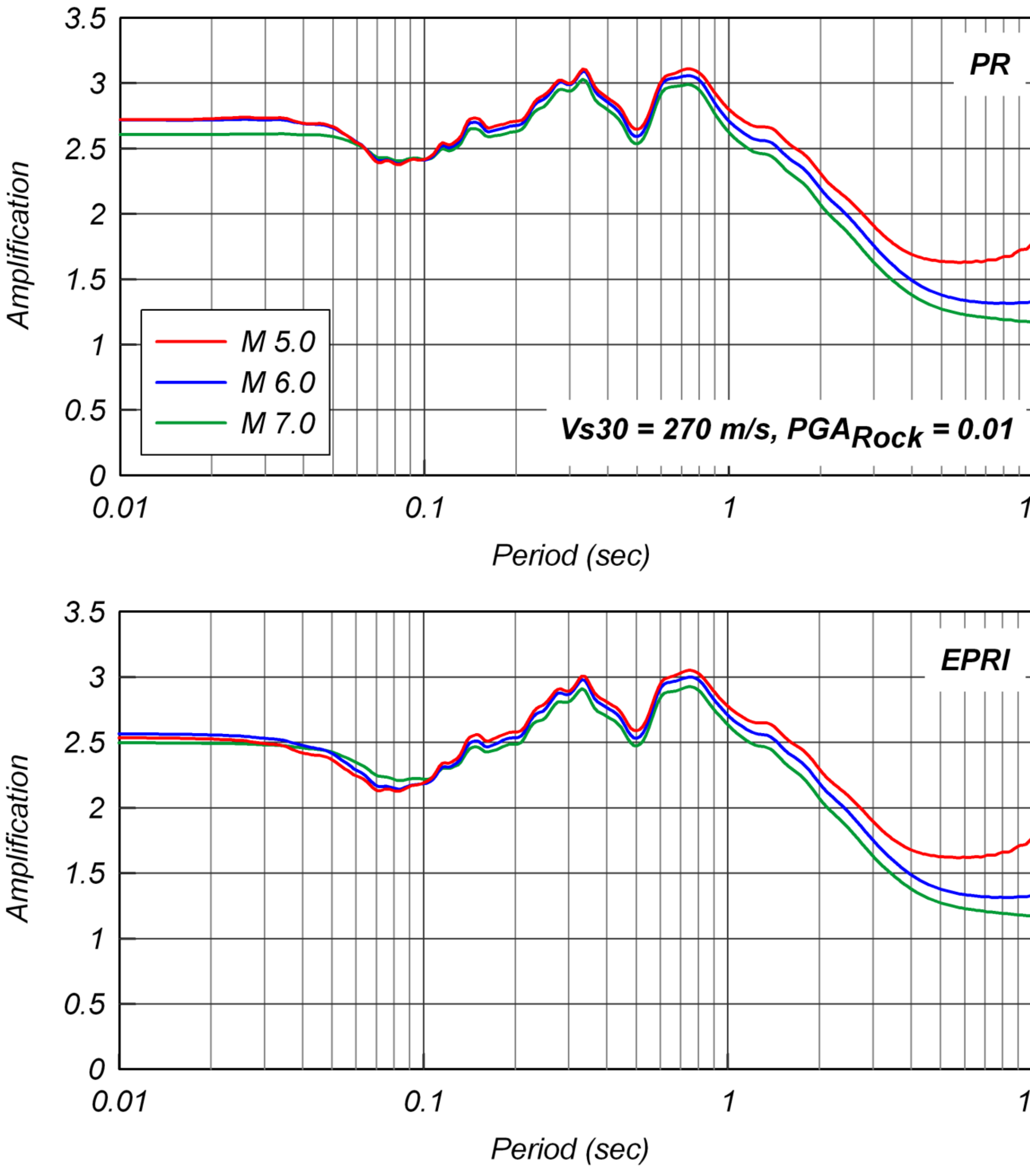

Figure 3.1 Magnitude dependence for a PR, V_{S30}=270 m/sec profile (top) and an EPRI, V_{S30}=270 m/sec profile (bottom) with PGA_{Rock}=0.01g.

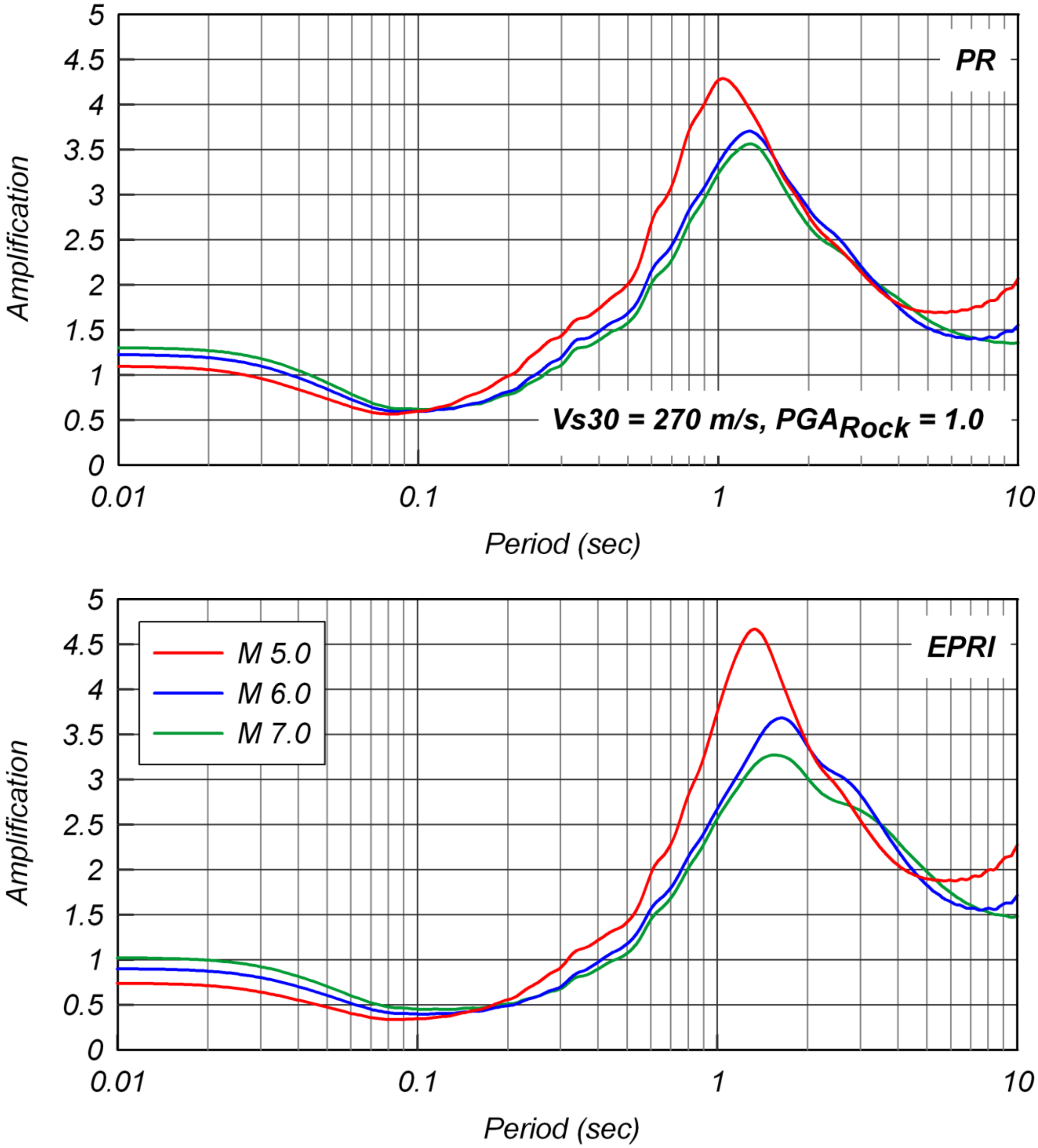

Figure 3.2. **Magnitude dependence for a PR, V_{S30}=270 m/sec profile (top) and an EPRI, V_{S30}=270 m/sec profile (bottom) with PGA_{Rock}=1.0g.**

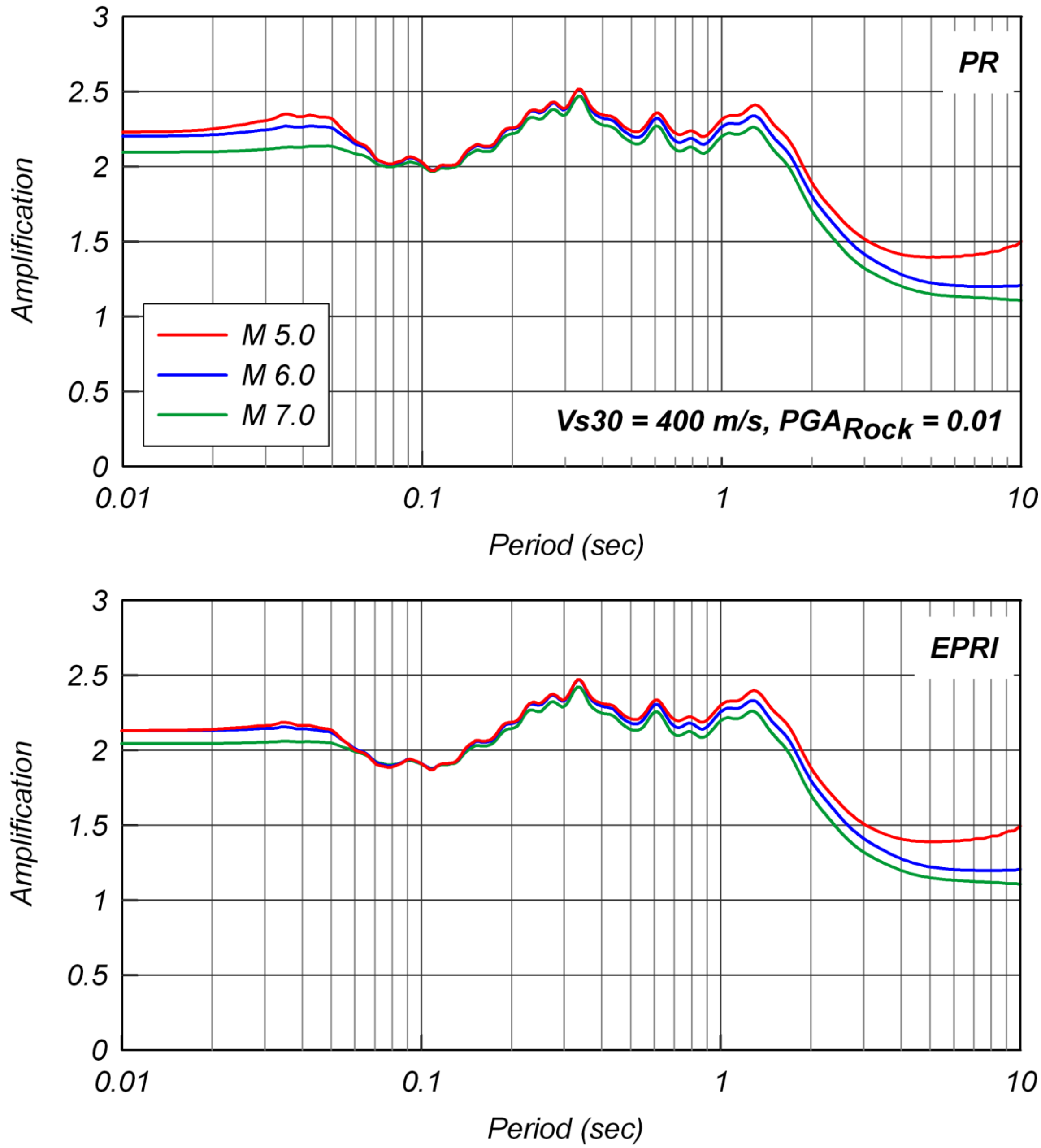

Figure 3.3 **Magnitude dependence for a PR, V_{S30}=400 m/sec profile (top) and an EPRI, V_{S30}=270 m/sec profile (bottom) with PGA_{Rock}=0.01g.**

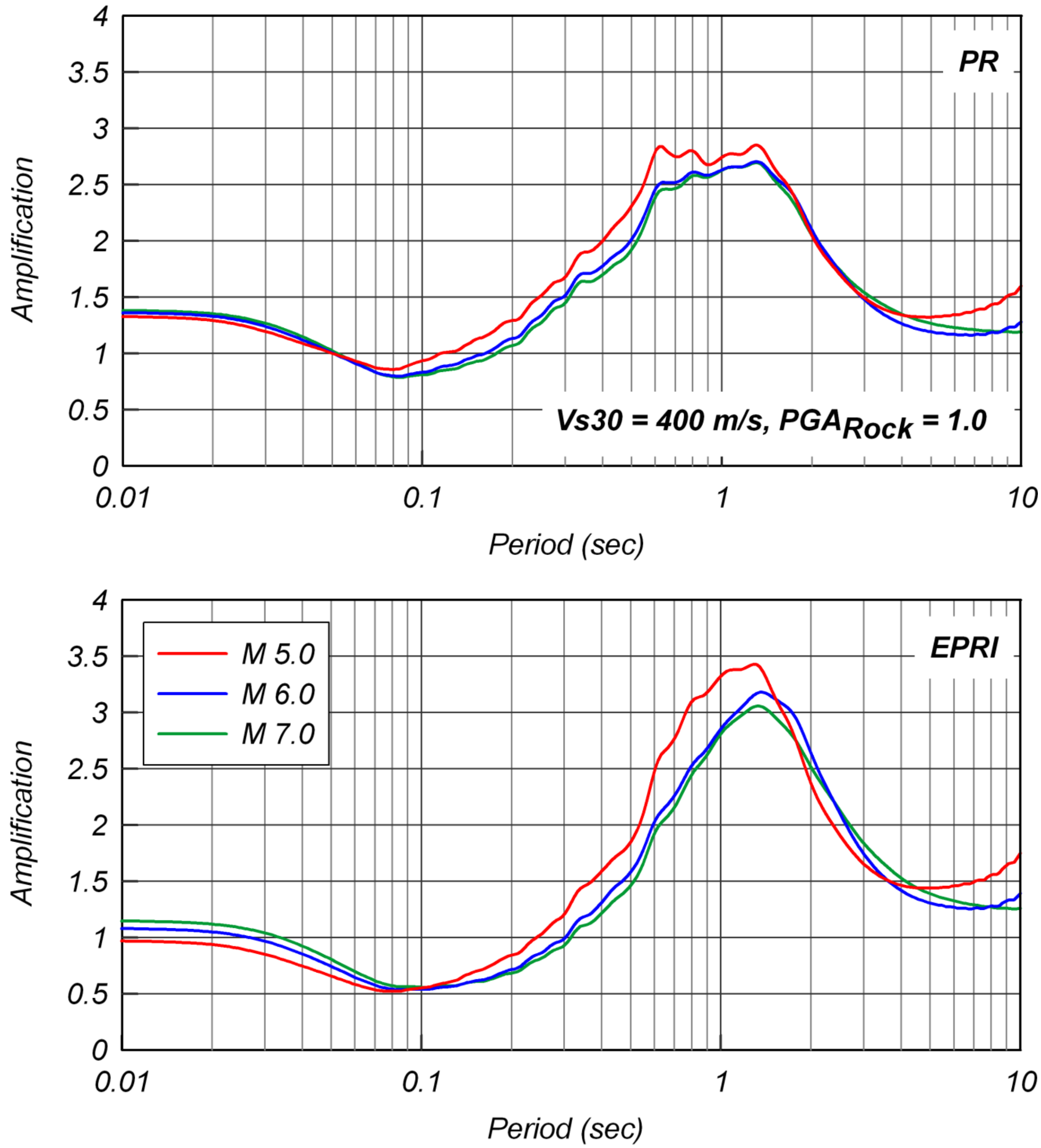

Figure 3.4 **Magnitude dependence for a PR, V_{S30}=400 m/sec profile (top) and an EPRI, V_{S30}=270 m/sec profile (bottom) with PGA_{Rock}=1.0g.**

3.3 SCALING FOR THE RANDOMIZED SOIL DEPTHS

The period dependence of the amplification in the linear range (PGA_{1170}=0.01g) for the twelve V_{S30} profiles are shown in Figures 3.5 and 3.6. Overall, there is an increase in the amplification as the V_{S30} is reduced.

The nonlinearity in the amplification for a range of V_{S30} profiles and soil models (BM, IV, PR and EPRI) is shown in Figures 3.7 to 3.12 for spectral periods of 0.01, 0.1, 0.2, 0.5, 1.0, and 2.0 sec. The strongest nonlinear effects are seen for T=0.1 sec (Figure 3.8). For spectral periods of 1.0 sec or longer and soil profiles with V_{S30} of 400 or greater, the amplification is nearly linear. However, in the softer profiles there are two competing trends. For example, for T=2sec the amplification is decreasing with increase in PGA_{Rock} for soil profiles with V_{s30} of 160-190 while it is increasing for profiles with V_{s30} of 270-400 due to the effects of period elongation at these higher levels of shaking.

The nonlinearity of the four soil models can also be compared in Figures 3.7 to 3.12. Note that each V_{s30} value is plotted with the same color on the upper and lower panels. These figures show that on average, the EPRI model is more nonlinear than the PR model. Also, the BM model is much more nonlinear than the IV model. The nonlinearity for the IV model (V_{S30}=190 m/sec) is similar to the nonlinearity for the EPRI model for V_{S30}=270 m/sec.

The standard deviation of the linear amplification PGA_{Rock}=0.01g is shown in Figures 3.13 and 3.14 for the PR soil profiles and the non-PR soil profiles (BM, IV, EPRI), respectively. For the smaller PGA_{Rock} values, the standard deviations of the amplification generally increase with period and decrease with increasing V_{S30}. For profiles with V_{S30}=270 m/sec or higher, the standard deviations of the linear amplification are generally between 0.15 and 0.3 natural log units. The PGA_{Rock} dependence of the standard deviations for all soil profiles are shown in Figures 3.15 to 3.17 for spectral periods of 0.01 sec, 0.2 sec and 1.0 sec, respectively. The increase in the standard deviation as a function of the PGA_{Rock} is due to the variability of the nonlinear properties that were randomized (G/G_{max} and damping).

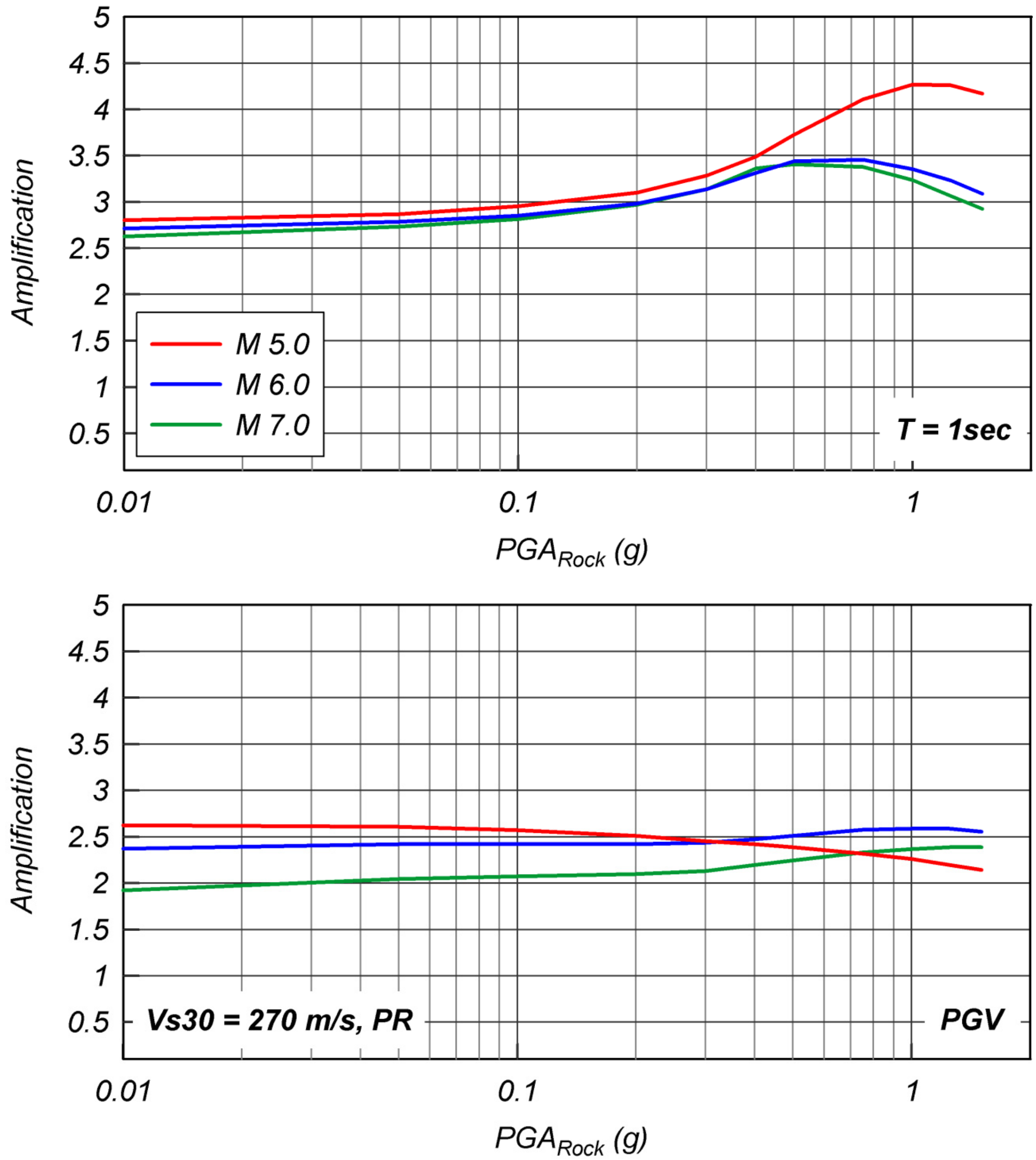

Figure 3.5. Magnitude dependence of the amplification at T=1 sec (top) and at PGV (bottom) for a PR, V_{S30}=270 m/sec profile.

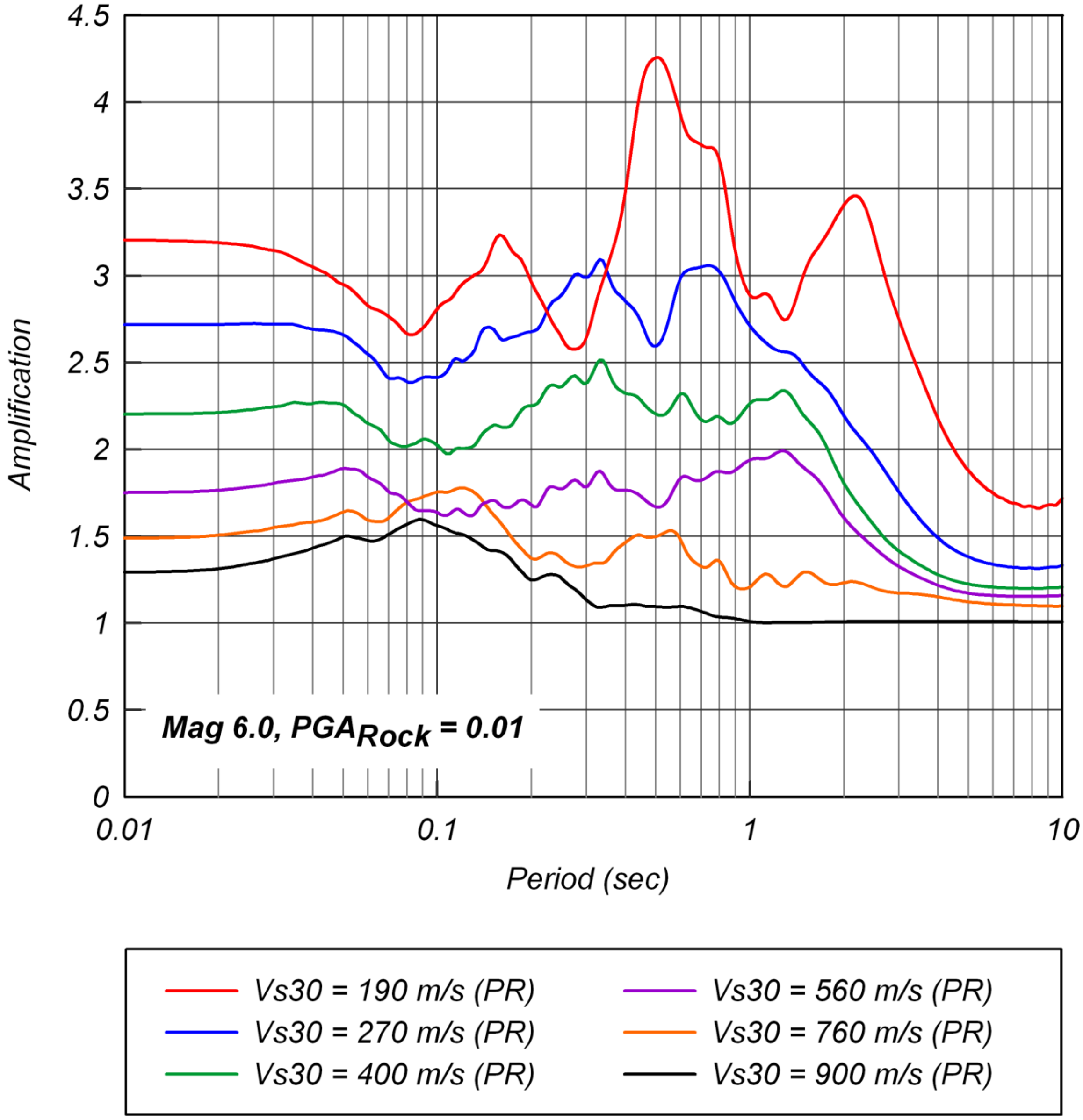

Figure 3.6. Period dependence of the linear amplification for six Vs profiles with PR and depths averaged over 30-1000 ft.

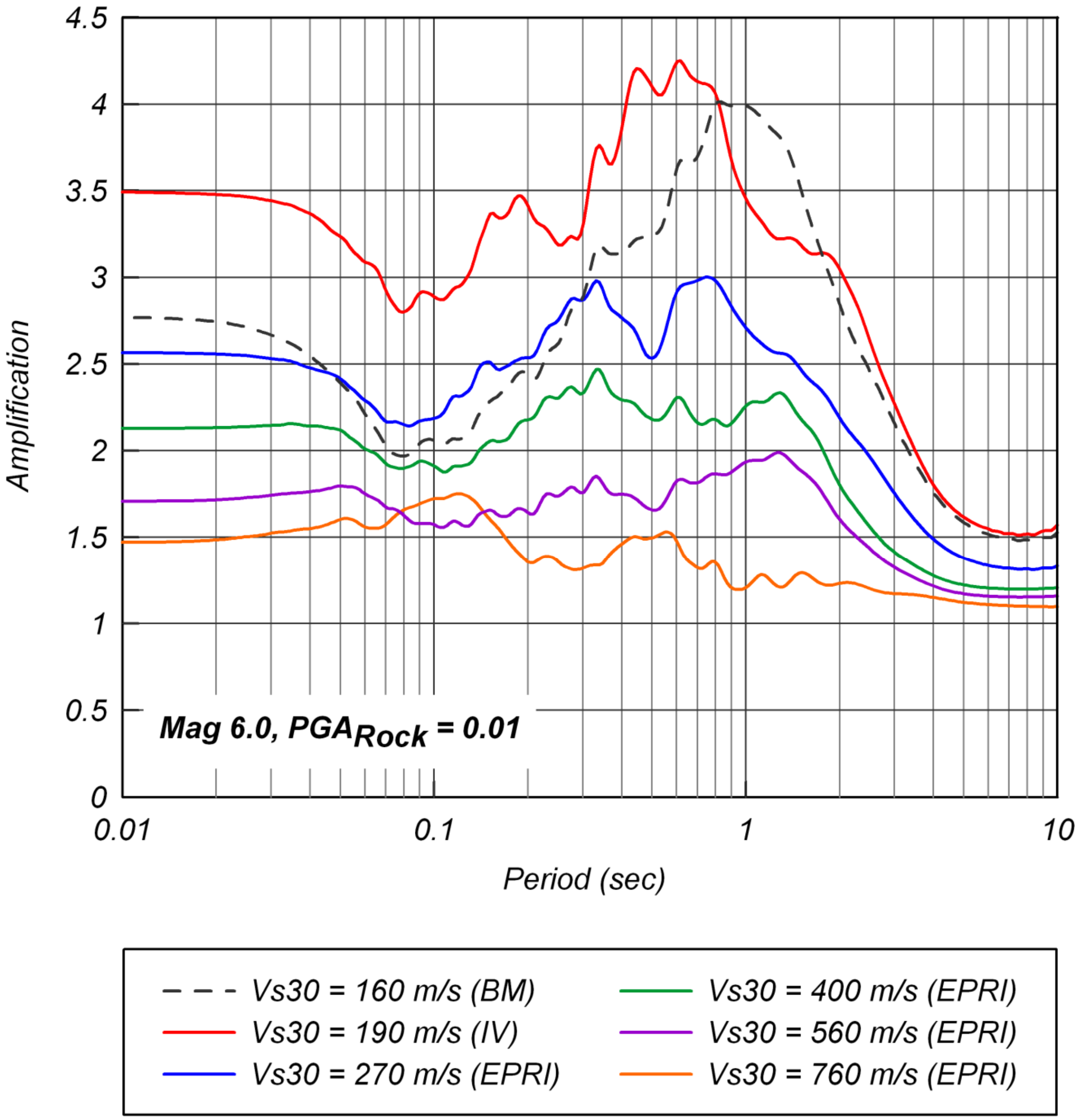

Figure 3.7 **Period dependence of the linear amplification for six Vs profiles with BM, IV, and EPRI, and soil depths averaged over 30–1000 ft.**

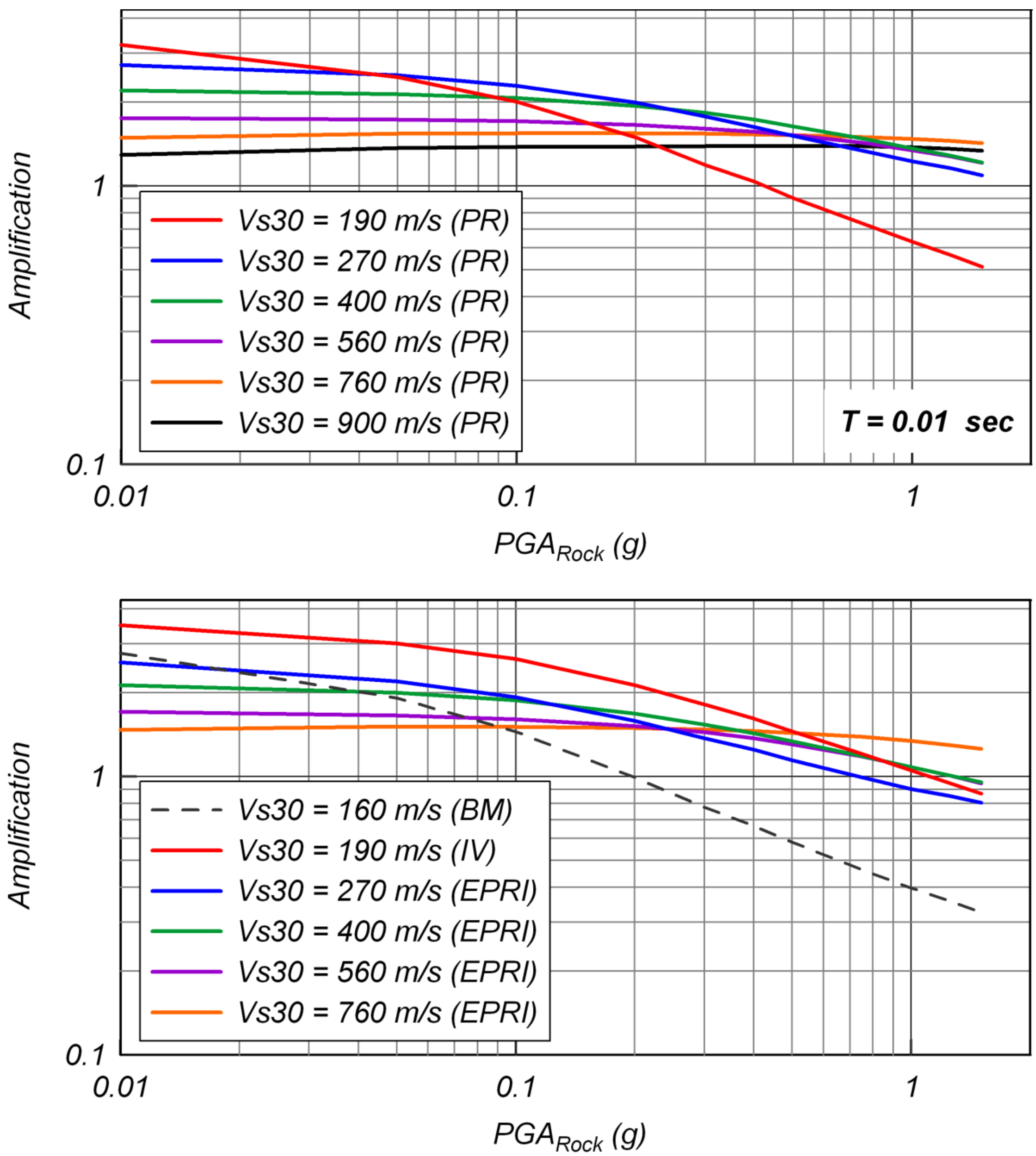

Figure 3.8 **PGA_{Rock} dependence of the soil amplification for T=0.01 sec for all soil profiles with a randomized soil depth.**

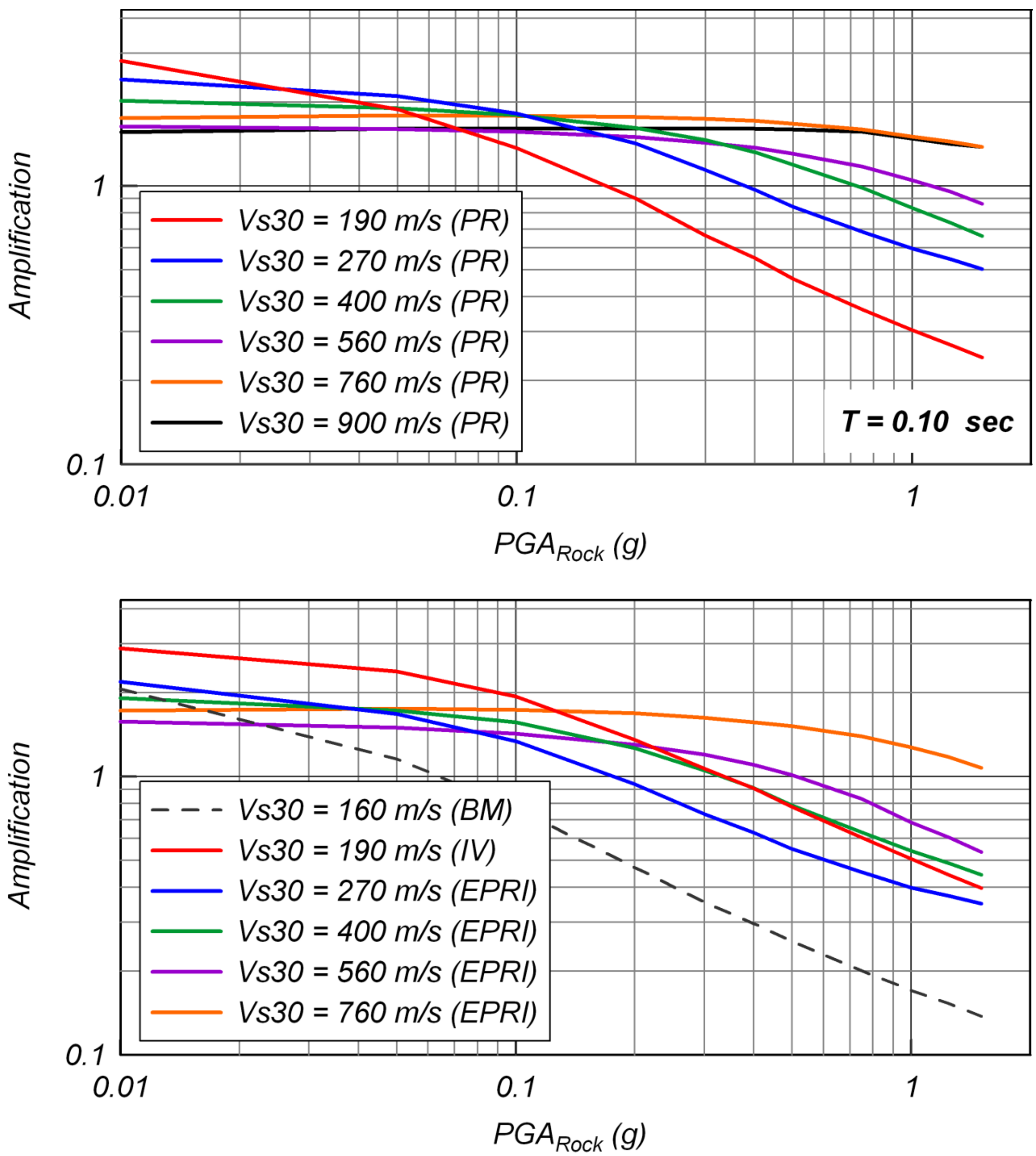

Figure 3.9 **PGA_{Rock} dependence of the soil amplification for T=0.1 sec for all soil profiles with a randomized soil depth.**

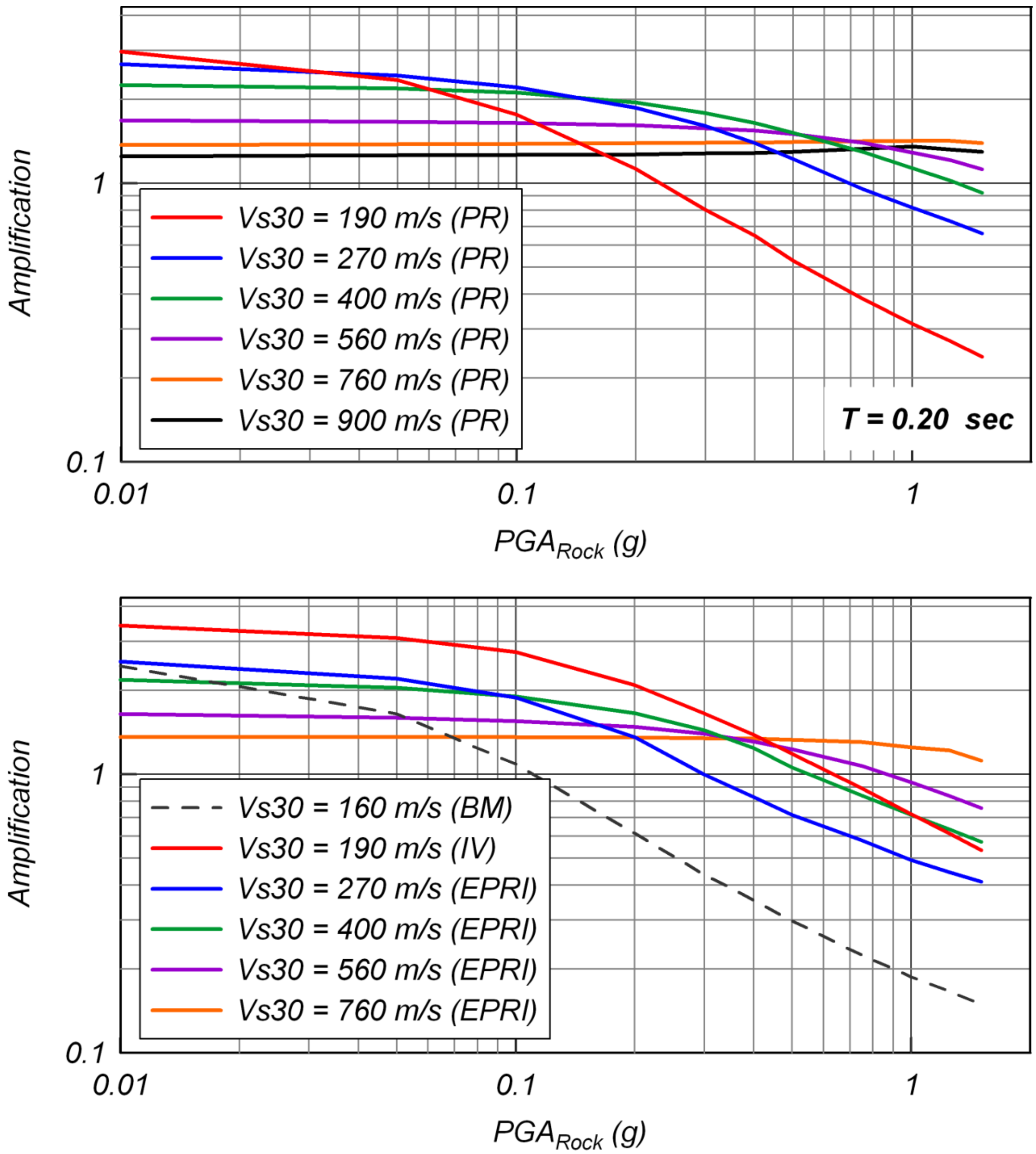

Figure 3.10 **PGA$_{Rock}$ dependence of the soil amplification for T=0.2 sec for all soil profiles with a randomized soil depth.**

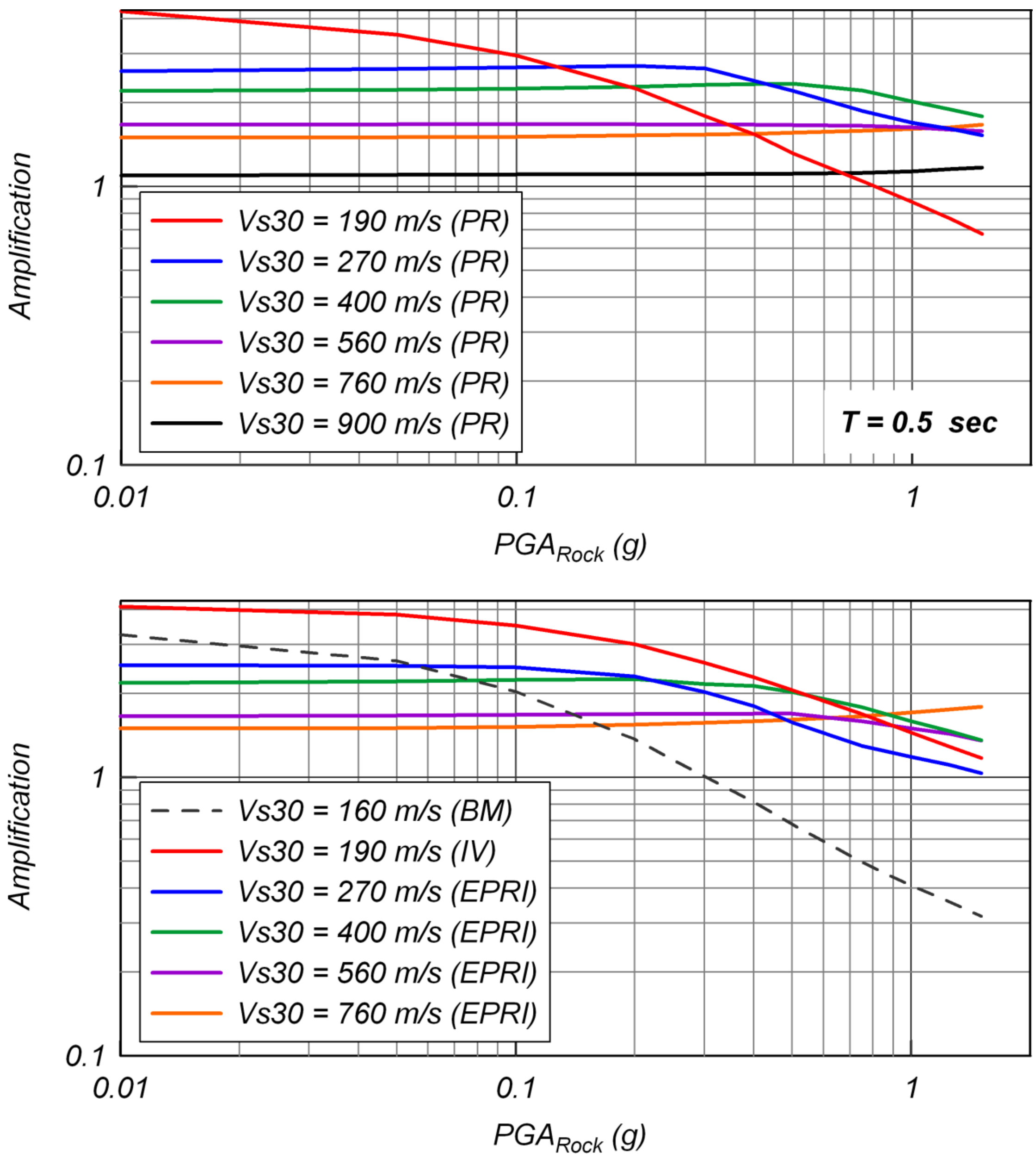

Figure 3.11 PGA$_{Rock}$ dependence of the soil amplification for T=0.5 sec for all soil profiles with a randomized soil depth.

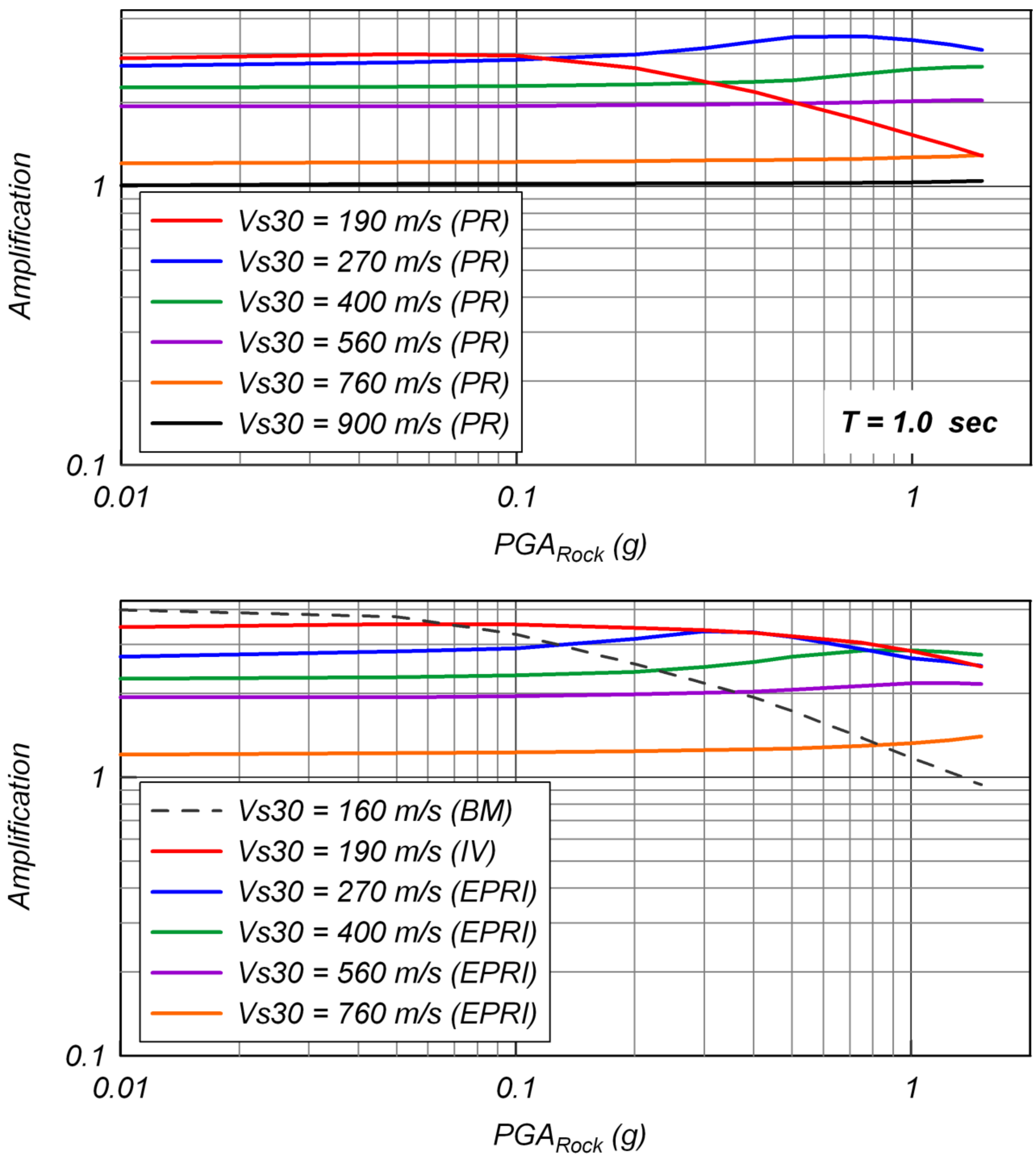

Figure 3.12 PGA_{Rock} dependence of the soil amplification for T=1.0 sec for all soil profiles with a randomized soil depth.

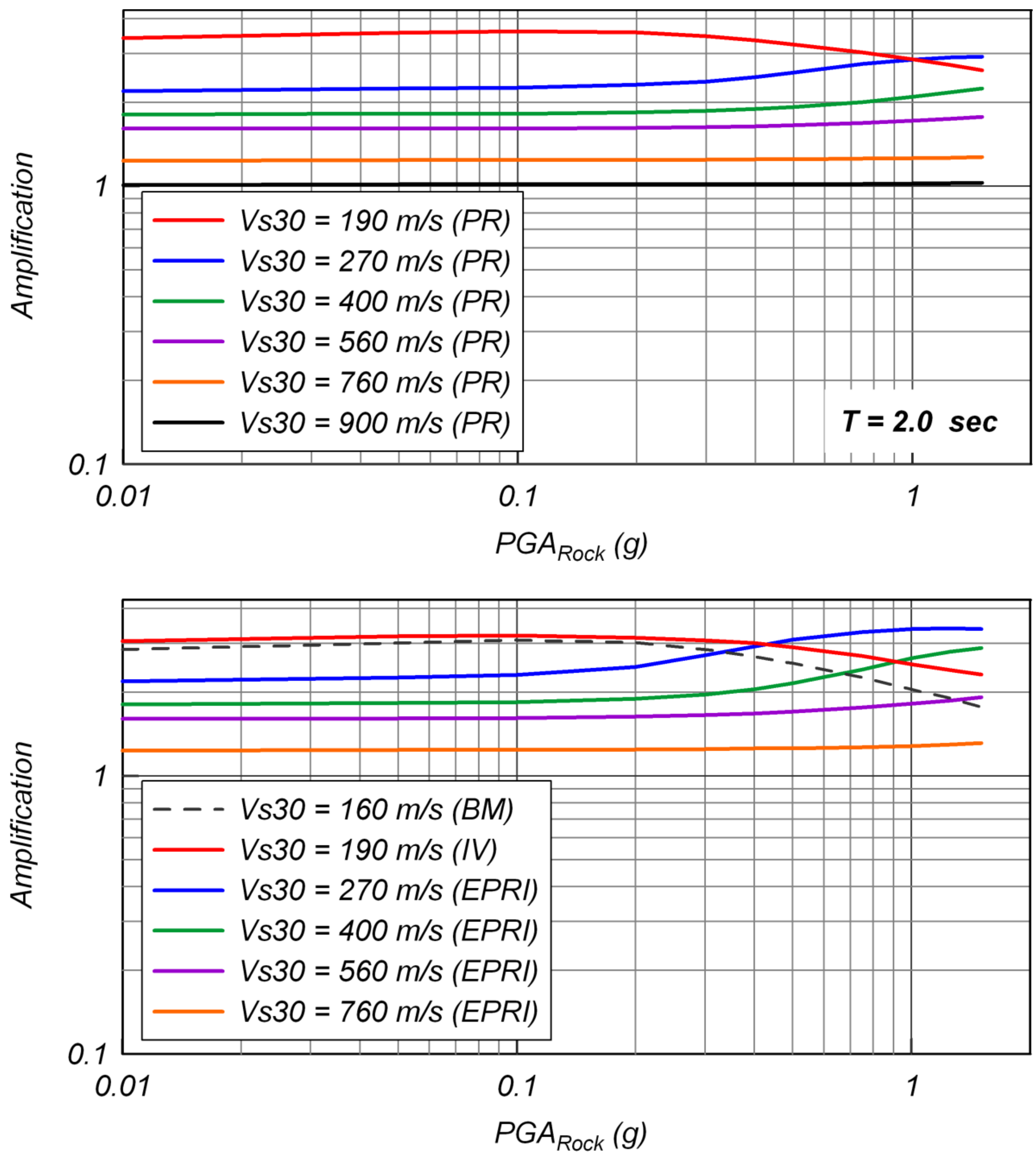

Figure 3.13. Nonlinear amplification for T=2 sec spectral acceleration for the EPRI and PR models using the soil depth averaged over 30-1000 ft.

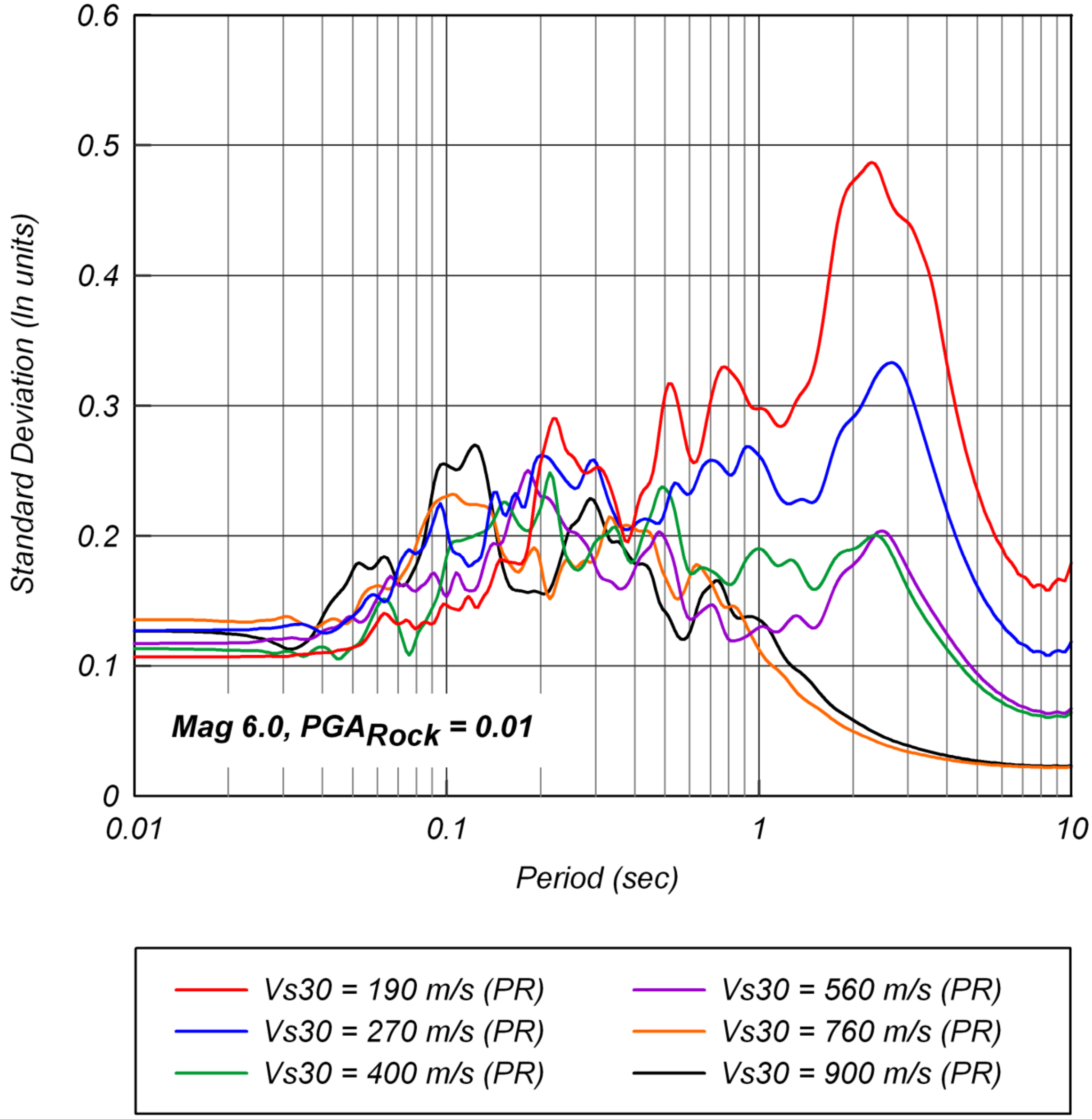

Figure 3.14 Standard deviations of the linear amplification (PGA_{Rock}=0.01g) for PR with randomized soil depth.

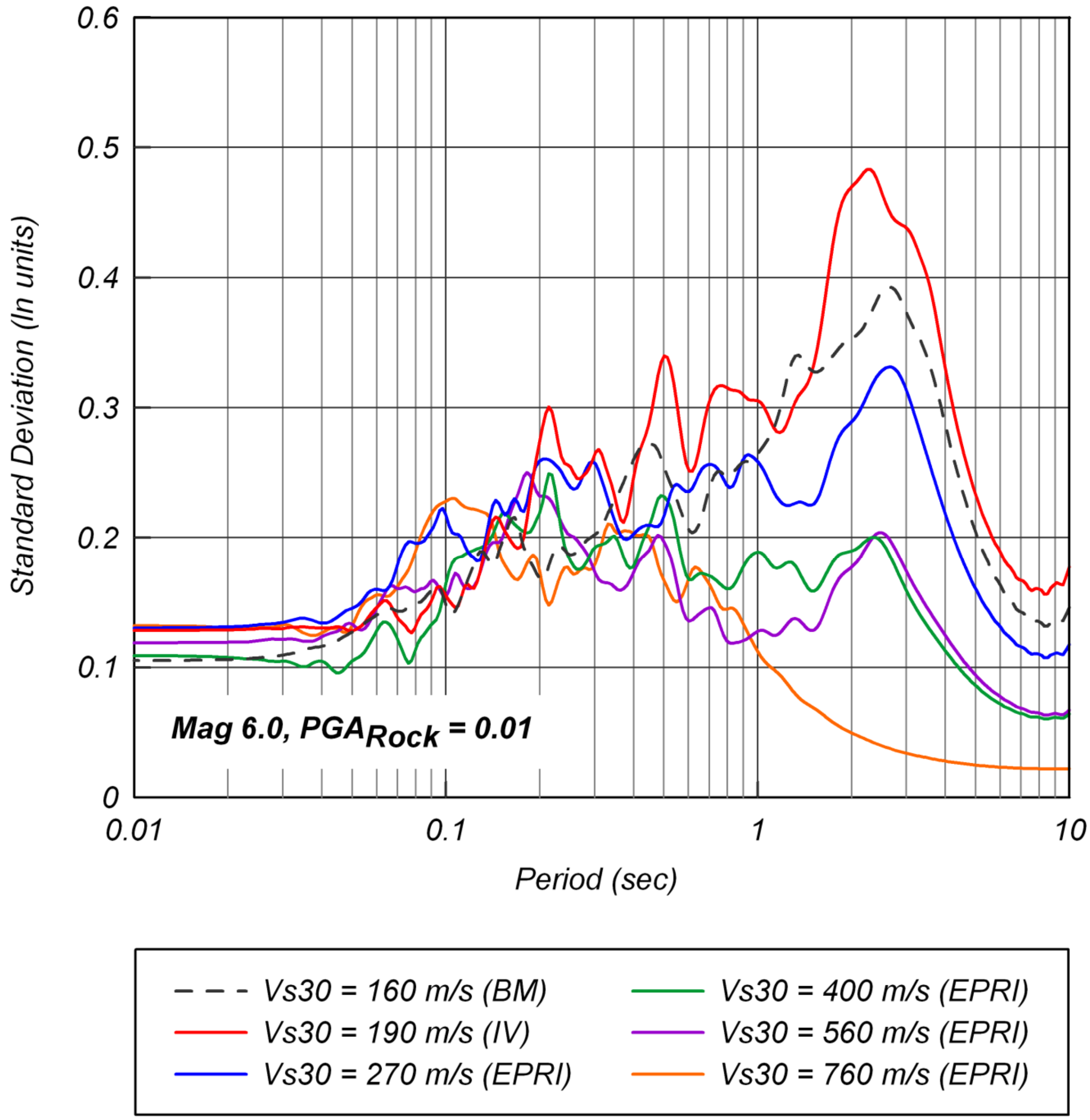

Figure 3.15 Standard deviations of the linear amplification (PGA_{Rock}=0.01g) for BM, IV, and EPRI with randomized soil depth.

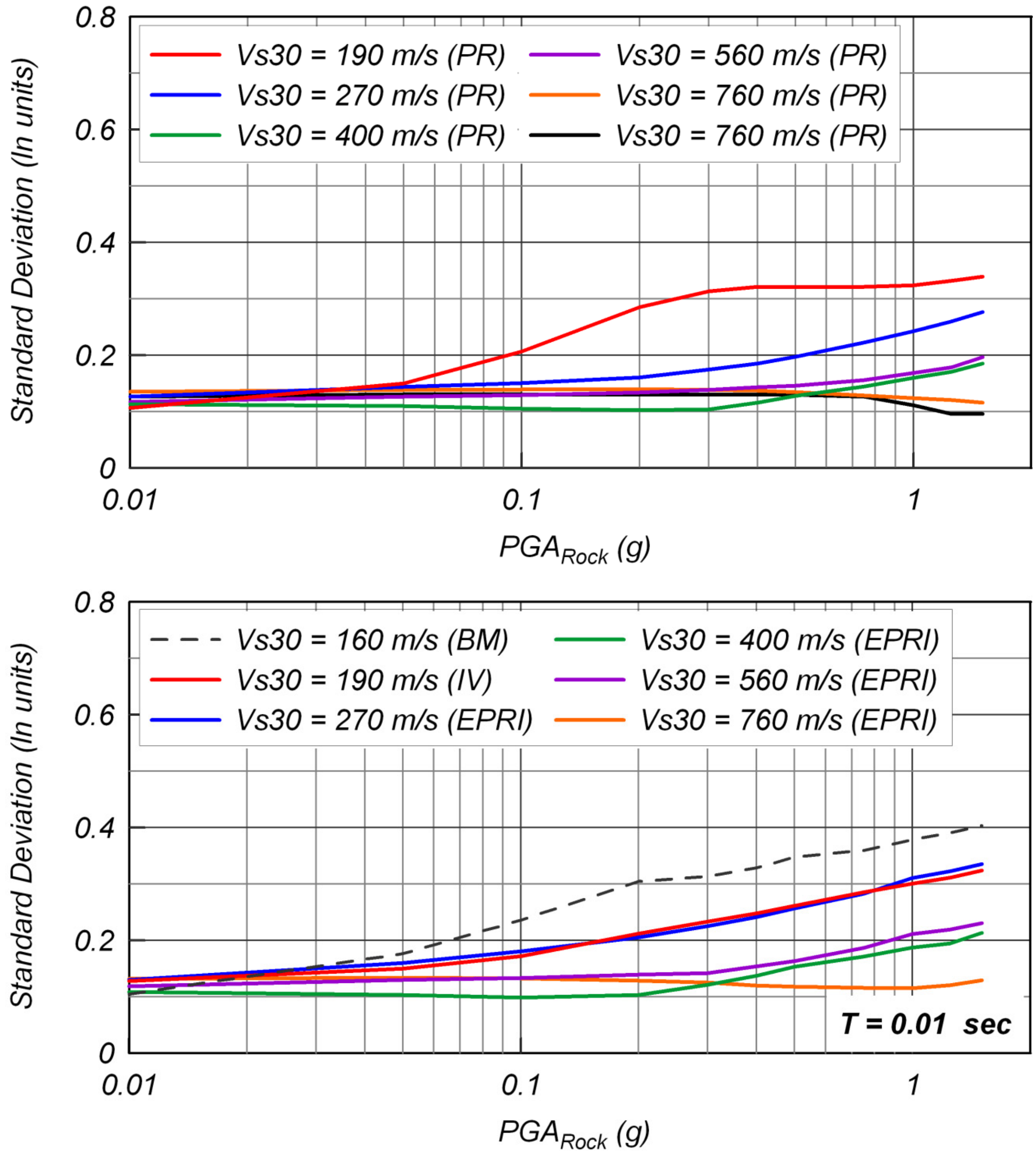

Figure 3.16 **PGA_{Rock} dependence of the standard deviations for T=0.01 sec for all soil profiles with a randomized soil depth.**

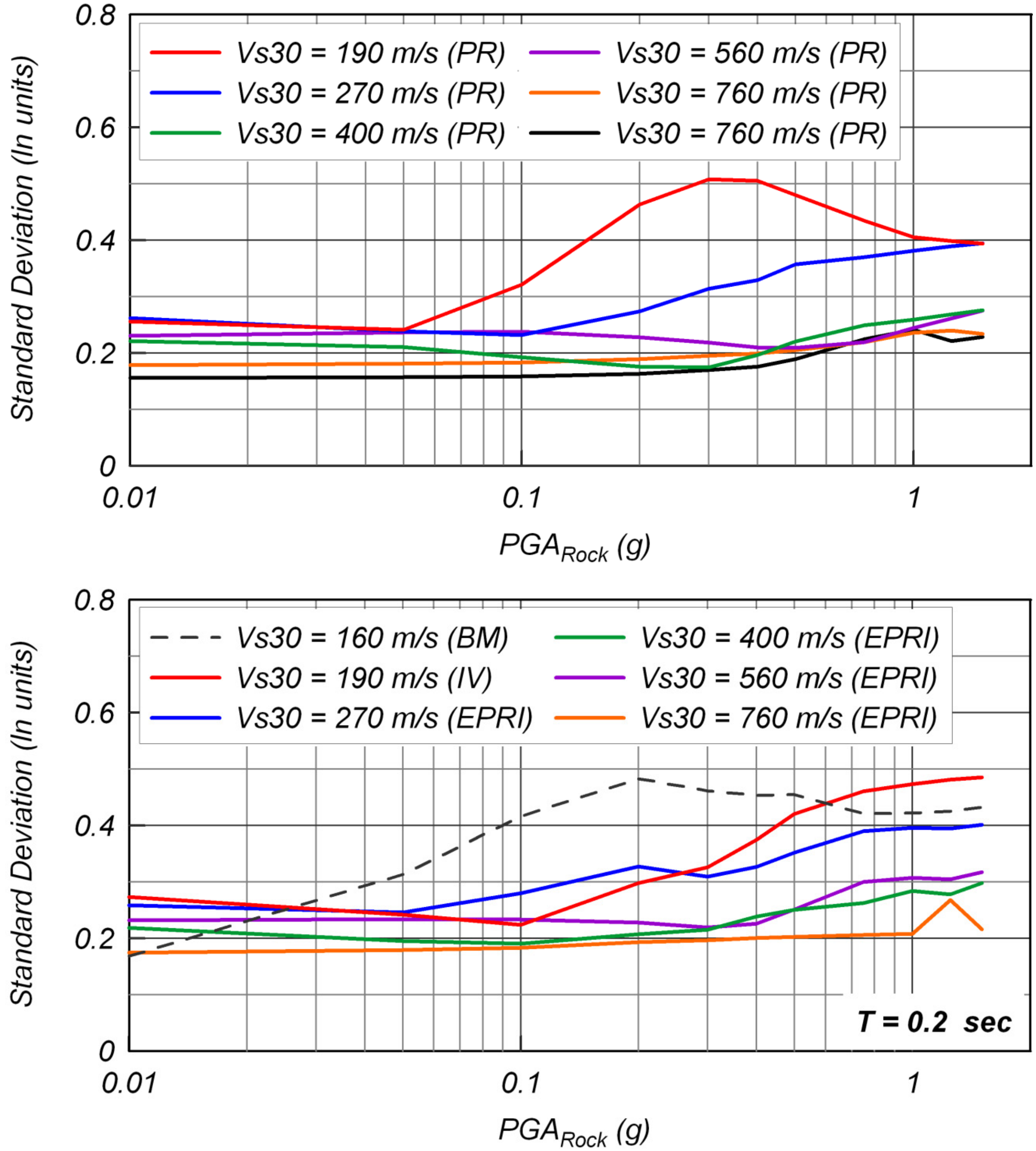

Figure 3.17 **PGA$_{Rock}$ dependence of the standard deviations for T=0.2 sec for all soil profiles with a randomized soil depth.**

3.4 SOIL DEPTH SCALING

The 1-D simulation results can also be used to estimate the effect of the soil depth on the amplification. Examples of the effect of the soil depth on the amplification are shown in Figures 3.18 to 3.20, for soil profiles with V_{S30} ranging from 160 m/sec to 760 m/sec. Similar plots show the effect of depth on the standard deviation of the linear amplification in Figures 3.21 to 3.23. The soil depth is parameterized by the depth to the layer with V_S=1.0 km/sec. These figures are for the linear site response (PGA_{Rock}=0.01g); therefore, they are independent of the nonlinear properties.

The soil depth scaling is shown in Figure 3.24 for soil profiles with V_{S30} values of 190 m/sec, 270 m/sec, 400 m/sec, and 560 m/sec. The soil depth effects are strongest for the softer soil profiles (lower V_{S30} values). For the softer profiles, there is strong scaling for soil depths from 8 to 300 m, but the scaling becomes weak for soil depths greater than 300 m, mostly due to the limitations of modeling deep soil profiles with a 1D soil column.

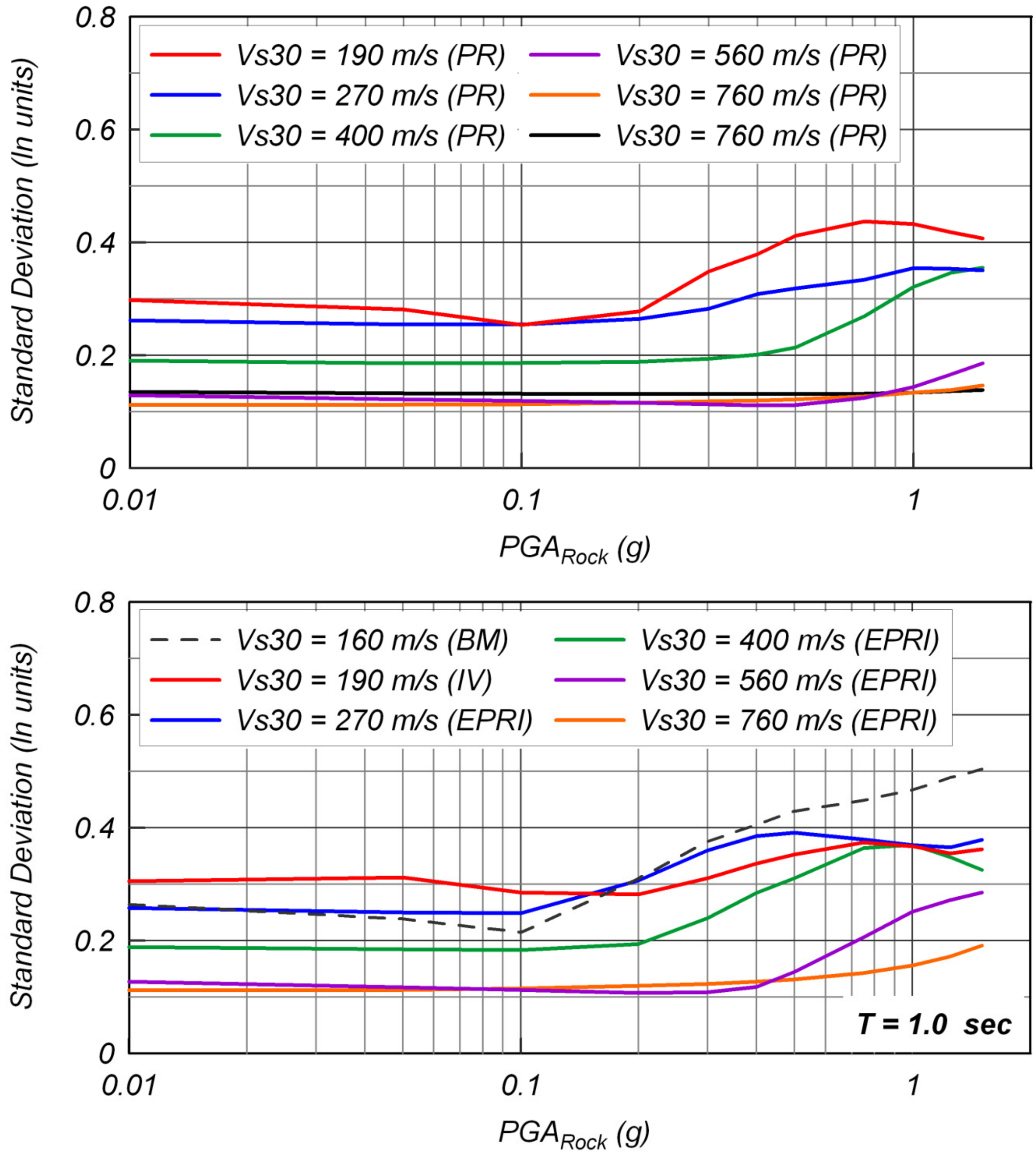

Figure 3.18 **PGA_{Rock} dependence of the standard deviations for T=1.0 sec for all soil profiles with a randomized soil depth.**

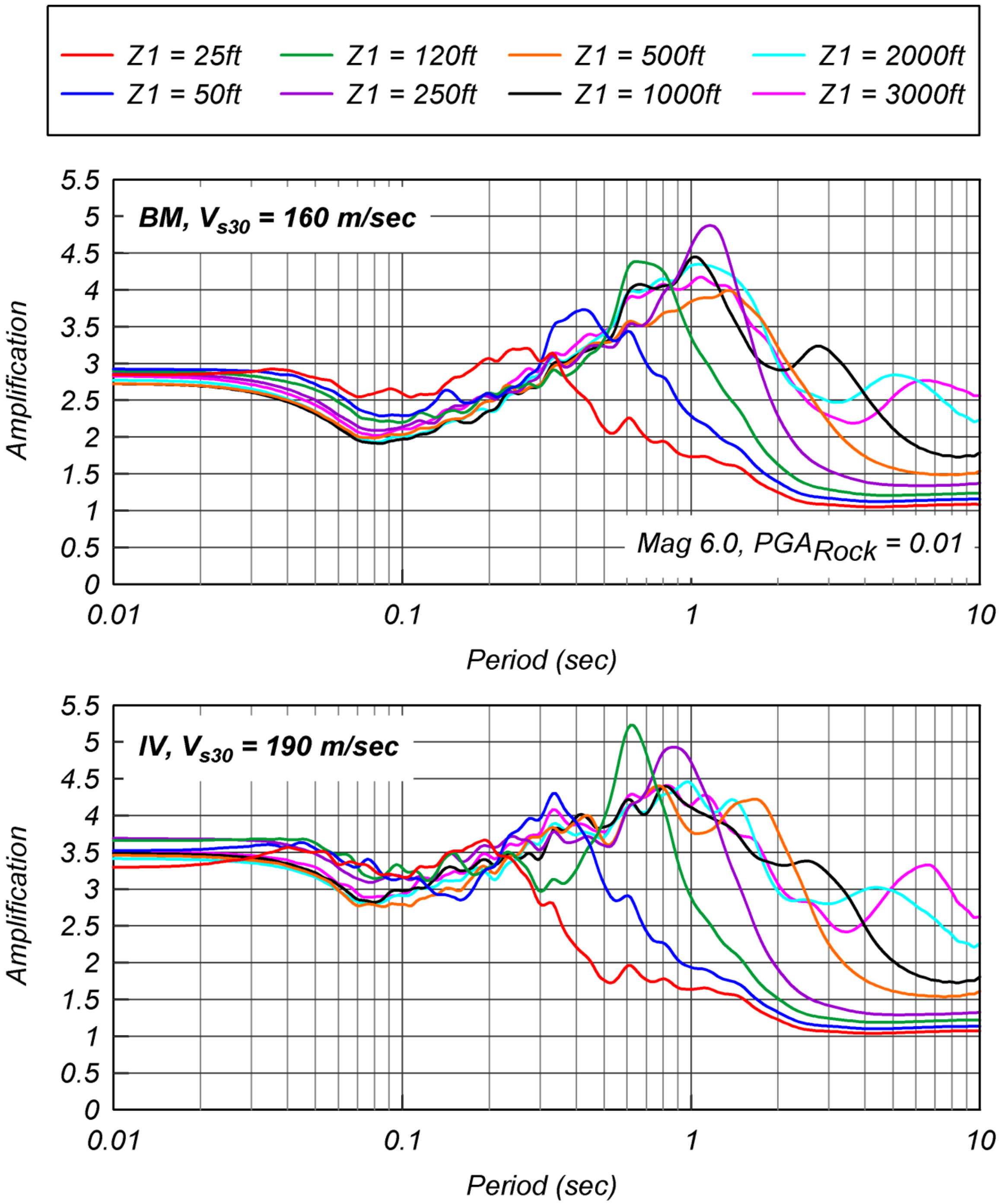

Figure 3.19 **Linear amplification for a range of soil depths for the V_{S30}=160 m/sec profile (top) and the V_{S30}=190 m/sec profile (bottom).**

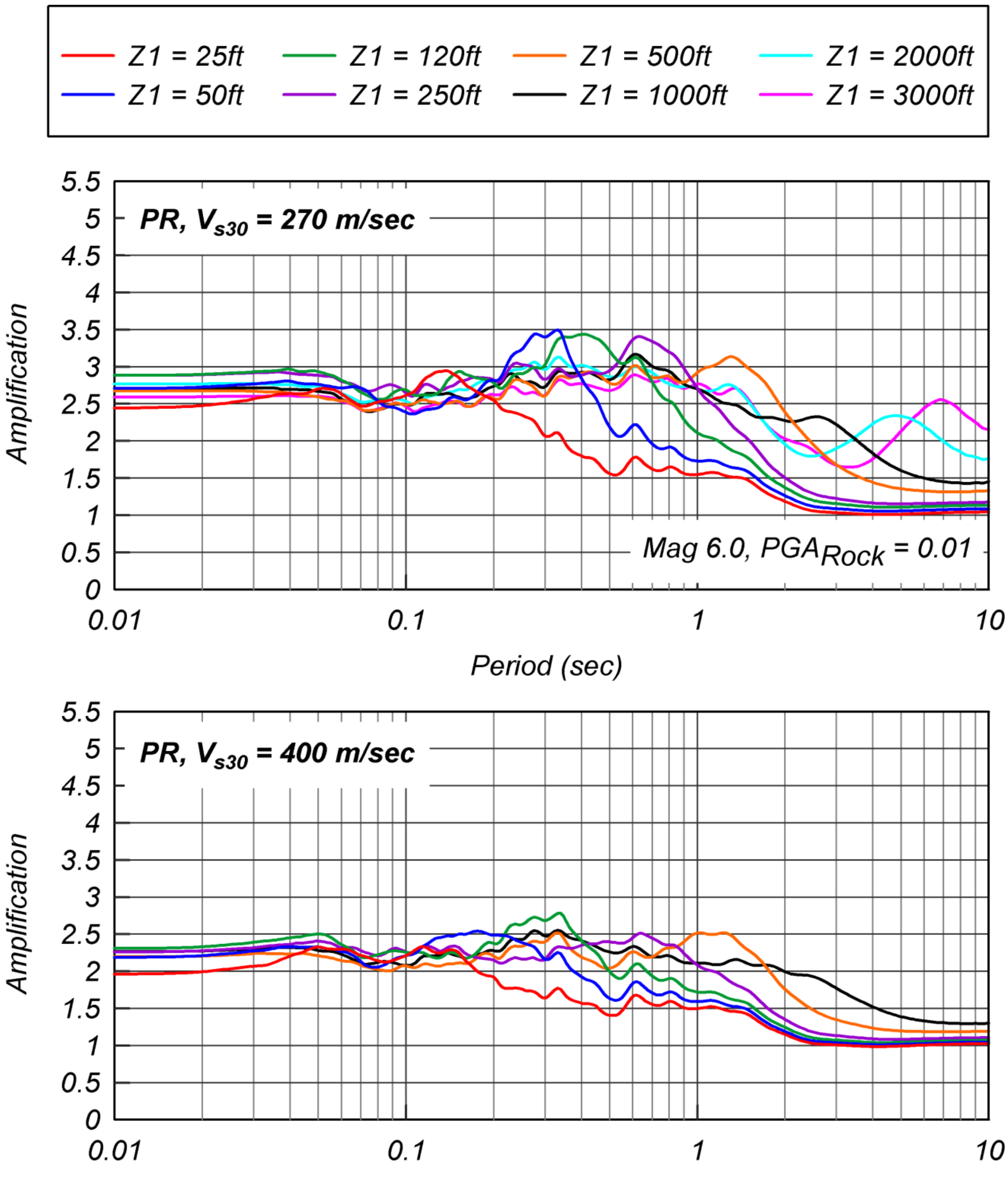

Figure 3.20 Linear amplification for a range of soil depths for the V_{S30}=270 m/sec profile (top) and the V_{S30}=400 m/sec profile (bottom).

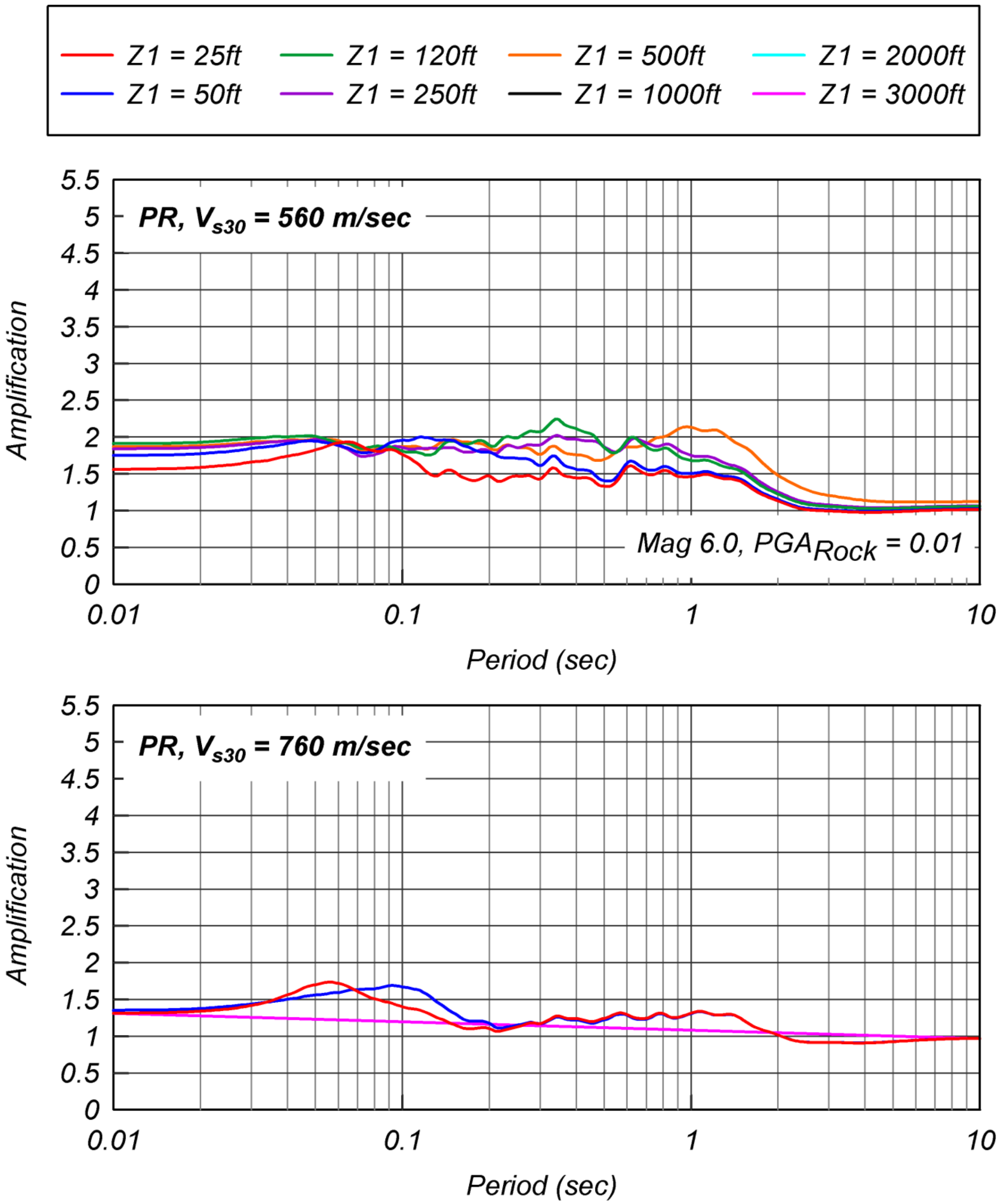

Figure 3.21 Linear amplification for a range of soil depths for the V_{S30}=560 m/sec profile (top) and the V_{S30}=760 m/sec profile (bottom).

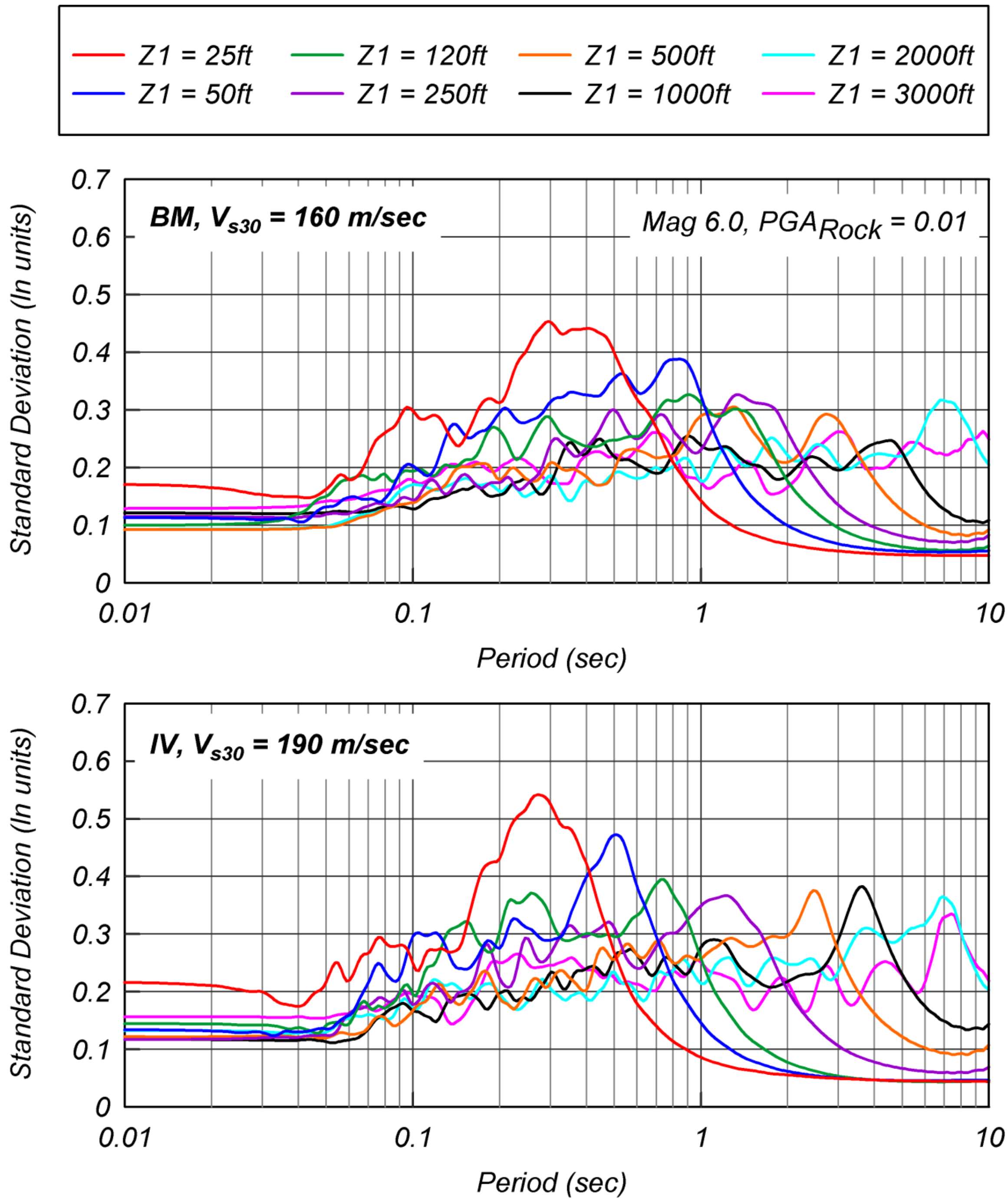

Figure 3.22 **Standard deviations of the linear amplification (PGA_{Rock}=0.01g) for a range of soil depths for the V_{S30}=160 m/sec profile (top) and the V_{S30}=190 m/sec profile (bottom).**

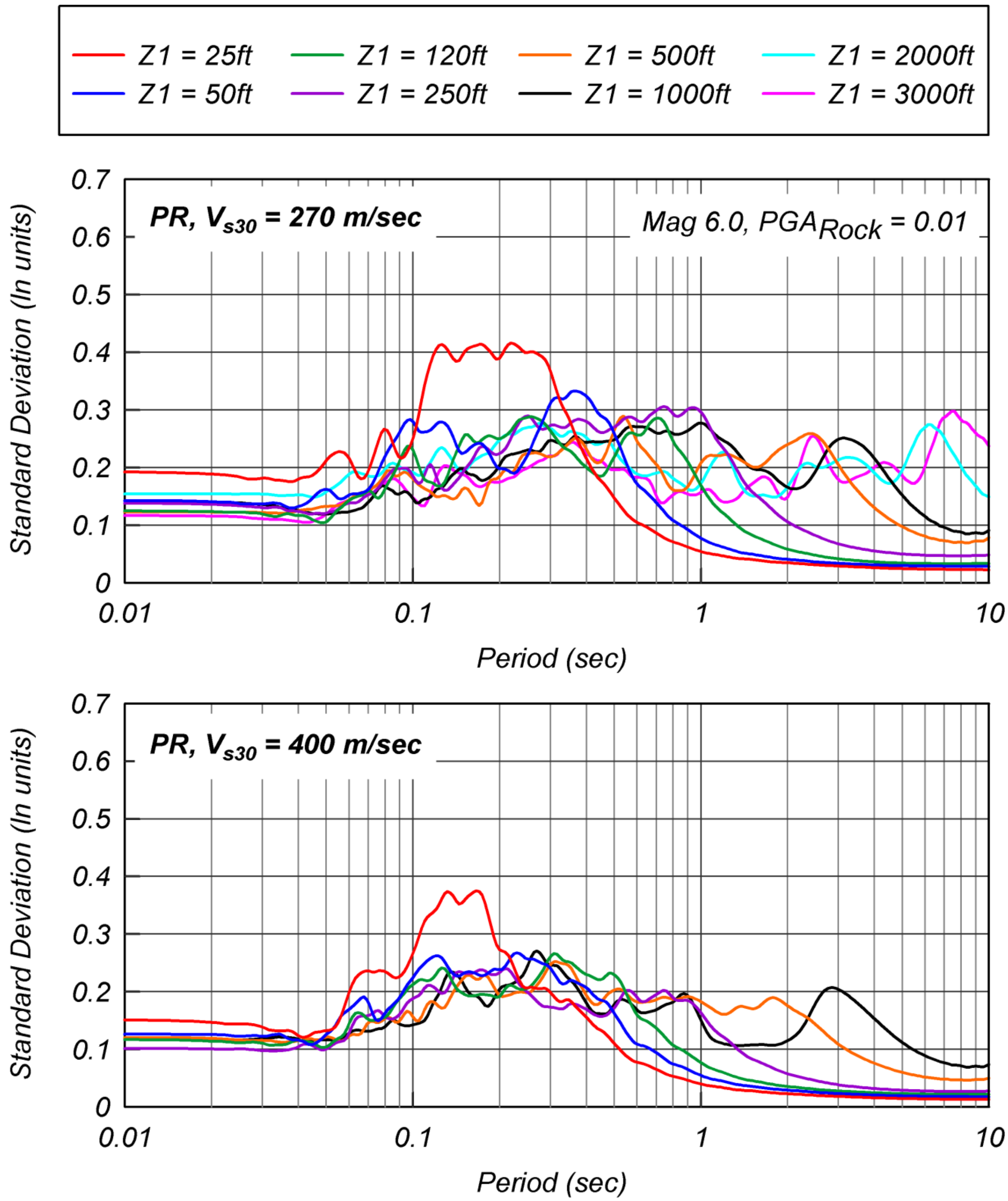

Figure 3.23 Standard deviations of the linear amplification (PGA_{Rock}=0.01g) for a range of soil depths for the V_{S30}=270 m/sec profile (top) and the V_{S30}=400 m/sec profile (bottom).

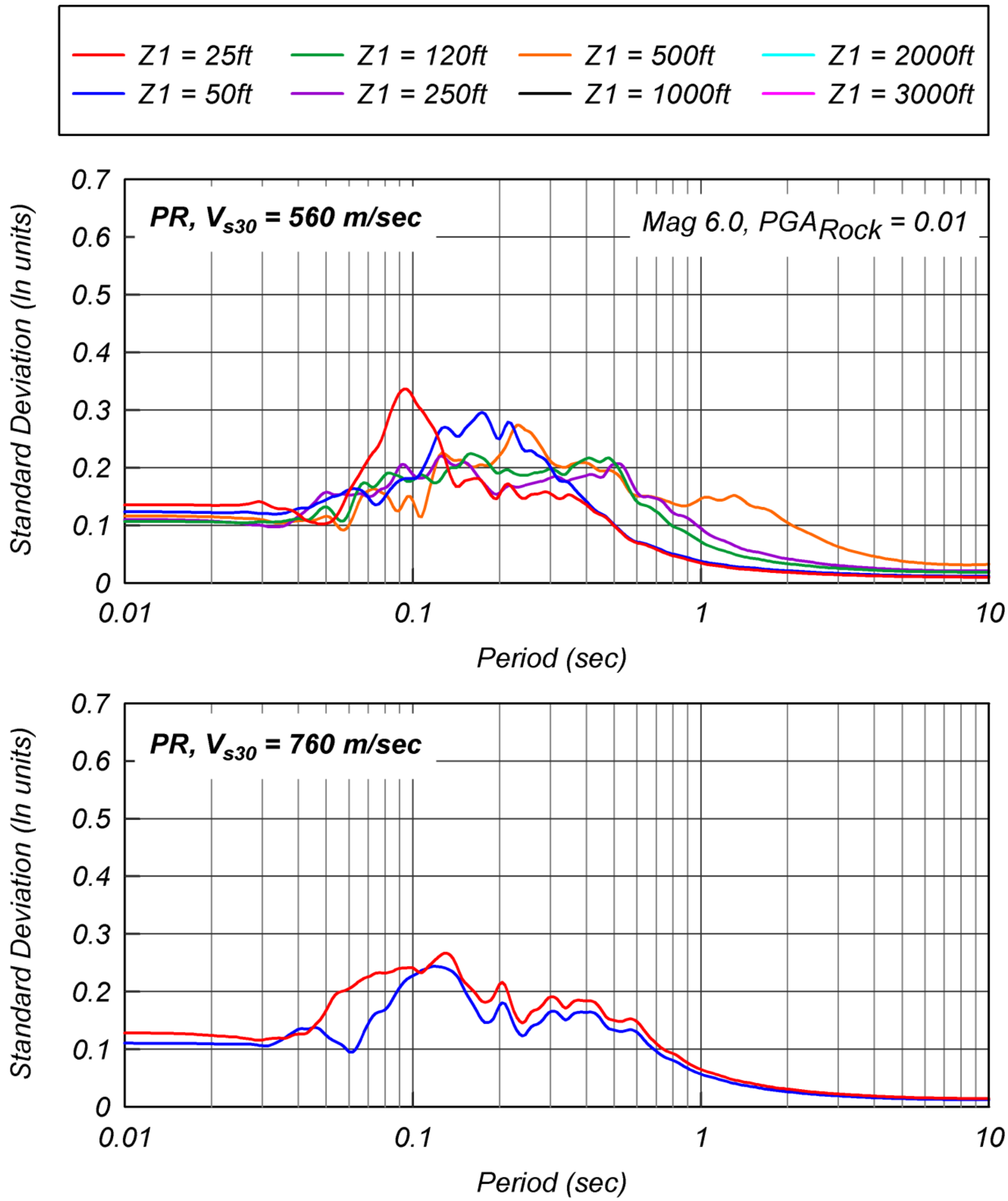

Figure 3.24 **Standard deviations of the linear amplification (PGA_{Rock}=0.01g) for a range of soil depths for the V_{S30}=560 m/sec profile (top) and the V_{S30}=760 m/sec profile (bottom).**

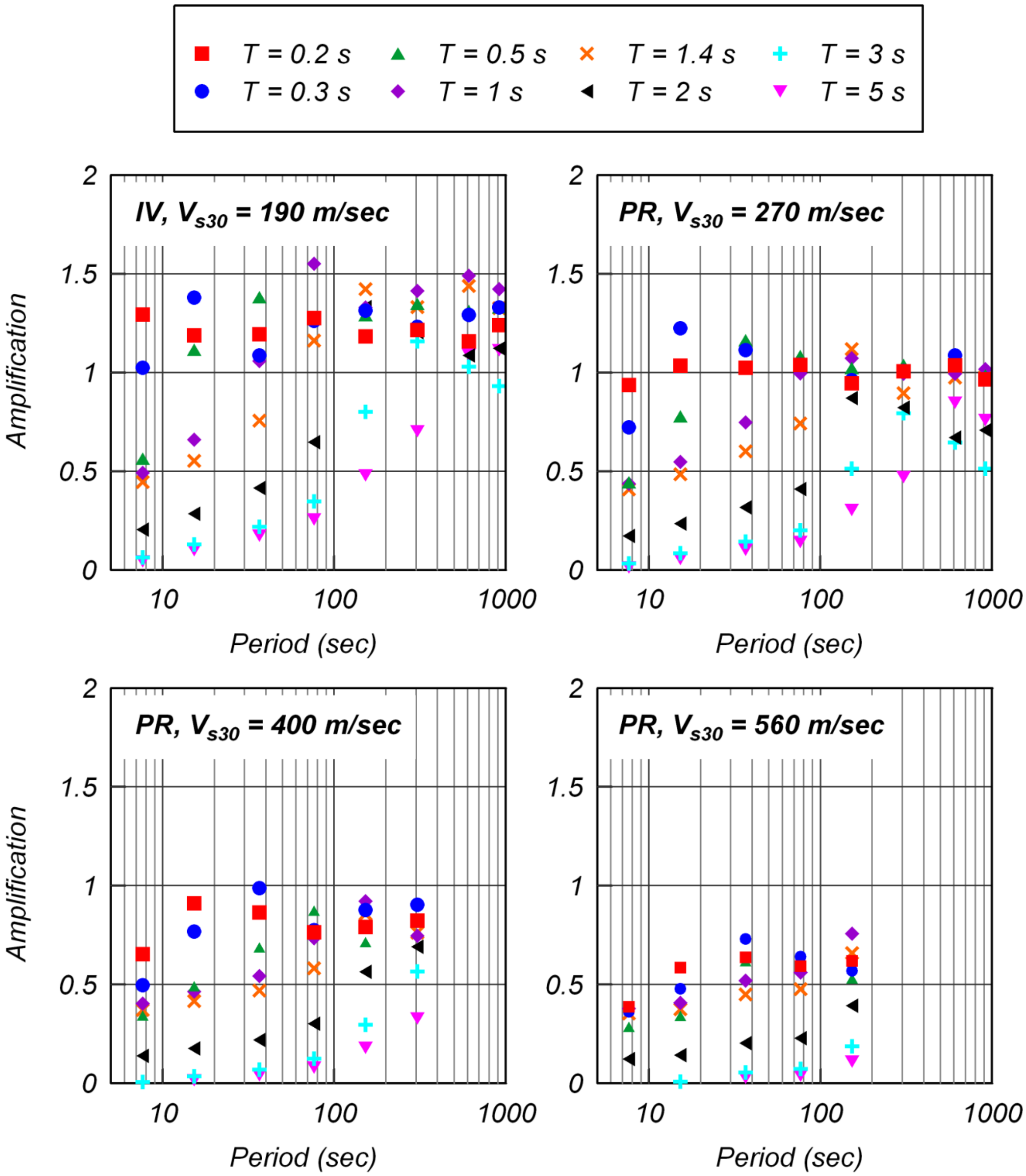

Figure 3.25 Soil depth dependence of the linear amplification.

4 Parametric Model for Nonlinear Site Amplification

4.1 INTRODUCTION

A subset of the simulation cases described above was used for the development of parametric models for the nonlinear response of soil sites to strong ground motions. The proposed models are updates to the models developed by Walling et al. (2008) in that they are based on an extended simulation dataset and use the same functional form.

The models developed by Walling et al. (2008) were revisited herein for two main reasons: (*a*) the simulation database on which the models were developed has been updated and extended, with additional magnitudes and soil profiles, and (*b*) two alternatives for the input shaking parameter are explored – the Peak Ground Acceleration (PGA) and the spectral acceleration for each period, ($Sa(T)$).

4.2 MODEL DEVELOPMENT

Four resulting models are presented below: for each of the soil models - Peninsular Range and EPRI - there is a one model based on *PGA* as input and one based on *Sa(T)* as input. All models are based on the randomized-depth soil profiles only. A summary of the simulation cases used for model development is presented in Table 4.1.

Table 4.1 List of simulation scenarios that were selected for model development.

V_{s30} (m/sec)	Depth to top of rock (V_{s30}=1 km/sec)	Material model used for nonlinear properties
190	9-305 m	PR
270	9-305 m	PR, EPRI
400	9-305 m	PR, EPRI
560	9-305 m	PR, EPRI
760	79 m	PR, EPRI
900	79 m	PR

4.2.1 Functional Form

The functional form is identical to that used in Walling et al. (2008). It can be written as the sum of a linear term and a nonlinear term:

$$\ln(Amp) = f_L(V_{s30}) + f_{NL}\,(GM_{Rock}, V_{s30}) \tag{4.1}$$

The linear term is a function of Vs30 only, whereas the nonlinear term is a function of Vs30 and a measure of the shaking intensity on rock. The ground motion intensity was defined in the Walling2008 model in term of PGA_{Rock}. Here we present two alternatives – for each soil model (PR and EPRI), we present one model in term of PGA_{Rock} and one in term of $Sa(T)_{Rock}$. Finally, the resulting functional forms for the two alternative models are given in Equations (4.2) and (4.3) for the PGA-based and the Sa(T)-based models, respectively:

$$\ln(Amp) = \begin{cases} a\,ln\left(\frac{V_{S30}^*}{V_{Lin}}\right) - b\,ln(PGA_{Rock} + c) \\ + b\,ln\left(PGA_{Rock} + c\left(\frac{V_{S30}^*}{V_{Lin}}\right)^n\right) + d \quad for\ V_{s30} < V_{Lin} \\ (a + bn)ln\left(\frac{V_{S30}^*}{V_{Lin}}\right) + d \qquad for\ V_{s30} \geq V_{Lin} \end{cases} \tag{4.2}$$

$$\ln(Amp) = \begin{cases} a\,ln\left(\frac{V_{S30}^*}{V_{Lin}}\right) - b\,ln(Sa_{Rock}(T) + c) \\ + b\,ln\left(Sa_{Rock}(T) + c\left(\frac{V_{S30}^*}{V_{Lin}}\right)^n\right) + d \quad for\ V_{s30} < V_{Lin} \\ (a + bn)ln\left(\frac{V_{S30}^*}{V_{Lin}}\right) + d \qquad for\ V_{s30} \geq V_{Lin} \end{cases} \tag{4.3}$$

where:

$$V_{S30}^* = \begin{cases} V_{s30} & for\ V_{s30} < V_1 \\ V_1 & for\ V_{s30} \geq V_1 \end{cases} \tag{4.4}$$

and V_1 corresponds to the Vs_{30} above which the soil amplification no longer scales linearly with respect to changes in Vs_{30} (Abrahamson and Silva, 2008).

Further explanation on the evolution of the form for the nonlinear term is provided in Walling et al. (2008).

4.2.2 Data Selection

For the models presented below, only simulations with randomized depth (30–1000 ft) are used. The simulations with smaller depth bins are used to constrain the depth term within the GMPE (e.g., Abrahamson and Silva 2008) but that part is not discussed in this report.

A Magnitude-Period constrain was placed on the dataset used for the model regression, due to an increased amplification at long periods for the smaller magnitudes (e.g., Figures 3.1 to 3.4), which is believed to be a numerical artifact of the simulation procedure. The simulation results used for model regression include the Magnitude 7.0 simulations within the available period range $0.01 < T < 10$ sec, Magnitude 6.0 simulations at $0.01 < T < 5$ sec and Magnitude 5.0 simulations at $0.01 < T < 2$ sec. The PGV model regression is performed on simulations from Magnitudes 6.0 and 7.0 only, as discussed in Section 3.2.

4.2.3 Model Parameters

Due to the nonlinearity of the functional form as shown in figure (4.2) and (4.3), the three parameters - b, n, and c - which appear in the nonlinear term are highly correlated and hence do not all need to be period-dependent. Hence, the parameters n and c were fixed along all periods and the parameter b was regressed as a period-dependent parameter. Fixing of n and c was done based on regressions of smaller subsets at short periods, where the nonlinearity is greatest. In the second step, the period-dependent reference shear-wave velocity, V_{Lin} was regressed and smoothed. V_{Lin} is intentionally kept identical for the two models of each soil group (i.e. the two PR models and the two EPRI models), since it represents a physical measure which should not depend on the input shaking. In the third step, the period-dependent nonlinear coefficient, *b*, was regressed and smoothed.

Smoothing of the period-dependent parameters was done by fitting a 7th order polynomial to the regressed values with some constraints at the low and high ends of the period range, following Equation (4.5).

$$x = \begin{cases} \beta_2 & T \geq T_2 \\ \propto_0 + \sum_{i=1}^{7} \propto_i \left[ln\left(\frac{T}{T_0}\right)\right]^i & T_1 < T < T_2 \\ \beta_1 & T \leq T_1 \end{cases} \tag{4.5}$$

The smoothed parameter x in Equation (4.5) is either $ln(V_{Lin})$ or b and T is the spectral period. The four pairs of the smoothed parameters (V_{lin} and b for each of the four models presented in this report) are compared with the smoothed parameters from Walling et al. (2008) in Figure 4.1. Note that while the parameter b was constrained in Walling et al. (2008) to be negative (or ≤ 0.15), it was allowed to be positive in the models below and was as high as 3.95 for the PR-Sa model. The positive b values allow an increase in amplification for increased levels of shaking, which can be related to period elongation, as will be shown below.

The list of parameters needed for reconstructing the nonlinear terms (following equation 5) are presented in Table 4.2. The smoothed values for V_{lin} and b are listed in Appendix A for the 111 periods that are in the NGA FlatFile. The parameters which appear in the linear term - a and d - are left unsmoothed, since they are correlated with other terms in the GMPE and should be regressed for each individual GMPE in which these site amplification models are applied.

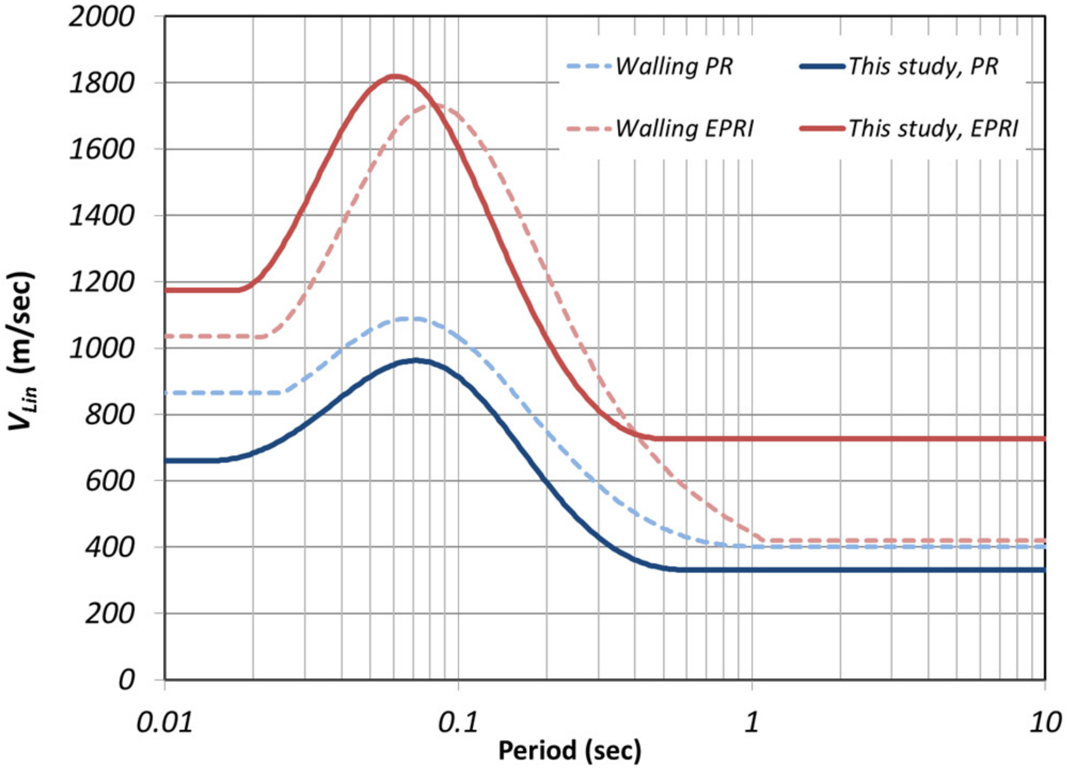

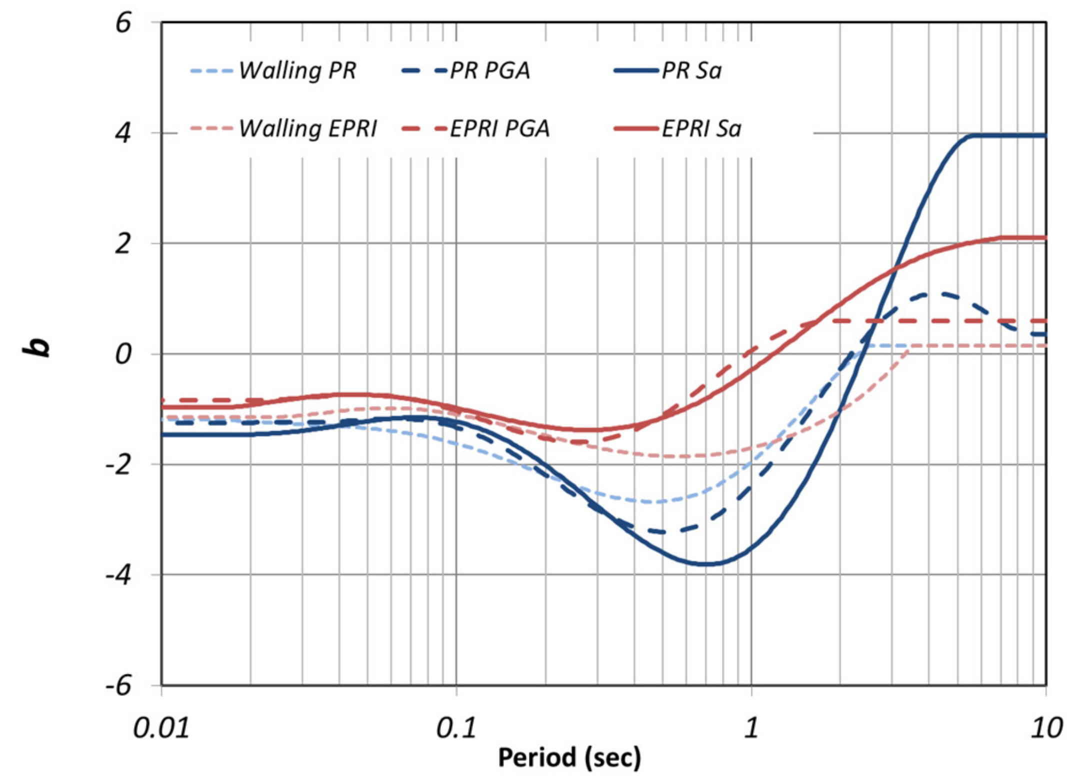

Figure 4.1 Period-dependence of the smoothed model parameters. V_{Lin} (top) and b (bottom).

Table 4.2 List of coefficients needed to reconstruct the smoothed model parameters.

	PR			EPRI		
		PGA	Sa		PGA	Sa
n		1.5	1.5		1.5	1.5
c		1.4	2.4 (*100 for PGV)		2.0	3.0 (*100 for PGV)
	V_{LIN}	***b***	***b***	V_{LIN}	***b***	***b***
PGV	332.00	-1.5140	-2.0200	728.00	0.5850	0.6025
T_0	0.010	0.020	0.012	0.014	0.010	0.02
T_1	0.015	0.020	0.018	0.018	0.022	0.018
T_2	0.550	9.000	5.500	0.460	1.820	7.000
a_0	6.5300	-1.2500	-1.6400	7.1360	-0.9039	-0.9241
a_1	-0.2000	0.2780	0.9474	-0.6500	1.1276	0.3081
a_2	0.2400	-1.3430	-2.0673	1.7860	-3.5267	0.2166
a_3	0.0940	2.4810	2.2630	-1.0370	4.4341	-0.5068
a_4	-0.0170	-1.8690	-1.0634	0.1237	-2.5880	0.1586
a_5	-0.0529	0.6040	0.2097	0.0421	0.7361	0.0006
a_6	0.0191	-0.0862	-0.0155	-0.0117	-0.0993	-0.0047
a_7	-0.0018	0.0045	0.0002	0.0008	0.0051	0.0004
β_1	6.493	-1.250	-1.470	7.068	-0.833	-0.960
β_2	5.805	0.360	3.950	6.590	0.600	2.100

4.3 SUMMARY OF RESULTS

The dependence of the amplification level on shaking intensity [in terms of PGA or Sa(f)] as well as on the soil profile (in terms of Vs_{30}) is presented in Figures 4.2 through 4.5 for the four different models, for periods 0.01, 0.2, 1, 2, 3, and 5 sec. The simulation results are represented by open symbols while the parametric model is shown by the solid line for each corresponding V_{s30}. All four models can be seen to capture the general response of the simulations, that is – increased amplification as V_{s30} decreases, nonlinearity at short periods, and period elongation (increased amplification for increased input motion) at long periods. The biggest discrepancy can be seen at T=1 sec for all four models. At that period, there are several aspects of the soil response that cannot be captured by the current functional form. For example, the two softest profiles for the PR model (V_{s30}=190 and V_{s30}=270) have opposite trends with shaking intensity, the amplification for low shaking intensity does not scale linearly with V_{s30}, and some of the profiles change their nonlinearity from positive to negative with shaking input. These discrepancies are also consistent with Figures 3.2 and 3.5, which suggest that at T=1 sec there is both resonance at the soft profiles and the greatest magnitude dependence. The model's agreement with simulation results at other periods seems to be much better for a range of V_{s30} and shaking intensity values.

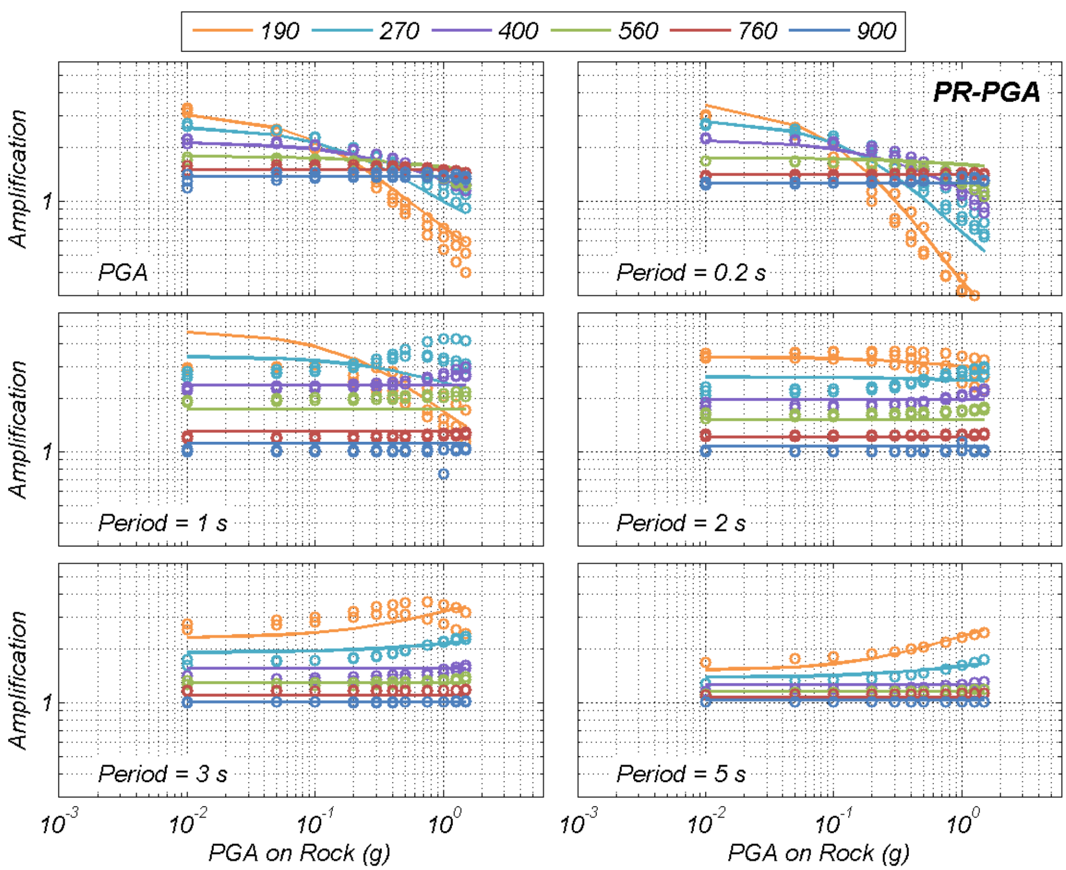

Figure 4.2 Model versus simulation results for the PR-PGA model for six representative periods.

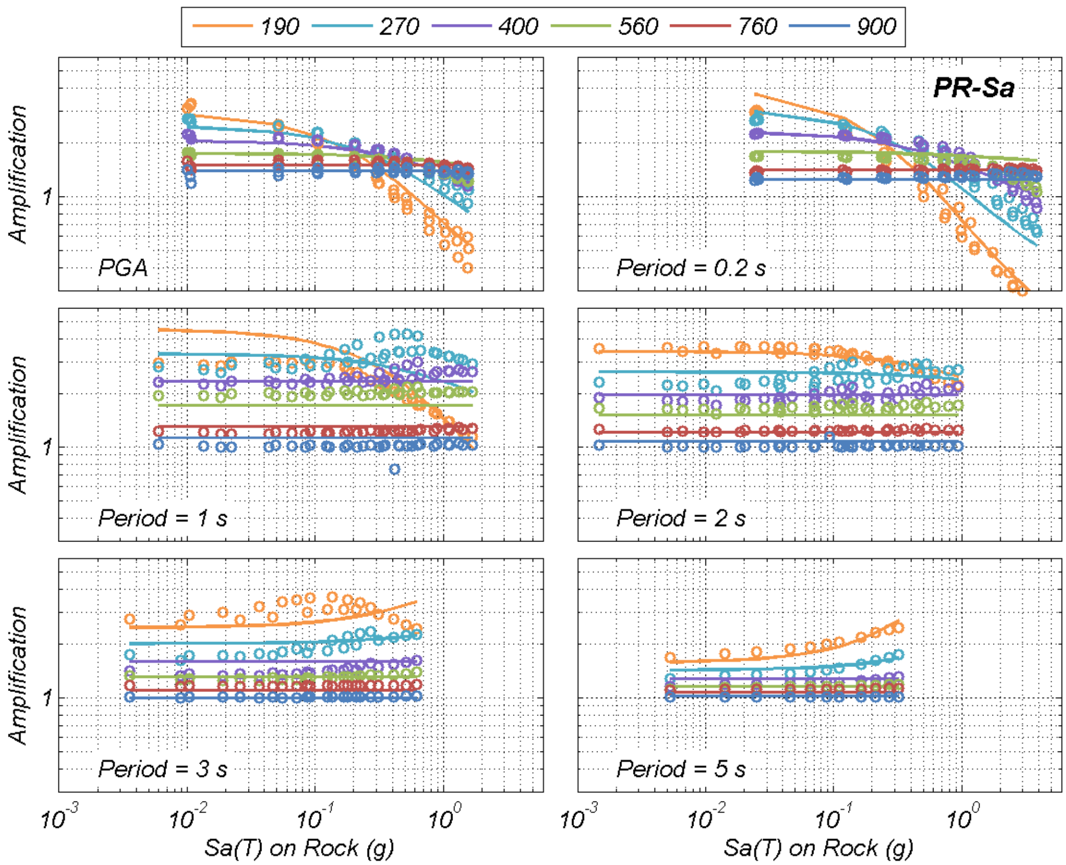

Figure 4.3 Model versus imulation results for the PR-Sa model for six representative periods.

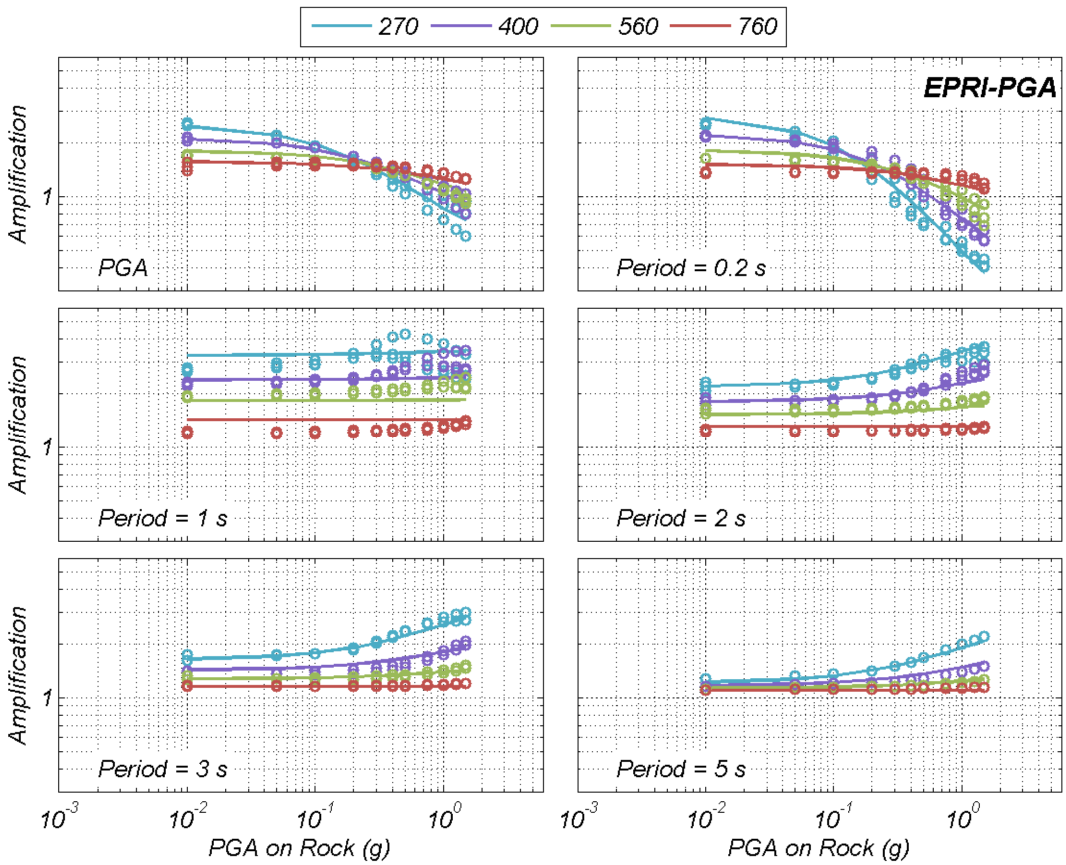

Figure 4.4 **Model versus simulation results for the EPRI-PGA model for six representative periods.**

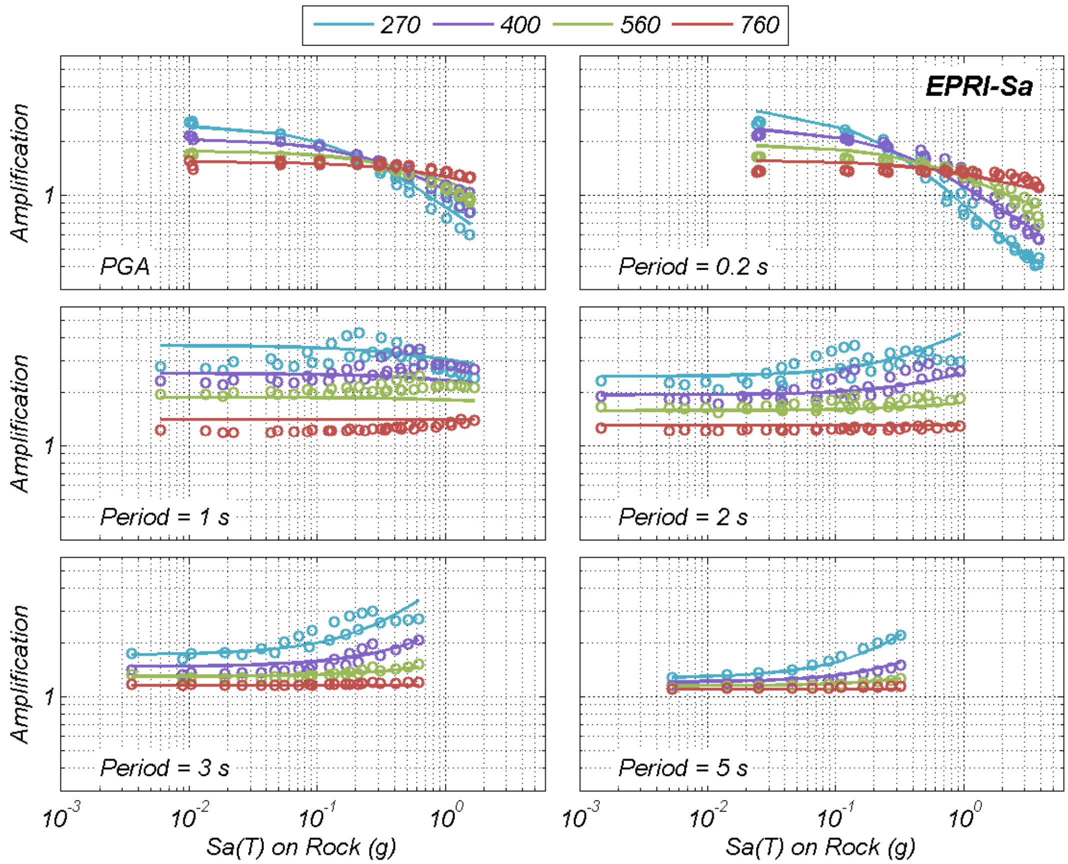

Figure 4.5 Model versus imulation results for the EPRI-Sa model for six representative periods.

The nonlinearity with respect to shaking intensity can be represented by the slope of the lines in Figures 4.2 through 4.5. This term is presented in Figure 4.6 for a profile with V_{s30}=270 m/sec, showing the slopes between reference PGA of 0.1g to 1g. The trends are similar for all four models and are also quite consistent with nonlinearity computed from the Walling(2008) models. The nonlinearity for the EPRI models is generally greater than that of the PR models, with the nonlinearity peaking at about T=0.2s for all models (as seen in the top panel, slope from 0.1g to 1g).

A comparison between the resulting spectral values on soil vs. the input motion on rock is presented in Figure 4.7 for the PR-Sa model, for the same six periods as shown in Figures 4.2 through 4.5. The expected spectral acceleration of the soil, given the input spectral acceleration on rock and the corresponding model amplification can be computed as:

$$Sa_{Soil}(f) = Sa_{Rock}(f) \cdot Amp(f) \tag{4.6}$$

It can be seen that at low rock shaking levels, all soil profiles amplify the response (all lines are above the 1:1 line). As shaking levels increase, the softer profiles de-amplify the response at shorter periods (lines cross below the 1:1 line). At the longer periods (above ~1 sec) there is no de-amplification even for high levels of shaking.

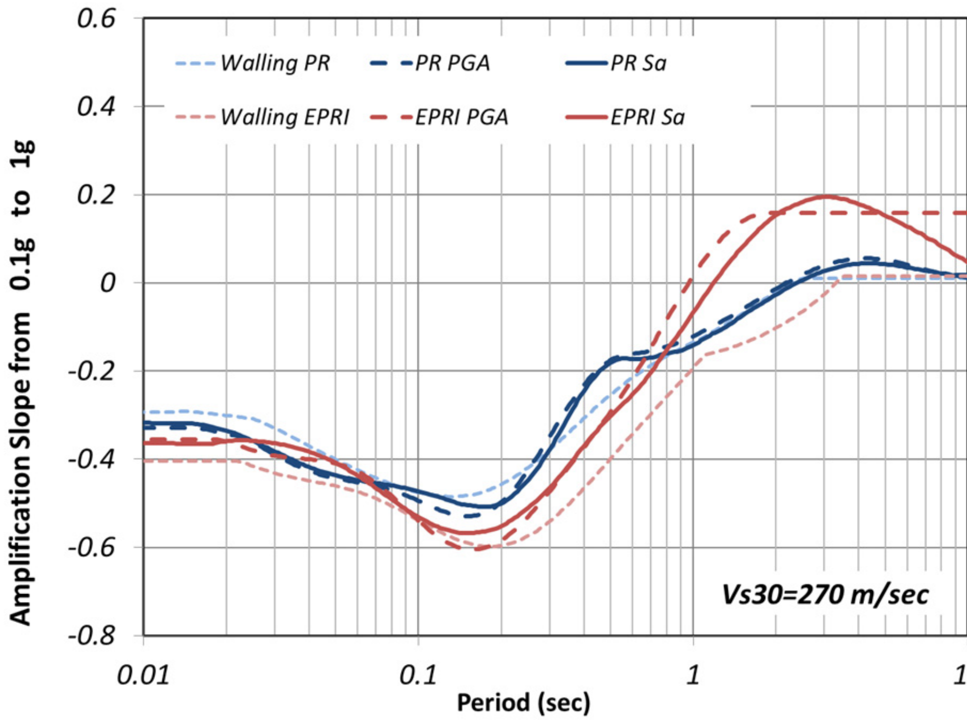

Figure 4.6 Period-dependence of the combined nonlinear term, computed as the slope of amplification from 0.1g to 1g.

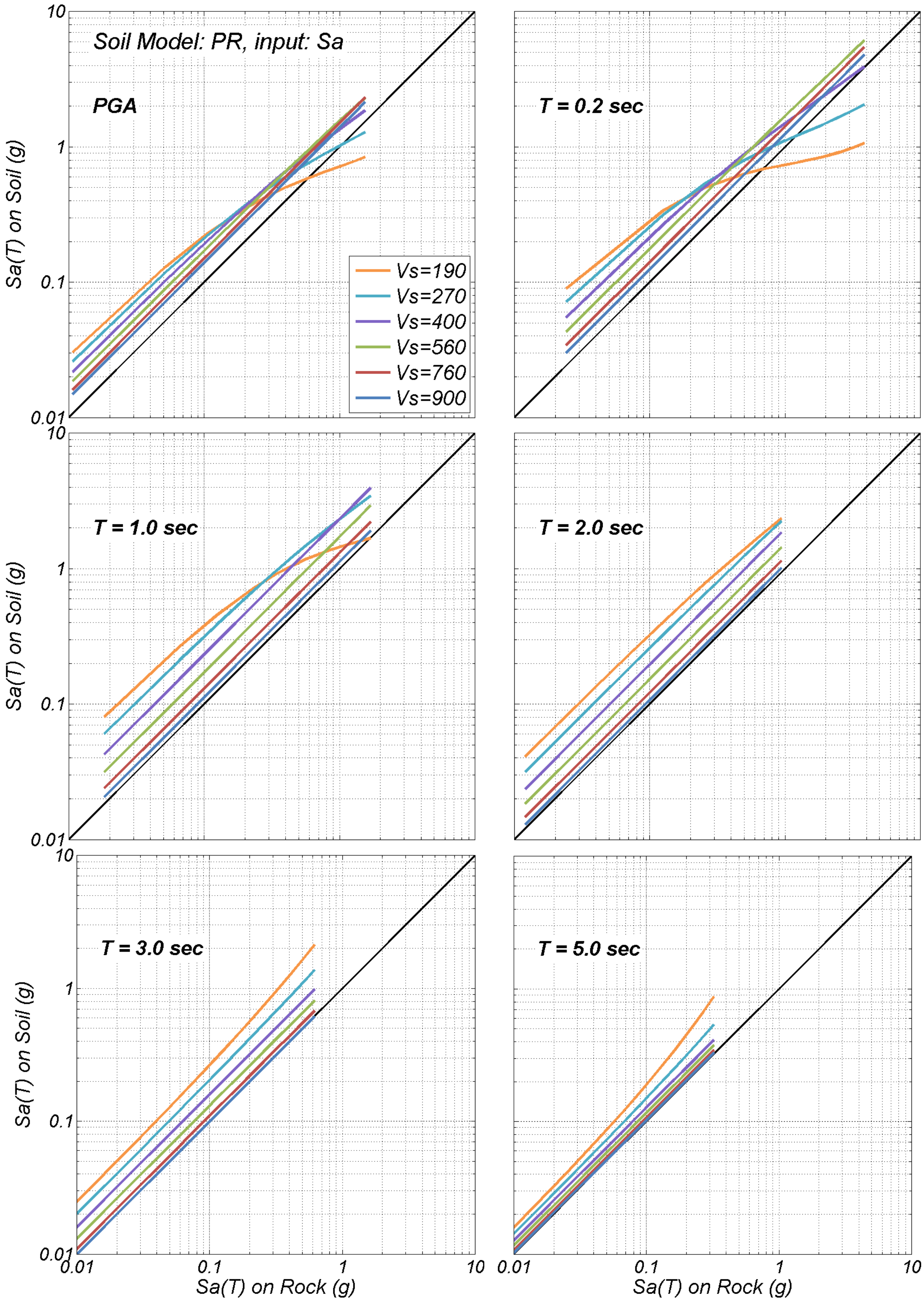

Figure 4.7 Sa on Soil vs. Sa on Rock, for the PR-Sa model.

The spectral shape of the rock and corresponding soil motions are presented in Figure 4.8 for four increasing shaking intensities – ranging from PGA_{1100} of 0.05g to 1g. The rock motions are shown in solid lines and the corresponding soil motions are in dashed lines. It can be seen that as shaking increases, there is more nonlinearity, and hence the soil softens and the peak response is shifted towards longer periods. This can also explain the upward trend of the amplification curve at T>2 sec in Figures 4.3 through 4.6.

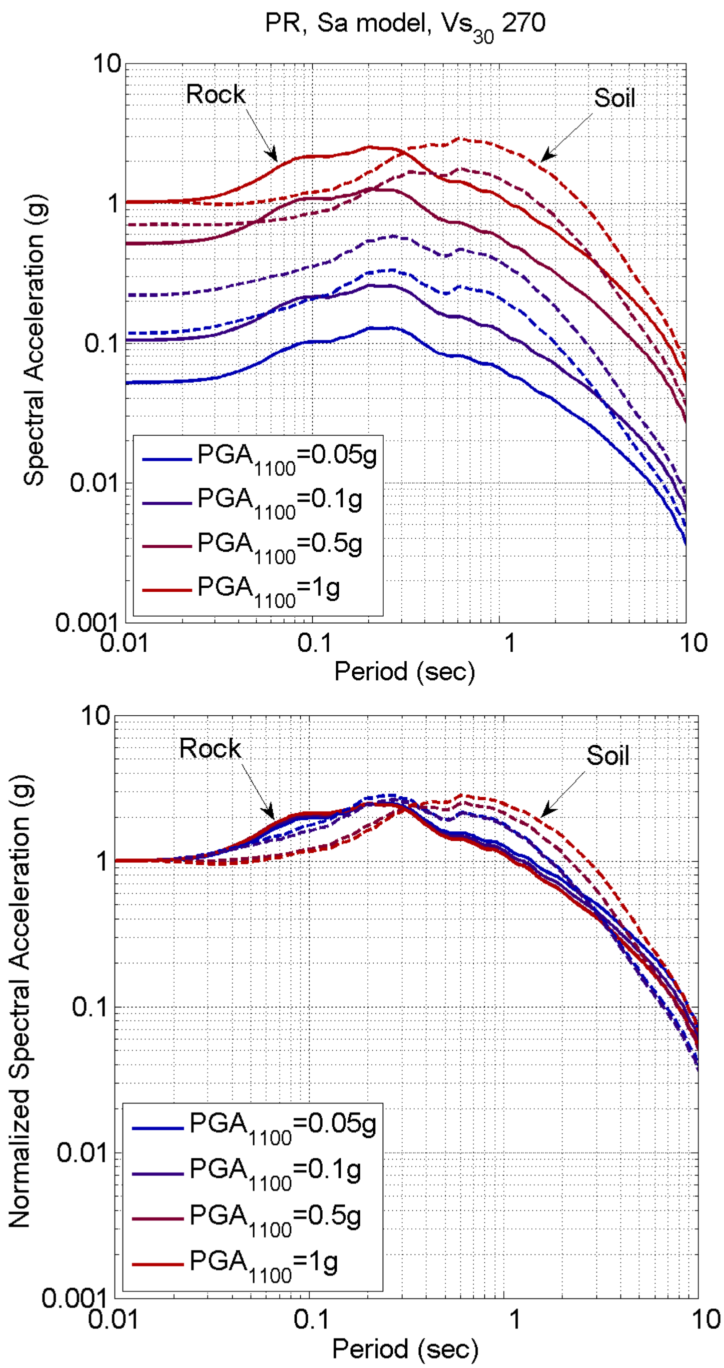

Figure 4.8 **Spectral acceleration (top) and Normalized spectral acceleration (bottom) vs. Period, for the PR-Sa model with Vs30=270 m/sec and under four different input shaking intensities.**

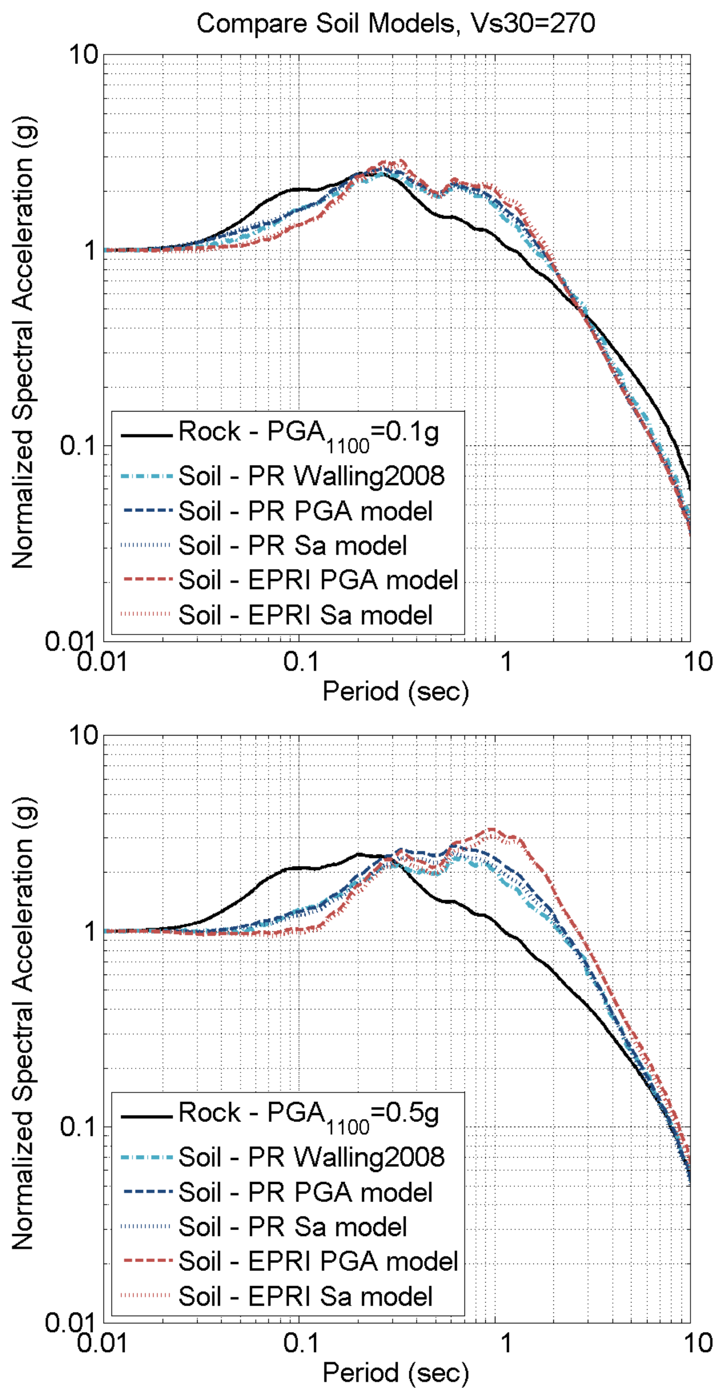

Figure 4.9 Normalized spectral acceleration vs. Period for a Vs_{30}=270 m/sec profile with PGA_{1100}=0.1g (left) and PGA_{1100}=0.5g (right).

The four amplification models are compared in Figure 4.9 in terms of their resulting soil spectra for Vs_{30}=270m/sec with PGA_{1100}=0.1g (left) and PGA_{1100}=0.5g (right). It can be seen that while all four models result in a largely similar soil spectra, there is a greater difference between the two nonlinear material models (i.e. PR vs. EPRI) rather than between the two forms of the input motion [i.e. PGA vs. Sa(T)].

The predictive power of the functional form can be tested by comparing the sigma of the model for different profiles and different functional forms. Since each combination of input shaking value and soil profile was simulated 30 times with randomization of the soil profile and material properties, the parametric model is regressed on the mean amplification of each of those sets. The standard deviation of the fit could therefore either include or not include the standard deviation of each set. A comparison between the two options is presented in Figure 4.10, which shows the standard deviation of the fit for the PR-Sa model, for each of the different soil profiles. On the left, σ_{res} is the standard deviation of the residuals between the simulation means and the parametric model. On the right, the total standard deviation includes the average standard deviation of the simulations for each of the profiles considered, computed as following:

$$\sigma_{res-total} = \sqrt{\overline{\sigma_{simulation}}^2 + \sigma_{res}^2} \tag{4.7}$$

where $\overline{\sigma_{simulation}}$ is the mean of the standard deviations for each set of 30 realizations performed for each profile and each shaking intensity (see Figures 3.14 through 3.18) and σ_{res} is the misfit between the mean of that set and the parametric model. In general, Figure 4.10 shows that σ_{res} increases as V_{s30} decreases. The average $\sigma_{res,}$ representing all soil profiles, is shown in black and can be seen to be mostly affected by the softer profiles with the larger σ_{res} while the average $\sigma_{res-total}$ is pulled down (relatively) by the lower $\sigma_{simulation}$ of the stiffer profiles.

The two different functional forms (PGA vs. Sa as shaking input parameter) are compared in Figure 4.11 for the Peninsular Range soil model, showing both σ_{res} and $\sigma_{res-total}$ for each of the forms. If one functional form would have fit the simulation results better, we would expect that form to have a lower standard deviation. However, both σ_{res} and $\sigma_{res-total}$are almost identical for the two forms, suggesting that there is no significant advantage for either of the functional forms. These findings are different than the conclusion of Bazzurro and Cornell (2004), who propagated 78 earthquake records through two soil profiles and explore seven functional forms for the amplification functions. A subset of their findings is also re-drawn in Figure 4.11, comparing the standard deviations of the residuals to two of their functional forms, using PGA and Sa(f) as single model parameters. Bazzurro and Cornell concluded that Sa(T) is the single most helpful parameter for the prediction of the amplification since it had the lowest σ_{res}. One of the main difference between our simulations and Bazzurro and Cornell's is that they use real time histories and by that account for variability in the spectral shape, whereas the simulations in this study were performed with the RVT method, which has a unique spectral shape and hence a strong correlation between PGA and Sa(T). Uncertainties in soil properties are accounted for in both studies, and do not add to the total uncertainty very much, as long as the general profile (depth, Vs30) stays the same.

We conclude that based on the analysis presented herein, there is no statistical preference for either of the forms (PGA or Sa as input-motion parameter), but we recommend using the Sa(T) model, for ease of use in forward applications of the GMPE model.

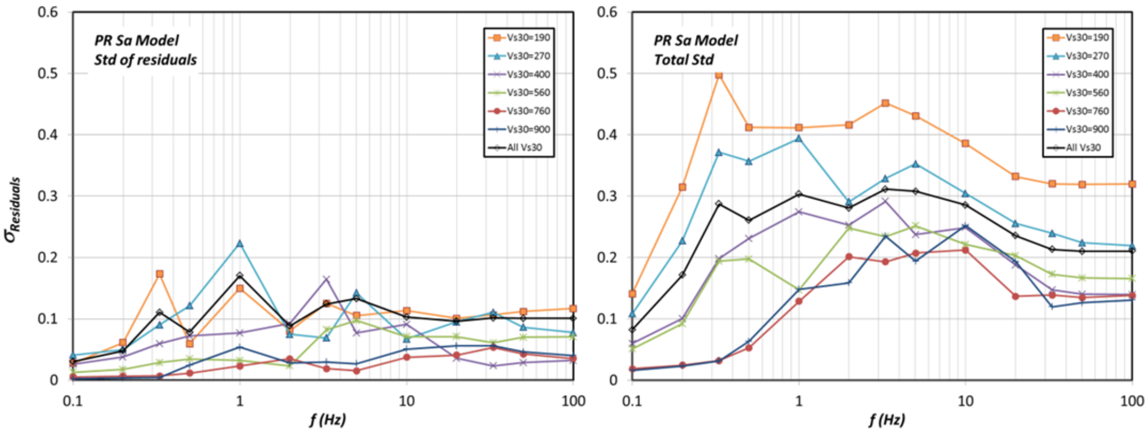

Figure 4.10 **Standard deviation of PR-Sa model, for a range of V_{s30} values. On the left σ_{res} is the standard deviation of the residuals to the fit, while on the right it is the total standard deviation, including the standard deviation of each set of 30 realizations.**

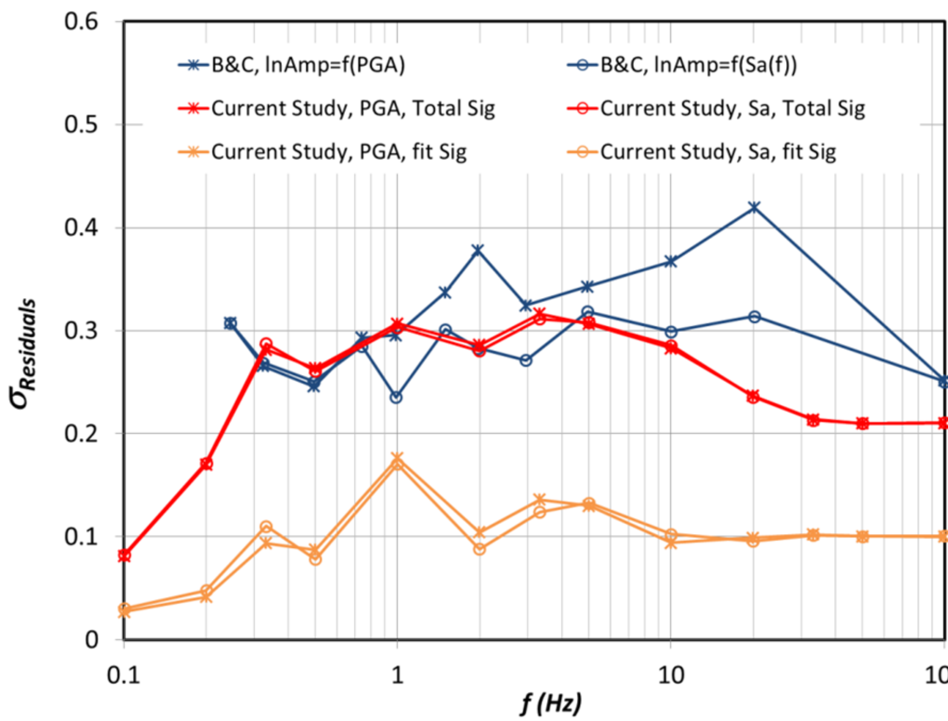

Figure 4.11 **Standard deviation of the PR models, averaged over all Vs30 profiles. Comparison between the two PR models from the current study and a subset of two corresponding models redrawn from Bazzurro and Cornell (2004).**

REFERENCES

Anderson J G., Hough S. (1984). A model for the shape of the Fourier amplitude spectrum of acceleration at high frequencies, *Bull. Seism. Soc. Am*., 74, 1969−1993.

Bazzurro P., Cornell A. (2004). Ground-motion amplification in nonlinear soil sites with uncertain properties, *Bull. Seism. Soc. Am.,* 96: 2090–2109.

Boore D.M. (1983). Stochastic simulation of high-frequency ground motion based on seismological models of the radiated spectra, *Bull. Seism. Soc. Am.,* 73: 1865−1894.

EPRI (1993). Guidelines for determining design basis ground motions, Electric Power Research Institute, Vol. 1−5, *EPRI TR-102293*.

Schnabel P.B., Lysmer J., Seed H.B. (1972). SHAKE: a computer program for earthquake response analysis of horizontal layered sites, *EERC Rept. No. 72−12,* Earthquake Engineering Research Center, University of California, Berkeley, CA.

Silva W.J. Lee K. (1987). WES RASCAL code for synthesizing earthquake ground motions, State-of-the-Art for Assessing Earthquake Hazards in the United States, *Report 24*, U.S. Army Engineers Waterways Experiment Station, Miscellaneous Paper S−73−1.

Silva W.J. (1992). Factors controlling strong ground motions and their associated uncertainties, *ASCE Symposium on High Level Nuclear Waste Repositories,* pp. 132−161.

Silva W. J, Abrahamson N.A., Toro G., Costantino C. (1997). Description and validation of the stochastic ground motion model, Pacific Engineering and Analysis Report, available at www.pacificengineering.org/rpts_page1.shtml

Turner E., Stokoe K.H. (1982). Static and dynamic properties of clayey soils subjected to19790 Imperial Valley Earthquake *Geotechnical Engineering Report GR82-26*, Geotech. Eng. Dept., University of Texas, Austin.

Vucetic M., Dobry R. (1991). Effects of soil plasticity on cyclic response, ASCE, *J. Geotech. Eng*., 117: 89−107.

Walling M., Silva W.J., Abrahamson N.A. (2008). Nonlinear site amplification factors for constraining the NGA models, *Earthq. Spectra*, 24(1): 243–255.

Appendix A: Table of Model Parameters

Table A.1. Model Parameters corresponding to the 111 periods in the NGA FlatFile.

	PR PGA Model		PR Sa Model		EPRI PGA Model		EPRI Sa Model	
n	1.5		1.5		1.5		1.5	
c	1.4		2.4 (*100 for PGV)		2.0		3.0 (*100 for PGV)	
Period (sec)	*VLIN*	*b*	*VLIN*	*b*	*VLIN*	*b*	*VLIN*	*b*
PGV	332.00	-1.514	332.00	-2.020	728.00	0.585	728.00	0.603
0.01	660.50	-1.250	660.50	-1.470	1173.80	-0.833	1173.80	-0.960
0.02	683.74	-1.250	683.74	-1.459	1195.76	-0.833	1195.76	-0.924
0.022	698.64	-1.234	698.64	-1.448	1232.97	-0.833	1232.97	-0.893
0.025	723.96	-1.232	723.96	-1.430	1304.69	-0.825	1304.69	-0.850
0.029	760.05	-1.236	760.05	-1.399	1409.62	-0.805	1409.62	-0.803
0.03	769.14	-1.237	769.14	-1.390	1435.59	-0.799	1435.59	-0.793
0.032	787.11	-1.237	787.11	-1.372	1486.02	-0.787	1486.02	-0.776
0.035	813.17	-1.233	813.17	-1.343	1556.26	-0.770	1556.26	-0.757
0.036	821.52	-1.231	821.52	-1.334	1577.95	-0.765	1577.95	-0.752
0.04	852.89	-1.220	852.89	-1.297	1655.02	-0.749	1655.02	-0.739
0.042	867.19	-1.214	867.19	-1.279	1687.55	-0.744	1687.55	-0.736
0.044	880.48	-1.208	880.48	-1.263	1716.06	-0.740	1716.06	-0.735
0.045	886.74	-1.205	886.74	-1.255	1728.85	-0.738	1728.85	-0.735
0.046	892.74	-1.201	892.74	-1.247	1740.67	-0.737	1740.67	-0.735
0.048	903.95	-1.196	903.95	-1.232	1761.51	-0.737	1761.51	-0.737
0.05	914.11	-1.190	914.11	-1.219	1778.77	-0.738	1778.77	-0.740
0.055	934.95	-1.180	934.95	-1.191	1807.65	-0.746	1807.65	-0.753
0.06	949.57	-1.175	949.57	-1.170	1818.90	-0.763	1818.90	-0.772
0.065	958.49	-1.176	958.49	-1.157	1815.95	-0.786	1815.95	-0.794
0.067	960.59	-1.178	960.59	-1.154	1811.51	-0.796	1811.51	-0.803
0.07	962.31	-1.183	962.31	-1.151	1801.90	-0.814	1801.90	-0.818
0.075	961.69	-1.196	961.69	-1.152	1779.42	-0.845	1779.42	-0.844
0.08	957.26	-1.214	957.26	-1.158	1750.74	-0.879	1750.74	-0.872
0.085	949.63	-1.237	949.63	-1.169	1717.67	-0.915	1717.67	-0.899
0.09	939.35	-1.264	939.35	-1.186	1681.64	-0.952	1681.64	-0.926
0.095	926.93	-1.294	926.93	-1.206	1643.80	-0.990	1643.80	-0.953
0.1	912.81	-1.328	912.81	-1.230	1605.04	-1.027	1605.04	-0.980

0.11	880.95	-1.404	880.95	-1.287	1527.26	-1.101	1527.26	-1.031
0.12	846.25	-1.487	846.25	-1.353	1451.92	-1.171	1451.92	-1.078
0.13	810.51	-1.574	810.51	-1.426	1380.93	-1.236	1380.93	-1.121
0.133	799.78	-1.601	799.78	-1.450	1360.64	-1.255	1360.64	-1.134
0.14	774.94	-1.664	774.94	-1.505	1315.18	-1.296	1315.18	-1.161
0.15	740.37	-1.755	740.37	-1.587	1254.92	-1.349	1254.92	-1.196
0.16	707.30	-1.846	707.30	-1.671	1200.08	-1.397	1200.08	-1.228
0.17	676.04	-1.935	676.04	-1.756	1150.38	-1.439	1150.38	-1.256
0.18	646.74	-2.022	646.74	-1.842	1105.46	-1.475	1105.46	-1.280
0.19	619.44	-2.107	619.44	-1.927	1064.92	-1.505	1064.92	-1.301
0.2	594.13	-2.188	594.13	-2.012	1028.37	-1.530	1028.37	-1.319
0.22	549.18	-2.342	549.18	-2.177	965.74	-1.567	965.74	-1.347
0.24	511.11	-2.481	511.11	-2.335	914.87	-1.586	914.87	-1.366
0.25	494.37	-2.545	494.37	-2.411	893.14	-1.590	893.14	-1.372
0.26	479.03	-2.606	479.03	-2.485	873.56	-1.591	873.56	-1.376
0.28	452.08	-2.717	452.08	-2.626	840.03	-1.584	840.03	-1.379
0.29	440.28	-2.768	440.28	-2.693	825.73	-1.576	825.73	-1.378
0.3	429.47	-2.815	429.47	-2.757	812.88	-1.566	812.88	-1.376
0.32	410.55	-2.900	410.55	-2.879	791.00	-1.540	791.00	-1.367
0.34	394.74	-2.973	394.74	-2.992	773.51	-1.507	773.51	-1.354
0.35	387.85	-3.005	387.85	-3.045	766.18	-1.488	766.18	-1.346
0.36	381.57	-3.034	381.57	-3.096	759.70	-1.468	759.70	-1.338
0.38	370.63	-3.086	370.63	-3.191	749.01	-1.424	749.01	-1.318
0.4	361.60	-3.128	361.60	-3.278	740.98	-1.376	740.98	-1.295
0.42	354.20	-3.162	354.20	-3.356	735.24	-1.326	735.24	-1.270
0.44	348.19	-3.187	348.19	-3.427	731.48	-1.273	731.48	-1.243
0.45	345.64	-3.197	345.64	-3.460	730.26	-1.246	730.26	-1.229
0.46	343.37	-3.205	343.37	-3.491	727.78	-1.218	727.78	-1.214
0.48	339.57	-3.217	339.57	-3.548	727.78	-1.162	727.78	-1.184
0.5	336.64	-3.222	336.64	-3.599	727.78	-1.106	727.78	-1.153
0.55	331.96	-3.212	331.96	-3.698	727.78	-0.963	727.78	-1.070
0.6	331.96	-3.174	331.96	-3.765	727.78	-0.822	727.78	-0.983
0.65	331.96	-3.114	331.96	-3.802	727.78	-0.685	727.78	-0.895
0.667	331.96	-3.089	331.96	-3.808	727.78	-0.640	727.78	-0.864
0.7	331.96	-3.037	331.96	-3.814	727.78	-0.554	727.78	-0.805
0.75	331.96	-2.946	331.96	-3.804	727.78	-0.431	727.78	-0.716
0.8	331.96	-2.845	331.96	-3.775	727.78	-0.316	727.78	-0.627
0.85	331.96	-2.737	331.96	-3.729	727.78	-0.209	727.78	-0.540
0.9	331.96	-2.622	331.96	-3.670	727.78	-0.111	727.78	-0.454
0.95	331.96	-2.504	331.96	-3.598	727.78	-0.021	727.78	-0.370
1	331.96	-2.383	331.96	-3.515	727.78	0.061	727.78	-0.288
1.1	331.96	-2.137	331.96	-3.323	727.78	0.202	727.78	-0.131
1.2	331.96	-1.892	331.96	-3.104	727.78	0.316	727.78	0.018
1.3	331.96	-1.653	331.96	-2.865	727.78	0.405	727.78	0.157
1.4	331.96	-1.421	331.96	-2.611	727.78	0.473	727.78	0.287

1.5	331.96	-1.199	331.96	-2.348	727.78	0.524	727.78	0.409
1.6	331.96	-0.989	331.96	-2.079	727.78	0.559	727.78	0.523
1.7	331.96	-0.791	331.96	-1.807	727.78	0.583	727.78	0.629
1.8	331.96	-0.605	331.96	-1.534	727.78	0.597	727.78	0.728
1.9	331.96	-0.431	331.96	-1.262	727.78	0.600	727.78	0.821
2	331.96	-0.269	331.96	-0.992	727.78	0.600	727.78	0.907
2.2	331.96	0.020	331.96	-0.466	727.78	0.600	727.78	1.062
2.4	331.96	0.264	331.96	0.038	727.78	0.600	727.78	1.198
2.5	331.96	0.371	331.96	0.281	727.78	0.600	727.78	1.259
2.6	331.96	0.468	331.96	0.516	727.78	0.600	727.78	1.315
2.8	331.96	0.636	331.96	0.963	727.78	0.600	727.78	1.418
3	331.96	0.772	331.96	1.379	727.78	0.600	727.78	1.507
3.2	331.96	0.879	331.96	1.763	727.78	0.600	727.78	1.585
3.4	331.96	0.961	331.96	2.114	727.78	0.600	727.78	1.653
3.5	331.96	0.993	331.96	2.277	727.78	0.600	727.78	1.684
3.6	331.96	1.020	331.96	2.432	727.78	0.600	727.78	1.712
3.8	331.96	1.060	331.96	2.718	727.78	0.600	727.78	1.764
4	331.96	1.084	331.96	2.972	727.78	0.600	727.78	1.809
4.2	331.96	1.093	331.96	3.195	727.78	0.600	727.78	1.848
4.4	331.96	1.089	331.96	3.388	727.78	0.600	727.78	1.883
4.6	331.96	1.076	331.96	3.551	727.78	0.600	727.78	1.913
4.8	331.96	1.053	331.96	3.685	727.78	0.600	727.78	1.939
5	331.96	1.024	331.96	3.792	727.78	0.600	727.78	1.963
5.5	331.96	0.927	331.96	3.950	727.78	0.600	727.78	2.010
6	331.96	0.813	331.96	3.950	727.78	0.600	727.78	2.046
6.5	331.96	0.694	331.96	3.950	727.78	0.600	727.78	2.075
7	331.96	0.584	331.96	3.950	727.78	0.600	727.78	2.100
7.5	331.96	0.490	331.96	3.950	727.78	0.600	727.78	2.100
8	331.96	0.418	331.96	3.950	727.78	0.600	727.78	2.100
8.5	331.96	0.376	331.96	3.950	727.78	0.600	727.78	2.100
9	331.96	0.360	331.96	3.950	727.78	0.600	727.78	2.100
9.5	331.96	0.360	331.96	3.950	727.78	0.600	727.78	2.100
10	331.96	0.360	331.96	3.950	727.78	0.600	727.78	2.100
11	331.96	0.360	331.96	3.950	727.78	0.600	727.78	2.100
12	331.96	0.360	331.96	3.950	727.78	0.600	727.78	2.100
13	331.96	0.360	331.96	3.950	727.78	0.600	727.78	2.100
14	331.96	0.360	331.96	3.950	727.78	0.600	727.78	2.100
15	331.96	0.360	331.96	3.950	727.78	0.600	727.78	2.100
20	331.96	0.360	331.96	3.950	727.78	0.600	727.78	2.100

Appendix B: Table of Amplification Factors for Two Hard Rock Profiles

http://peer.berkeley.edu/publications/peer_reports/reports_2013/reports_2013.html

Appendix C: Table of Amplification Factors for the Soil Profiles by Depth Bins

http://peer.berkeley.edu/publications/peer_reports/reports_2013/reports_2013.html

Appendix D: Table of Amplification Factors for the Soil Profiles with Randomized Depth

http://peer.berkeley.edu/publications/peer_reports/reports_2013/reports_2013.html

PEER REPORTS

PEER reports are available as a free PDF download from http://peer.berkeley.edu/publications/peer_reports_complete.html. Printed hard copies of PEER reports can be ordered directly from our printer by following the instructions at http://peer.berkeley.edu/publications/peer_reports.html. For other related questions about the PEER Report Series, contact the Pacific Earthquake Engineering Research Center, 325 Davis Hall mail code 1792, Berkeley, CA 94720. Tel.: (510) 642-3437; Fax: (510) 665-1655; Email: peer_editor@berkeley.edu

PEER 2013/12 *Nonlinear Horizontal Site Response for the NGA-West2 Project.* Ronnie Kamai, Norman A. Abramson, Walter J. Silva. May 2013.

PEER 2013/11 *Epistemic Uncertainty for NGA-West2 Models.* Linda Al Atik and Robert R. Youngs. May 2013.

PEER 2013/10 *NGA-West2 Models for Ground-Motion Directionality.* Shrey K. Shahi and Jack W. Baker. May 2013.

PEER 2013/09 *Final Report of the NGA-West2 Directivity Working Group.* Paul Spudich, Jeffrey R. Bayless, Jack W. Baker, Brian S.J. Chiou, Badie Rowshandel, Shrey K. Shahi, and Paul Somerville. May 2013.

PEER 2013/08 *NGA-West2 Model for Estimating Average Horizontal Values of Pseudo-Absolute Spectral Accelerations Generated by Crustal Earthquakes.* I. M. Idriss. May 2013.

PEER 2013/07 *Update of the Chiou and Youngs NGA Ground Motion Model for Average Horizontal Component of Peak Ground Motion and Response Spectra.* Brian S.J. Chiou and Robert R. Youngs. May 2013.

PEER 2013/06 *NGA-West2 Campbell-Bozorgnia Ground Motion Model for the Horizontal Components of PGA, PGV, and 5%-Damped Elastic Pseudo-Acceleration Response Spectra for Periods Ranging from 0.01 to 10 sec.* Kenneth W. Campbell and Yousef Bozorgnia. May 2013.

PEER 2013/05 *NGA-West2 Equations for Predicting Response Spectral Accelerations for Shallow Crustal Earthquakes.* David M. Boore, Jonathan P. Stewart, Emel Seyhan, Gail M. Atkinson. May 2013.

PEER 2013/04 *Update of the AS08 Ground-Motion Prediction Equations Based on the NGA-West2 Data Set.* Norman A. Abrahamson, Walter J. Silva, and Ronnie Kamai. May 2013.

PEER 2013/03 *PEER NGA-West2 Database.* Timothy D. Ancheta, Robert B. Darragh, Jonathan P. Stewart, Emel Seyhan, Walter J. Silva, Brian S.J. Chiou, Katie E. Wooddell, Robert W. Graves, Albert R. Kottke, David M. Boore, Tadahiro Kishida, and Jennifer L. Donahue. May 2013.

PEER 2013/02 *Hybrid Simulation of the Seismic Response of Squat Reinforced Concrete Shear Walls.* Catherine A. Whyte and Bozidar Stojadinovic. May 2013.

PEER 2013/01 *Housing Recovery in Chile: A Qualitative Mid-program Review.* Mary C. Comerio. February 2013.

PEER 2012/08 *Guidelines for Estimation of Shear Wave Velocity.* Bernard R. Wair, Jason T. DeJong, and Thomas Shantz. December 2012.

PEER 2012/07 *Earthquake Engineering for Resilient Communities: 2012 PEER Internship Program Research Report Collection.* Heidi Tremayne (Editor), Stephen A. Mahin (Editor), Collin Anderson, Dustin Cook, Michael Erceg, Carlos Esparza, Jose Jimenez, Dorian Krausz, Andrew Lo, Stephanie Lopez, Nicole McCurdy, Paul Shipman, Alexander Strum, Eduardo Vega. December 2012.

PEER 2012/06 *Fragilities for Precarious Rocks at Yucca Mountain.* Matthew D. Purvance, Rasool Anooshehpoor, and James N. Brune. December 2012.

PEER 2012/05 *Development of Simplified Analysis Procedure for Piles in Laterally Spreading Layered Soils.* Christopher R. McGann, Pedro Arduino, and Peter Mackenzie–Helnwein. December 2012.

PEER 2012/04 *Unbonded Pre-Tensioned Columns for Bridges in Seismic Regions.* Phillip M. Davis, Todd M. Janes, Marc O. Eberhard, and John F. Stanton. December 2012.

PEER 2012/03 *Experimental and Analytical Studies on Reinforced Concrete Buildings with Seismically Vulnerable Beam-Column Joints.* Sangjoon Park and Khalid M. Mosalam. October 2012.

PEER 2012/02 *Seismic Performance of Reinforced Concrete Bridges Allowed to Uplift during Multi-Directional Excitation.* Andres Oscar Espinoza and Stephen A. Mahin. July 2012.

PEER 2012/01 *Spectral Damping Scaling Factors for Shallow Crustal Earthquakes in Active Tectonic Regions.* Sanaz Rezaeian, Yousef Bozorgnia, I. M. Idriss, Kenneth Campbell, Norman Abrahamson, and Walter Silva. July 2012.

PEER 2011/10 *Earthquake Engineering for Resilient Communities: 2011 PEER Internship Program Research Report Collection.* Eds. Heidi Faison and Stephen A. Mahin. December 2011.

PEER 2011/09 *Calibration of Semi-Stochastic Procedure for Simulating High-Frequency Ground Motions.* Jonathan P. Stewart, Emel Seyhan, and Robert W. Graves. December 2011.

PEER 2011/08 *Water Supply in regard to Fire Following Earthquake.* Charles Scawthorn. November 2011.

PEER 2011/07 *Seismic Risk Management in Urban Areas. Proceedings of a U.S.-Iran-Turkey Seismic Workshop.* September 2011.

PEER 2011/06 *The Use of Base Isolation Systems to Achieve Complex Seismic Performance Objectives.* Troy A. Morgan and Stephen A. Mahin. July 2011.

PEER 2011/05 *Case Studies of the Seismic Performance of Tall Buildings Designed by Alternative Means.* Task 12 Report for the Tall Buildings Initiative. Jack Moehle, Yousef Bozorgnia, Nirmal Jayaram, Pierson Jones, Mohsen Rahnama, Nilesh Shome, Zeynep Tuna, John Wallace, Tony Yang, and Farzin Zareian. July 2011.

PEER 2011/04 *Recommended Design Practice for Pile Foundations in Laterally Spreading Ground.* Scott A. Ashford, Ross W. Boulanger, and Scott J. Brandenberg. June 2011.

PEER 2011/03 *New Ground Motion Selection Procedures and Selected Motions for the PEER Transportation Research Program.* Jack W. Baker, Ting Lin, Shrey K. Shahi, and Nirmal Jayaram. March 2011.

PEER 2011/02 *A Bayesian Network Methodology for Infrastructure Seismic Risk Assessment and Decision Support.* Michelle T. Bensi, Armen Der Kiureghian, and Daniel Straub. March 2011.

PEER 2011/01 *Demand Fragility Surfaces for Bridges in Liquefied and Laterally Spreading Ground.* Scott J. Brandenberg, Jian Zhang, Pirooz Kashighandi, Yili Huo, and Minxing Zhao. March 2011.

PEER 2010/05 *Guidelines for Performance-Based Seismic Design of Tall Buildings.* Developed by the Tall Buildings Initiative. November 2010.

PEER 2010/04 *Application Guide for the Design of Flexible and Rigid Bus Connections between Substation Equipment Subjected to Earthquakes.* Jean-Bernard Dastous and Armen Der Kiureghian. September 2010.

PEER 2010/03 *Shear Wave Velocity as a Statistical Function of Standard Penetration Test Resistance and Vertical Effective Stress at Caltrans Bridge Sites.* Scott J. Brandenberg, Naresh Bellana, and Thomas Shantz. June 2010.

PEER 2010/02 *Stochastic Modeling and Simulation of Ground Motions for Performance-Based Earthquake Engineering.* Sanaz Rezaeian and Armen Der Kiureghian. June 2010.

PEER 2010/01 *Structural Response and Cost Characterization of Bridge Construction Using Seismic Performance Enhancement Strategies.* Ady Aviram, Božidar Stojadinović, Gustavo J. Parra-Montesinos, and Kevin R. Mackie. March 2010.

PEER 2009/03 *The Integration of Experimental and Simulation Data in the Study of Reinforced Concrete Bridge Systems Including Soil-Foundation-Structure Interaction.* Matthew Dryden and Gregory L. Fenves. November 2009.

PEER 2009/02 *Improving Earthquake Mitigation through Innovations and Applications in Seismic Science, Engineering, Communication, and Response. Proceedings of a U.S.-Iran Seismic Workshop.* October 2009.

PEER 2009/01 *Evaluation of Ground Motion Selection and Modification Methods: Predicting Median Interstory Drift Response of Buildings.* Curt B. Haselton, Ed. June 2009.

PEER 2008/10 *Technical Manual for Strata.* Albert R. Kottke and Ellen M. Rathje. February 2009.

PEER 2008/09 *NGA Model for Average Horizontal Component of Peak Ground Motion and Response Spectra.* Brian S.-J. Chiou and Robert R. Youngs. November 2008.

PEER 2008/08 *Toward Earthquake-Resistant Design of Concentrically Braced Steel Structures.* Patxi Uriz and Stephen A. Mahin. November 2008.

PEER 2008/07 *Using OpenSees for Performance-Based Evaluation of Bridges on Liquefiable Soils.* Stephen L. Kramer, Pedro Arduino, and HyungSuk Shin. November 2008.

PEER 2008/06 *Shaking Table Tests and Numerical Investigation of Self-Centering Reinforced Concrete Bridge Columns.* Hyung IL Jeong, Junichi Sakai, and Stephen A. Mahin. September 2008.

PEER 2008/05 *Performance-Based Earthquake Engineering Design Evaluation Procedure for Bridge Foundations Undergoing Liquefaction-Induced Lateral Ground Displacement.* Christian A. Ledezma and Jonathan D. Bray. August 2008.

PEER 2008/04 *Benchmarking of Nonlinear Geotechnical Ground Response Analysis Procedures.* Jonathan P. Stewart, Annie On-Lei Kwok, Yousseff M. A. Hashash, Neven Matasovic, Robert Pyke, Zhiliang Wang, and Zhaohui Yang. August 2008.

PEER 2008/03 *Guidelines for Nonlinear Analysis of Bridge Structures in California.* Ady Aviram, Kevin R. Mackie, and Božidar Stojadinović. August 2008.

PEER 2008/02 *Treatment of Uncertainties in Seismic-Risk Analysis of Transportation Systems.* Evangelos Stergiou and Anne S. Kiremidjian. July 2008.

PEER 2008/01 *Seismic Performance Objectives for Tall Buildings.* William T. Holmes, Charles Kircher, William Petak, and Nabih Youssef. August 2008.

PEER 2007/12 *An Assessment to Benchmark the Seismic Performance of a Code-Conforming Reinforced Concrete Moment-Frame Building.* Curt Haselton, Christine A. Goulet, Judith Mitrani-Reiser, James L. Beck, Gregory G. Deierlein, Keith A. Porter, Jonathan P. Stewart, and Ertugrul Taciroglu. August 2008.

PEER 2007/11 *Bar Buckling in Reinforced Concrete Bridge Columns.* Wayne A. Brown, Dawn E. Lehman, and John F. Stanton. February 2008.

PEER 2007/10 *Computational Modeling of Progressive Collapse in Reinforced Concrete Frame Structures.* Mohamed M. Talaat and Khalid M. Mosalam. May 2008.

PEER 2007/09 *Integrated Probabilistic Performance-Based Evaluation of Benchmark Reinforced Concrete Bridges.* Kevin R. Mackie, John-Michael Wong, and Božidar Stojadinović. January 2008.

PEER 2007/08 *Assessing Seismic Collapse Safety of Modern Reinforced Concrete Moment-Frame Buildings.* Curt B. Haselton and Gregory G. Deierlein. February 2008.

PEER 2007/07 *Performance Modeling Strategies for Modern Reinforced Concrete Bridge Columns.* Michael P. Berry and Marc O. Eberhard. April 2008.

PEER 2007/06 *Development of Improved Procedures for Seismic Design of Buried and Partially Buried Structures.* Linda Al Atik and Nicholas Sitar. June 2007.

PEER 2007/05 *Uncertainty and Correlation in Seismic Risk Assessment of Transportation Systems.* Renee G. Lee and Anne S. Kiremidjian. July 2007.

PEER 2007/04 *Numerical Models for Analysis and Performance-Based Design of Shallow Foundations Subjected to Seismic Loading.* Sivapalan Gajan, Tara C. Hutchinson, Bruce L. Kutter, Prishati Raychowdhury, José A. Ugalde, and Jonathan P. Stewart. May 2008.

PEER 2007/03 *Beam-Column Element Model Calibrated for Predicting Flexural Response Leading to Global Collapse of RC Frame Buildings.* Curt B. Haselton, Abbie B. Liel, Sarah Taylor Lange, and Gregory G. Deierlein. May 2008.

PEER 2007/02 *Campbell-Bozorgnia NGA Ground Motion Relations for the Geometric Mean Horizontal Component of Peak and Spectral Ground Motion Parameters.* Kenneth W. Campbell and Yousef Bozorgnia. May 2007.

PEER 2007/01 *Boore-Atkinson NGA Ground Motion Relations for the Geometric Mean Horizontal Component of Peak and Spectral Ground Motion Parameters.* David M. Boore and Gail M. Atkinson. May. May 2007.

PEER 2006/12 *Societal Implications of Performance-Based Earthquake Engineering.* Peter J. May. May 2007.

PEER 2006/11 *Probabilistic Seismic Demand Analysis Using Advanced Ground Motion Intensity Measures, Attenuation Relationships, and Near-Fault Effects.* Polsak Tothong and C. Allin Cornell. March 2007.

PEER 2006/10 *Application of the PEER PBEE Methodology to the I-880 Viaduct.* Sashi Kunnath. February 2007.

PEER 2006/09 *Quantifying Economic Losses from Travel Forgone Following a Large Metropolitan Earthquake.* James Moore, Sungbin Cho, Yue Yue Fan, and Stuart Werner. November 2006.

PEER 2006/08 *Vector-Valued Ground Motion Intensity Measures for Probabilistic Seismic Demand Analysis.* Jack W. Baker and C. Allin Cornell. October 2006.

PEER 2006/07 *Analytical Modeling of Reinforced Concrete Walls for Predicting Flexural and Coupled–Shear-Flexural Responses.* Kutay Orakcal, Leonardo M. Massone, and John W. Wallace. October 2006.

PEER 2006/06 *Nonlinear Analysis of a Soil-Drilled Pier System under Static and Dynamic Axial Loading.* Gang Wang and Nicholas Sitar. November 2006.

PEER 2006/05 *Advanced Seismic Assessment Guidelines.* Paolo Bazzurro, C. Allin Cornell, Charles Menun, Maziar Motahari, and Nicolas Luco. September 2006.

PEER 2006/04 *Probabilistic Seismic Evaluation of Reinforced Concrete Structural Components and Systems.* Tae Hyung Lee and Khalid M. Mosalam. August 2006.

PEER 2006/03 *Performance of Lifelines Subjected to Lateral Spreading.* Scott A. Ashford and Teerawut Juirnarongrit. July 2006.

PEER 2006/02 *Pacific Earthquake Engineering Research Center Highway Demonstration Project.* Anne Kiremidjian, James Moore, Yue Yue Fan, Nesrin Basoz, Ozgur Yazali, and Meredith Williams. April 2006.

PEER 2006/01 *Bracing Berkeley. A Guide to Seismic Safety on the UC Berkeley Campus.* Mary C. Comerio, Stephen Tobriner, and Ariane Fehrenkamp. January 2006.

PEER 2005/16 *Seismic Response and Reliability of Electrical Substation Equipment and Systems.* Junho Song, Armen Der Kiureghian, and Jerome L. Sackman. April 2006.

PEER 2005/15 *CPT-Based Probabilistic Assessment of Seismic Soil Liquefaction Initiation.* R. E. S. Moss, R. B. Seed, R. E. Kayen, J. P. Stewart, and A. Der Kiureghian. April 2006.

PEER 2005/14 *Workshop on Modeling of Nonlinear Cyclic Load-Deformation Behavior of Shallow Foundations.* Bruce L. Kutter, Geoffrey Martin, Tara Hutchinson, Chad Harden, Sivapalan Gajan, and Justin Phalen. March 2006.

PEER 2005/13 *Stochastic Characterization and Decision Bases under Time-Dependent Aftershock Risk in Performance-Based Earthquake Engineering.* Gee Liek Yeo and C. Allin Cornell. July 2005.

PEER 2005/12 *PEER Testbed Study on a Laboratory Building: Exercising Seismic Performance Assessment.* Mary C. Comerio, editor. November 2005.

PEER 2005/11 *Van Nuys Hotel Building Testbed Report: Exercising Seismic Performance Assessment.* Helmut Krawinkler, editor. October 2005.

PEER 2005/10 *First NEES/E-Defense Workshop on Collapse Simulation of Reinforced Concrete Building Structures.* September 2005.

PEER 2005/09 *Test Applications of Advanced Seismic Assessment Guidelines.* Joe Maffei, Karl Telleen, Danya Mohr, William Holmes, and Yuki Nakayama. August 2006.

PEER 2005/08 *Damage Accumulation in Lightly Confined Reinforced Concrete Bridge Columns.* R. Tyler Ranf, Jared M. Nelson, Zach Price, Marc O. Eberhard, and John F. Stanton. April 2006.

PEER 2005/07 *Experimental and Analytical Studies on the Seismic Response of Freestanding and Anchored Laboratory Equipment.* Dimitrios Konstantinidis and Nicos Makris. January 2005.

PEER 2005/06 *Global Collapse of Frame Structures under Seismic Excitations.* Luis F. Ibarra and Helmut Krawinkler. September 2005.

PEER 2005//05 *Performance Characterization of Bench- and Shelf-Mounted Equipment.* Samit Ray Chaudhuri and Tara C. Hutchinson. May 2006.

PEER 2005/04 *Numerical Modeling of the Nonlinear Cyclic Response of Shallow Foundations.* Chad Harden, Tara Hutchinson, Geoffrey R. Martin, and Bruce L. Kutter. August 2005.

PEER 2005/03 *A Taxonomy of Building Components for Performance-Based Earthquake Engineering.* Keith A. Porter. September 2005.

PEER 2005/02 *Fragility Basis for California Highway Overpass Bridge Seismic Decision Making.* Kevin R. Mackie and Božidar Stojadinović. June 2005.

PEER 2005/01 *Empirical Characterization of Site Conditions on Strong Ground Motion.* Jonathan P. Stewart, Yoojoong Choi, and Robert W. Graves. June 2005.

PEER 2004/09 *Electrical Substation Equipment Interaction: Experimental Rigid Conductor Studies.* Christopher Stearns and André Filiatrault. February 2005.

PEER 2004/08 *Seismic Qualification and Fragility Testing of Line Break 550-kV Disconnect Switches.* Shakhzod M. Takhirov, Gregory L. Fenves, and Eric Fujisaki. January 2005.

PEER 2004/07 *Ground Motions for Earthquake Simulator Qualification of Electrical Substation Equipment.* Shakhzod M. Takhirov, Gregory L. Fenves, Eric Fujisaki, and Don Clyde. January 2005.

PEER 2004/06 *Performance-Based Regulation and Regulatory Regimes.* Peter J. May and Chris Koski. September 2004.

PEER 2004/05 *Performance-Based Seismic Design Concepts and Implementation: Proceedings of an International Workshop.* Peter Fajfar and Helmut Krawinkler, editors. September 2004.

PEER 2004/04 *Seismic Performance of an Instrumented Tilt-up Wall Building.* James C. Anderson and Vitelmo V. Bertero. July 2004.

PEER 2004/03 *Evaluation and Application of Concrete Tilt-up Assessment Methodologies.* Timothy Graf and James O. Malley. October 2004.

PEER 2004/02 *Analytical Investigations of New Methods for Reducing Residual Displacements of Reinforced Concrete Bridge Columns.* Junichi Sakai and Stephen A. Mahin. August 2004.

PEER 2004/01 *Seismic Performance of Masonry Buildings and Design Implications.* Kerri Anne Taeko Tokoro, James C. Anderson, and Vitelmo V. Bertero. February 2004.

PEER 2003/18 *Performance Models for Flexural Damage in Reinforced Concrete Columns.* Michael Berry and Marc Eberhard. August 2003.

PEER 2003/17 *Predicting Earthquake Damage in Older Reinforced Concrete Beam-Column Joints.* Catherine Pagni and Laura Lowes. October 2004.

PEER 2003/16 *Seismic Demands for Performance-Based Design of Bridges.* Kevin Mackie and Božidar Stojadinović. August 2003.

PEER 2003/15 *Seismic Demands for Nondeteriorating Frame Structures and Their Dependence on Ground Motions.* Ricardo Antonio Medina and Helmut Krawinkler. May 2004.

PEER 2003/14 *Finite Element Reliability and Sensitivity Methods for Performance-Based Earthquake Engineering.* Terje Haukaas and Armen Der Kiureghian. April 2004.

PEER 2003/13 *Effects of Connection Hysteretic Degradation on the Seismic Behavior of Steel Moment-Resisting Frames.* Janise E. Rodgers and Stephen A. Mahin. March 2004.

PEER 2003/12 *Implementation Manual for the Seismic Protection of Laboratory Contents: Format and Case Studies.* William T. Holmes and Mary C. Comerio. October 2003.

PEER 2003/11 *Fifth U.S.-Japan Workshop on Performance-Based Earthquake Engineering Methodology for Reinforced Concrete Building Structures.* February 2004.

PEER 2003/10 *A Beam-Column Joint Model for Simulating the Earthquake Response of Reinforced Concrete Frames.* Laura N. Lowes, Nilanjan Mitra, and Arash Altoontash. February 2004.

PEER 2003/09 *Sequencing Repairs after an Earthquake: An Economic Approach.* Marco Casari and Simon J. Wilkie. April 2004.

PEER 2003/08 *A Technical Framework for Probability-Based Demand and Capacity Factor Design (DCFD) Seismic Formats*. Fatemeh Jalayer and C. Allin Cornell. November 2003.

PEER 2003/07 *Uncertainty Specification and Propagation for Loss Estimation Using FOSM Methods.* Jack W. Baker and C. Allin Cornell. September 2003.

PEER 2003/06 *Performance of Circular Reinforced Concrete Bridge Columns under Bidirectional Earthquake Loading*. Mahmoud M. Hachem, Stephen A. Mahin, and Jack P. Moehle. February 2003.

PEER 2003/05 *Response Assessment for Building-Specific Loss Estimation.* Eduardo Miranda and Shahram Taghavi. September 2003.

PEER 2003/04 *Experimental Assessment of Columns with Short Lap Splices Subjected to Cyclic Loads*. Murat Melek, John W. Wallace, and Joel Conte. April 2003.

PEER 2003/03 *Probabilistic Response Assessment for Building-Specific Loss Estimation.* Eduardo Miranda and Hesameddin Aslani. September 2003.

PEER 2003/02 *Software Framework for Collaborative Development of Nonlinear Dynamic Analysis Program.* Jun Peng and Kincho H. Law. September 2003.

PEER 2003/01 *Shake Table Tests and Analytical Studies on the Gravity Load Collapse of Reinforced Concrete Frames.* Kenneth John Elwood and Jack P. Moehle. November 2003.

PEER 2002/24 *Performance of Beam to Column Bridge Joints Subjected to a Large Velocity Pulse.* Natalie Gibson, André Filiatrault, and Scott A. Ashford. April 2002.

PEER 2002/23 *Effects of Large Velocity Pulses on Reinforced Concrete Bridge Columns.* Greg L. Orozco and Scott A. Ashford. April 2002.

PEER 2002/22 *Characterization of Large Velocity Pulses for Laboratory Testing.* Kenneth E. Cox and Scott A. Ashford. April 2002.

PEER 2002/21 *Fourth U.S.-Japan Workshop on Performance-Based Earthquake Engineering Methodology for Reinforced Concrete Building Structures.* December 2002.

PEER 2002/20 *Barriers to Adoption and Implementation of PBEE Innovations.* Peter J. May. August 2002.

PEER 2002/19 *Economic-Engineered Integrated Models for Earthquakes: Socioeconomic Impacts.* Peter Gordon, James E. Moore II, and Harry W. Richardson. July 2002.

PEER 2002/18 *Assessment of Reinforced Concrete Building Exterior Joints with Substandard Details.* Chris P. Pantelides, Jon Hansen, Justin Nadauld, and Lawrence D. Reaveley. May 2002.

PEER 2002/17 *Structural Characterization and Seismic Response Analysis of a Highway Overcrossing Equipped with Elastomeric Bearings and Fluid Dampers: A Case Study.* Nicos Makris and Jian Zhang. November 2002.

PEER 2002/16 *Estimation of Uncertainty in Geotechnical Properties for Performance-Based Earthquake Engineering.* Allen L. Jones, Steven L. Kramer, and Pedro Arduino. December 2002.

PEER 2002/15 *Seismic Behavior of Bridge Columns Subjected to Various Loading Patterns.* Asadollah Esmaeily-Gh. and Yan Xiao. December 2002.

PEER 2002/14 *Inelastic Seismic Response of Extended Pile Shaft Supported Bridge Structures.* T.C. Hutchinson, R.W. Boulanger, Y.H. Chai, and I.M. Idriss. December 2002.

PEER 2002/13 *Probabilistic Models and Fragility Estimates for Bridge Components and Systems.* Paolo Gardoni, Armen Der Kiureghian, and Khalid M. Mosalam. June 2002.

PEER 2002/12 *Effects of Fault Dip and Slip Rake on Near-Source Ground Motions: Why Chi-Chi Was a Relatively Mild M7.6 Earthquake.* Brad T. Aagaard, John F. Hall, and Thomas H. Heaton. December 2002.

PEER 2002/11 *Analytical and Experimental Study of Fiber-Reinforced Strip Isolators*. James M. Kelly and Shakhzod M. Takhirov. September 2002.

PEER 2002/10 *Centrifuge Modeling of Settlement and Lateral Spreading with Comparisons to Numerical Analyses***.** Sivapalan Gajan and Bruce L. Kutter. January 2003.

PEER 2002/09 *Documentation and Analysis of Field Case Histories of Seismic Compression during the 1994 Northridge, California, Earthquake.* Jonathan P. Stewart, Patrick M. Smith, Daniel H. Whang, and Jonathan D. Bray. October 2002.

PEER 2002/08 *Component Testing, Stability Analysis and Characterization of Buckling-Restrained Unbonded Braces™.* Cameron Black, Nicos Makris, and Ian Aiken. September 2002.

PEER 2002/07 *Seismic Performance of Pile-Wharf Connections.* Charles W. Roeder, Robert Graff, Jennifer Soderstrom, and Jun Han Yoo. December 2001.

PEER 2002/06 *The Use of Benefit-Cost Analysis for Evaluation of Performance-Based Earthquake Engineering Decisions*. Richard O. Zerbe and Anthony Falit-Baiamonte. September 2001.

PEER 2002/05 *Guidelines, Specifications, and Seismic Performance Characterization of Nonstructural Building Components and Equipment*. André Filiatrault, Constantin Christopoulos, and Christopher Stearns. September 2001.

PEER 2002/04 *Consortium of Organizations for Strong-Motion Observation Systems and the Pacific Earthquake Engineering Research Center Lifelines Program: Invited Workshop on Archiving and Web Dissemination of Geotechnical Data, 4–5 October 2001*. September 2002.

PEER 2002/03 *Investigation of Sensitivity of Building Loss Estimates to Major Uncertain Variables for the Van Nuys Testbed.* Keith A. Porter, James L. Beck, and Rustem V. Shaikhutdinov. August 2002.

PEER 2002/02 *The Third U.S.-Japan Workshop on Performance-Based Earthquake Engineering Methodology for Reinforced Concrete Building Structures*. July 2002.

PEER 2002/01 *Nonstructural Loss Estimation: The UC Berkeley Case Study.* Mary C. Comerio and John C. Stallmeyer. December 2001.

PEER 2001/16 *Statistics of SDF-System Estimate of Roof Displacement for Pushover Analysis of Buildings.* Anil K. Chopra, Rakesh K. Goel, and Chatpan Chintanapakdee. December 2001.

PEER 2001/15 *Damage to Bridges during the 2001 Nisqually Earthquake.* R. Tyler Ranf, Marc O. Eberhard, and Michael P. Berry. November 2001.

PEER 2001/14 *Rocking Response of Equipment Anchored to a Base Foundation.* Nicos Makris and Cameron J. Black. September 2001.

PEER 2001/13 *Modeling Soil Liquefaction Hazards for Performance-Based Earthquake Engineering.* Steven L. Kramer and Ahmed-W. Elgamal. February 2001.

PEER 2001/12 *Development of Geotechnical Capabilities in OpenSees.* Boris Jeremić. September 2001.

PEER 2001/11 *Analytical and Experimental Study of Fiber-Reinforced Elastomeric Isolators*. James M. Kelly and Shakhzod M. Takhirov. September 2001.

PEER 2001/10 *Amplification Factors for Spectral Acceleration in Active Regions.* Jonathan P. Stewart, Andrew H. Liu, Yoojoong Choi, and Mehmet B. Baturay. December 2001.

PEER 2001/09 *Ground Motion Evaluation Procedures for Performance-Based Design.* Jonathan P. Stewart, Shyh-Jeng Chiou, Jonathan D. Bray, Robert W. Graves, Paul G. Somerville, and Norman A. Abrahamson. September 2001.

PEER 2001/08 *Experimental and Computational Evaluation of Reinforced Concrete Bridge Beam-Column Connections for Seismic Performance*. Clay J. Naito, Jack P. Moehle, and Khalid M. Mosalam. November 2001.

PEER 2001/07 *The Rocking Spectrum and the Shortcomings of Design Guidelines.* Nicos Makris and Dimitrios Konstantinidis. August 2001.

PEER 2001/06 *Development of an Electrical Substation Equipment Performance Database for Evaluation of Equipment Fragilities*. Thalia Agnanos. April 1999.

PEER 2001/05 *Stiffness Analysis of Fiber-Reinforced Elastomeric Isolators.* Hsiang-Chuan Tsai and James M. Kelly. May 2001.

PEER 2001/04 *Organizational and Societal Considerations for Performance-Based Earthquake Engineering.* Peter J. May. April 2001.

PEER 2001/03 *A Modal Pushover Analysis Procedure to Estimate Seismic Demands for Buildings: Theory and Preliminary Evaluation.* Anil K. Chopra and Rakesh K. Goel. January 2001.

PEER 2001/02 *Seismic Response Analysis of Highway Overcrossings Including Soil-Structure Interaction.* Jian Zhang and Nicos Makris. March 2001.

PEER 2001/01 *Experimental Study of Large Seismic Steel Beam-to-Column Connections.* Egor P. Popov and Shakhzod M. Takhirov. November 2000.

PEER 2000/10 *The Second U.S.-Japan Workshop on Performance-Based Earthquake Engineering Methodology for Reinforced Concrete Building Structures.* March 2000.

PEER 2000/09 *Structural Engineering Reconnaissance of the August 17, 1999 Earthquake: Kocaeli (Izmit), Turkey.* Halil Sezen, Kenneth J. Elwood, Andrew S. Whittaker, Khalid Mosalam, John J. Wallace, and John F. Stanton. December 2000.

PEER 2000/08 *Behavior of Reinforced Concrete Bridge Columns Having Varying Aspect Ratios and Varying Lengths of Confinement.* Anthony J. Calderone, Dawn E. Lehman, and Jack P. Moehle. January 2001.

PEER 2000/07 *Cover-Plate and Flange-Plate Reinforced Steel Moment-Resisting Connections.* Taejin Kim, Andrew S. Whittaker, Amir S. Gilani, Vitelmo V. Bertero, and Shakhzod M. Takhirov. September 2000.

PEER 2000/06 *Seismic Evaluation and Analysis of 230-kV Disconnect Switches.* Amir S. J. Gilani, Andrew S. Whittaker, Gregory L. Fenves, Chun-Hao Chen, Henry Ho, and Eric Fujisaki. July 2000.

PEER 2000/05 *Performance-Based Evaluation of Exterior Reinforced Concrete Building Joints for Seismic Excitation.* Chandra Clyde, Chris P. Pantelides, and Lawrence D. Reaveley. July 2000.

PEER 2000/04 *An Evaluation of Seismic Energy Demand: An Attenuation Approach.* Chung-Che Chou and Chia-Ming Uang. July 1999.

PEER 2000/03 *Framing Earthquake Retrofitting Decisions: The Case of Hillside Homes in Los Angeles.* Detlof von Winterfeldt, Nels Roselund, and Alicia Kitsuse. March 2000.

PEER 2000/02 *U.S.-Japan Workshop on the Effects of Near-Field Earthquake Shaking.* Andrew Whittaker, ed. July 2000.

PEER 2000/01 *Further Studies on Seismic Interaction in Interconnected Electrical Substation Equipment.* Armen Der Kiureghian, Kee-Jeung Hong, and Jerome L. Sackman. November 1999.

PEER 1999/14 *Seismic Evaluation and Retrofit of 230-kV Porcelain Transformer Bushings.* Amir S. Gilani, Andrew S. Whittaker, Gregory L. Fenves, and Eric Fujisaki. December 1999.

PEER 1999/13 *Building Vulnerability Studies: Modeling and Evaluation of Tilt-up and Steel Reinforced Concrete Buildings.* John W. Wallace, Jonathan P. Stewart, and Andrew S. Whittaker, editors. December 1999.

PEER 1999/12 *Rehabilitation of Nonductile RC Frame Building Using Encasement Plates and Energy-Dissipating Devices.* Mehrdad Sasani, Vitelmo V. Bertero, James C. Anderson. December 1999.

PEER 1999/11 *Performance Evaluation Database for Concrete Bridge Components and Systems under Simulated Seismic Loads.* Yael D. Hose and Frieder Seible. November 1999.

PEER 1999/10 *U.S.-Japan Workshop on Performance-Based Earthquake Engineering Methodology for Reinforced Concrete Building Structures.* December 1999.

PEER 1999/09 *Performance Improvement of Long Period Building Structures Subjected to Severe Pulse-Type Ground Motions*. James C. Anderson, Vitelmo V. Bertero, and Raul Bertero. October 1999.

PEER 1999/08 *Envelopes for Seismic Response Vectors.* Charles Menun and Armen Der Kiureghian. July 1999.

PEER 1999/07 *Documentation of Strengths and Weaknesses of Current Computer Analysis Methods for Seismic Performance of Reinforced Concrete Members.* William F. Cofer. November 1999.

PEER 1999/06 *Rocking Response and Overturning of Anchored Equipment under Seismic Excitations.* Nicos Makris and Jian Zhang. November 1999.

PEER 1999/05 *Seismic Evaluation of 550 kV Porcelain Transformer Bushings.* Amir S. Gilani, Andrew S. Whittaker, Gregory L. Fenves, and Eric Fujisaki. October 1999.

PEER 1999/04 *Adoption and Enforcement of Earthquake Risk-Reduction Measures.* Peter J. May, Raymond J. Burby, T. Jens Feeley, and Robert Wood.

PEER 1999/03 *Task 3 Characterization of Site Response General Site Categories*. Adrian Rodriguez-Marek, Jonathan D. Bray, and Norman Abrahamson. February 1999.

PEER 1999/02 *Capacity-Demand-Diagram Methods for Estimating Seismic Deformation of Inelastic Structures: SDF Systems.* Anil K. Chopra and Rakesh Goel. April 1999.

PEER 1999/01 *Interaction in Interconnected Electrical Substation Equipment Subjected to Earthquake Ground Motions.* Armen Der Kiureghian, Jerome L. Sackman, and Kee-Jeung Hong. February 1999.

PEER 1998/08 *Behavior and Failure Analysis of a Multiple-Frame Highway Bridge in the 1994 Northridge Earthquake.* Gregory L. Fenves and Michael Ellery. December 1998.

PEER 1998/07 *Empirical Evaluation of Inertial Soil-Structure Interaction Effects.* Jonathan P. Stewart, Raymond B. Seed, and Gregory L. Fenves. November 1998.

PEER 1998/06 *Effect of Damping Mechanisms on the Response of Seismic Isolated Structures.* Nicos Makris and Shih-Po Chang. November 1998.

PEER 1998/05 *Rocking Response and Overturning of Equipment under Horizontal Pulse-Type Motions.* Nicos Makris and Yiannis Roussos. October 1998.

PEER 1998/04 *Pacific Earthquake Engineering Research Invitational Workshop Proceedings, May 14–15, 1998: Defining the Links between Planning, Policy Analysis, Economics and Earthquake Engineering.* Mary Comerio and Peter Gordon. September 1998.

PEER 1998/03 *Repair/Upgrade Procedures for Welded Beam to Column Connections.* James C. Anderson and Xiaojing Duan. May 1998.

PEER 1998/02 *Seismic Evaluation of 196 kV Porcelain Transformer Bushings.* Amir S. Gilani, Juan W. Chavez, Gregory L. Fenves, and Andrew S. Whittaker. May 1998.

PEER 1998/01 *Seismic Performance of Well-Confined Concrete Bridge Columns.* Dawn E. Lehman and Jack P. Moehle. December 2000.

ONLINE PEER REPORTS

The following PEER reports are available by Internet only at http://peer.berkeley.edu/publications/peer_reports_complete.html.

PEER 2012/103 *Performance-Based Seismic Demand Assessment of Concentrically Braced Steel Frame Buildings.* Chui-Hsin Chen and Stephen A. Mahin. December 2012.

PEER 2012/102 *Procedure to Restart an Interrupted Hybrid Simulation: Addendum to PEER Report 2010/103.* Vesna Terzic and Bozidar Stojadinovic. October 2012.

PEER 2012/101 *Mechanics of Fiber Reinforced Bearings.* James M. Kelly and Andrea Calabrese. February 2012.

PEER 2011/107 *Nonlinear Site Response and Seismic Compression at Vertical Array Strongly Shaken by 2007 Niigata-ken Chuetsu-oki Earthquake.* Eric Yee, Jonathan P. Stewart, and Kohji Tokimatsu. December 2011.

PEER 2011/106 *Self Compacting Hybrid Fiber Reinforced Concrete Composites for Bridge Columns.* Pardeep Kumar, Gabriel Jen, William Trono, Marios Panagiotou, and Claudia Ostertag. September 2011.

PEER 2011/105 *Stochastic Dynamic Analysis of Bridges Subjected to Spacially Varying Ground Motions.* Katerina Konakli and Armen Der Kiureghian. August 2011.

PEER 2011/104 *Design and Instrumentation of the 2010 E-Defense Four-Story Reinforced Concrete and Post-Tensioned Concrete Buildings.* Takuya Nagae, Kenichi Tahara, Taizo Matsumori, Hitoshi Shiohara, Toshimi Kabeyasawa, Susumu Kono, Minehiro Nishiyama (Japanese Research Team) and John Wallace, Wassim Ghannoum, Jack Moehle, Richard Sause, Wesley Keller, Zeynep Tuna (U.S. Research Team). June 2011.

PEER 2011/103 *In-Situ Monitoring of the Force Output of Fluid Dampers: Experimental Investigation.* Dimitrios Konstantinidis, James M. Kelly, and Nicos Makris. April 2011.

PEER 2011/102 *Ground-motion prediction equations 1964 - 2010.* John Douglas. April 2011.

PEER 2011/101 *Report of the Eighth Planning Meeting of NEES/E-Defense Collaborative Research on Earthquake Engineering.* Convened by the Hyogo Earthquake Engineering Research Center (NIED), NEES Consortium, Inc. February 2011.

PEER 2010/111 *Modeling and Acceptance Criteria for Seismic Design and Analysis of Tall Buildings.* Task 7 Report for the Tall Buildings Initiative - Published jointly by the Applied Technology Council. October 2010.

PEER 2010/110 *Seismic Performance Assessment and Probabilistic Repair Cost Analysis of Precast Concrete Cladding Systems for Multistory Buildlings.* Jeffrey P. Hunt and Božidar Stojadinovic. November 2010.

PEER 2010/109 *Report of the Seventh Joint Planning Meeting of NEES/E-Defense Collaboration on Earthquake Engineering. Held at the E-Defense, Miki, and Shin-Kobe, Japan, September 18–19, 2009.* August 2010.

PEER 2010/108 *Probabilistic Tsunami Hazard in California.* Hong Kie Thio, Paul Somerville, and Jascha Polet, preparers. October 2010.

PEER 2010/107 *Performance and Reliability of Exposed Column Base Plate Connections for Steel Moment-Resisting Frames.* Ady Aviram, Božidar Stojadinovic, and Armen Der Kiureghian. August 2010.

PEER 2010/106 *Verification of Probabilistic Seismic Hazard Analysis Computer Programs.* Patricia Thomas, Ivan Wong, and Norman Abrahamson. May 2010.

PEER 2010/105 *Structural Engineering Reconnaissance of the April 6, 2009, Abruzzo, Italy, Earthquake, and Lessons Learned.* M. Selim Günay and Khalid M. Mosalam. April 2010.

PEER 2010/104 *Simulating the Inelastic Seismic Behavior of Steel Braced Frames, Including the Effects of Low-Cycle Fatigue.* Yuli Huang and Stephen A. Mahin. April 2010.

PEER 2010/103 *Post-Earthquake Traffic Capacity of Modern Bridges in California.* Vesna Terzic and Božidar Stojadinović. March 2010.

PEER 2010/102 *Analysis of Cumulative Absolute Velocity (CAV) and JMA Instrumental Seismic Intensity (I_{JMA}) Using the PEER–NGA Strong Motion Database.* Kenneth W. Campbell and Yousef Bozorgnia. February 2010.

PEER 2010/101 *Rocking Response of Bridges on Shallow Foundations.* Jose A. Ugalde, Bruce L. Kutter, and Boris Jeremic. April 2010.

PEER 2009/109 *Simulation and Performance-Based Earthquake Engineering Assessment of Self-Centering Post-Tensioned Concrete Bridge Systems.* Won K. Lee and Sarah L. Billington. December 2009.

PEER 2009/108 *PEER Lifelines Geotechnical Virtual Data Center.* J. Carl Stepp, Daniel J. Ponti, Loren L. Turner, Jennifer N. Swift, Sean Devlin, Yang Zhu, Jean Benoit, and John Bobbitt. September 2009.

PEER 2009/107 *Experimental and Computational Evaluation of Current and Innovative In-Span Hinge Details in Reinforced Concrete Box-Girder Bridges: Part 2: Post-Test Analysis and Design Recommendations.* Matias A. Hube and Khalid M. Mosalam. December 2009.

PEER 2009/106 *Shear Strength Models of Exterior Beam-Column Joints without Transverse Reinforcement.* Sangjoon Park and Khalid M. Mosalam. November 2009.

PEER 2009/105 *Reduced Uncertainty of Ground Motion Prediction Equations through Bayesian Variance Analysis.* Robb Eric S. Moss. November 2009.

PEER 2009/104 *Advanced Implementation of Hybrid Simulation.* Andreas H. Schellenberg, Stephen A. Mahin, Gregory L. Fenves. November 2009.

PEER 2009/103 *Performance Evaluation of Innovative Steel Braced Frames.* T. Y. Yang, Jack P. Moehle, and Božidar Stojadinovic. August 2009.

PEER 2009/102 *Reinvestigation of Liquefaction and Nonliquefaction Case Histories from the 1976 Tangshan Earthquake.* Robb Eric Moss, Robert E. Kayen, Liyuan Tong, Songyu Liu, Guojun Cai, and Jiaer Wu. August 2009.

PEER 2009/101 *Report of the First Joint Planning Meeting for the Second Phase of NEES/E-Defense Collaborative Research on Earthquake Engineering.* Stephen A. Mahin et al. July 2009.

PEER 2008/104 *Experimental and Analytical Study of the Seismic Performance of Retaining Structures.* Linda Al Atik and Nicholas Sitar. January 2009.

PEER 2008/103 *Experimental and Computational Evaluation of Current and Innovative In-Span Hinge Details in Reinforced Concrete Box-Girder Bridges. Part 1: Experimental Findings and Pre-Test Analysis.* Matias A. Hube and Khalid M. Mosalam. January 2009.

PEER 2008/102 *Modeling of Unreinforced Masonry Infill Walls Considering In-Plane and Out-of-Plane Interaction.* Stephen Kadysiewski and Khalid M. Mosalam. January 2009.

PEER 2008/101 *Seismic Performance Objectives for Tall Buildings.* William T. Holmes, Charles Kircher, William Petak, and Nabih Youssef. August 2008.

PEER 2007/101 *Generalized Hybrid Simulation Framework for Structural Systems Subjected to Seismic Loading.* Tarek Elkhoraibi and Khalid M. Mosalam. July 2007.

PEER 2007/100 *Seismic Evaluation of Reinforced Concrete Buildings Including Effects of Masonry Infill Walls.* Alidad Hashemi and Khalid M. Mosalam. July 2007.

The Pacific Earthquake Engineering Research Center (PEER) is a multi-institutional research and education center with headquarters at the University of California, Berkeley. Investigators from over 20 universities, several consulting companies, and researchers at various state and federal government agencies contribute to research programs focused on performance-based earthquake engineering.

These research programs aim to identify and reduce the risks from major earthquakes to life safety and to the economy by including research in a wide variety of disciplines including structural and geotechnical engineering, geology/seismology, lifelines, transportation, architecture, economics, risk management, and public policy.

PEER is supported by federal, state, local, and regional agencies, together with industry partners.

PEER Core Institutions:
University of California, Berkeley (Lead Institution)
California Institute of Technology
Oregon State University
Stanford University
University of California, Davis
University of California, Irvine
University of California, Los Angeles
University of California, San Diego
University of Southern California
University of Washington

PEER reports can be ordered at http://peer.berkeley.edu/publications/peer_reports.html or by contacting

Pacific Earthquake Engineering Research Center
University of California, Berkeley
325 Davis Hall, mail code 1792
Berkeley, CA 94720-1792
Tel: 510-642-3437
Fax: 510-642-1655
Email: peer_editor@berkeley.edu

ISSN 1547-0587X